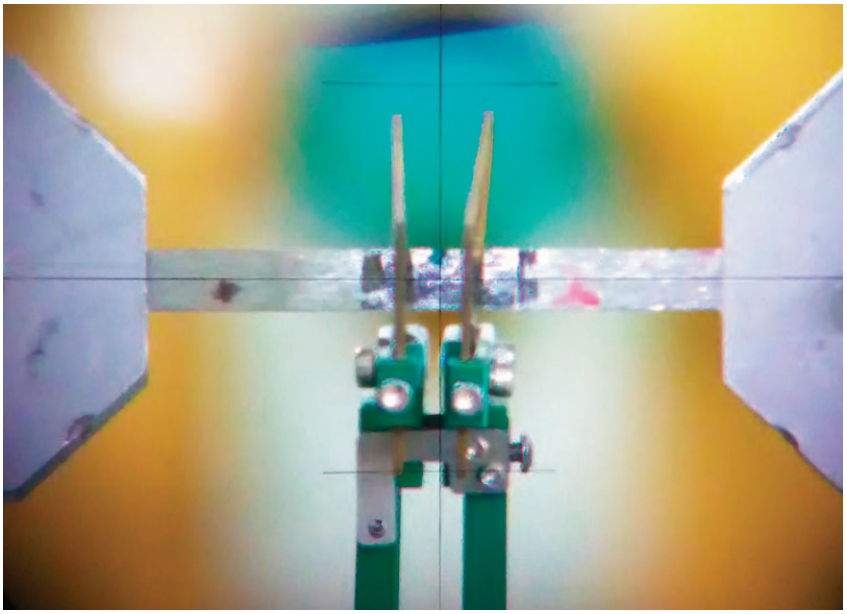

J-PARC

ANNUAL REPORT 2019

Vol.1: Highlight

Editorial Board (April 2020 – March 2021)

Cover photographs

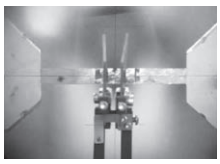
Photograph ① : Sample alignment for neutron experiment
Image credit: Stefanus HARJO

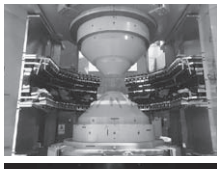
Photograph ② : The Lead Glass Calorimeter for J-PARC E16
Image credit: Sakiko ASHIKAGA

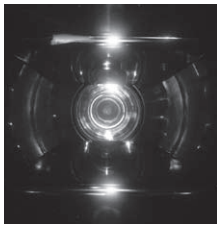
Photograph ③ : Abyss
Image credit: Taihei ADACHI

J-PARC Annual Report 2019

Contents

Preface 1

Accelerators 3

- Overview of the Accelerator 3
- Linac 6
- RCS 9
- MR 12

Materials and Life Science Experimental Facility 15

- Overview 15
- Neutron Source Section 16
- Neutron Science Section 17
- Neutron Device 18
- Muon Section 19
- Technology Development Section 20

Particle and Nuclear Physics 23

- Neutrino Experiment 23
- Hadron Experimental Facility 24
- Strangeness / Hadron Physics Experiments 25
- Kaon Decay Experiment 25
- Muon Experiments 25
- Highlight: T2K data place the strongest constraint on the leptonic CP violating phase in neutrino oscillation 26

Cryogenics Section 29

- Overview 29
- Cryogen Supply and Technical Support 30
- Superconducting Magnet System for T2K 30
- Superconducting Magnet Systems at the MLF 31
- Superconducting Magnet Systems at the HEF 31
- R&D for the Future Projects at J-PARC 32

Information System 33

- Overview 33
- Status of Networking 33
- Internet Connection Services for Visitors and Public Users of J-PARC 35
- Status of Computing 36

Transmutation Studies 39
Overview 39
Research and development 40
International cooperation 44
Safety 47
Safety 48
User Service 51
Users Office (UO) 52
User Statistics 54
MLF Proposals Summary - FY2019 55
J-PARC PAC Approval Summary for the 2019 Rounds 57
Organization and Committees 59
Organization Structure 60
Members of the Committees Organized for J-PARC 61
Main Parameters 67
Events 69
Events 69
Publications 75
Publications in Periodical Journals 76
Conference Reports and Books 84
KEK Reports 91
JAEA Reports 91
Others 91

Preface

We are facing an extraordinary crisis of human life with the new coronavirus which is still spreading all over the world. We hope you and your loved ones are in good health. In many countries, non-essential activities have been postponed and people are asked to stay home or even more severe regulations are enforced. In Japan, a national state of emergency was raised back in April, 2020. Consequently, we have decided to pause the operation of entire J-PARC facility as of April 20th, especially to contribute to subsiding the spread by staying home, hence, a reduction of contact chances.

We were able to resume the facility operation of Material and Life science experimental Facility (MLF) in mid-May. The hadron experimental facility (HEF) was able to start its upgraded operation which was delayed by the corona-related slowing down in the regulation review process. While the user's presence at the facility were not fully recovered, we were able to conclude the operation before summer shutdown with the successful 1 MW operation at MLF. Scientific outcome of this period will be reported in the next annual report.

While the challenges still remain, we think it is important to resume the research activities not only to maintain the research itself as an irreducible part of human civilization, but also to learn about an operation of a research facility like ours in the

similar situations possibly coming back again in the near future. Of course, it is extremely important to protect society against further spread of infections and secure staff and users from risks of infections. Therefore, we continue to reinforce the counter measures based on the best possible knowledge obtained to date. At the same time, the scientific research activity is undoubtedly important not only for an immediate benefit, but also for the incubation of novel ideas and fostering the next generations with scientific competence. Along this line, we are open for any research interests directly or indirectly related to COVID-19 at our facility.

While we were forced to stay home and keep distance from others in the last several months, I think everybody recognizes how important to cooperate with each other, share ideas, and even disagree sometimes.

Therefore, keep in touch, and stay connected towards the society with resilience, which can be accelerated by the research facilities like J-PARC.

In this volume, we report the progress made at J-PARC in fiscal year 2019, from April 2019 through March 2020. The neutrino group has established a significant constraint on the CP phase. The hadron experimental facility is now equipped with the new target system which can handle more beam power, and a new beamline, B-Line to receive a primary proton beam. The MLF is provided with more robust targetry for neutron and muon, and new instruments *e.g.* T0 chopper to produce increasing number of results with users from academic and industrial sectors, which are reported in the separated volume.

Even under pandemic, our slogan does not change, however, it now implies deeper engagements towards the future of our world.

"High power beams for the next stage of our life!"

Naohito SAITO
On behalf of the J-PARC staff members,
Director of J-PARC Center

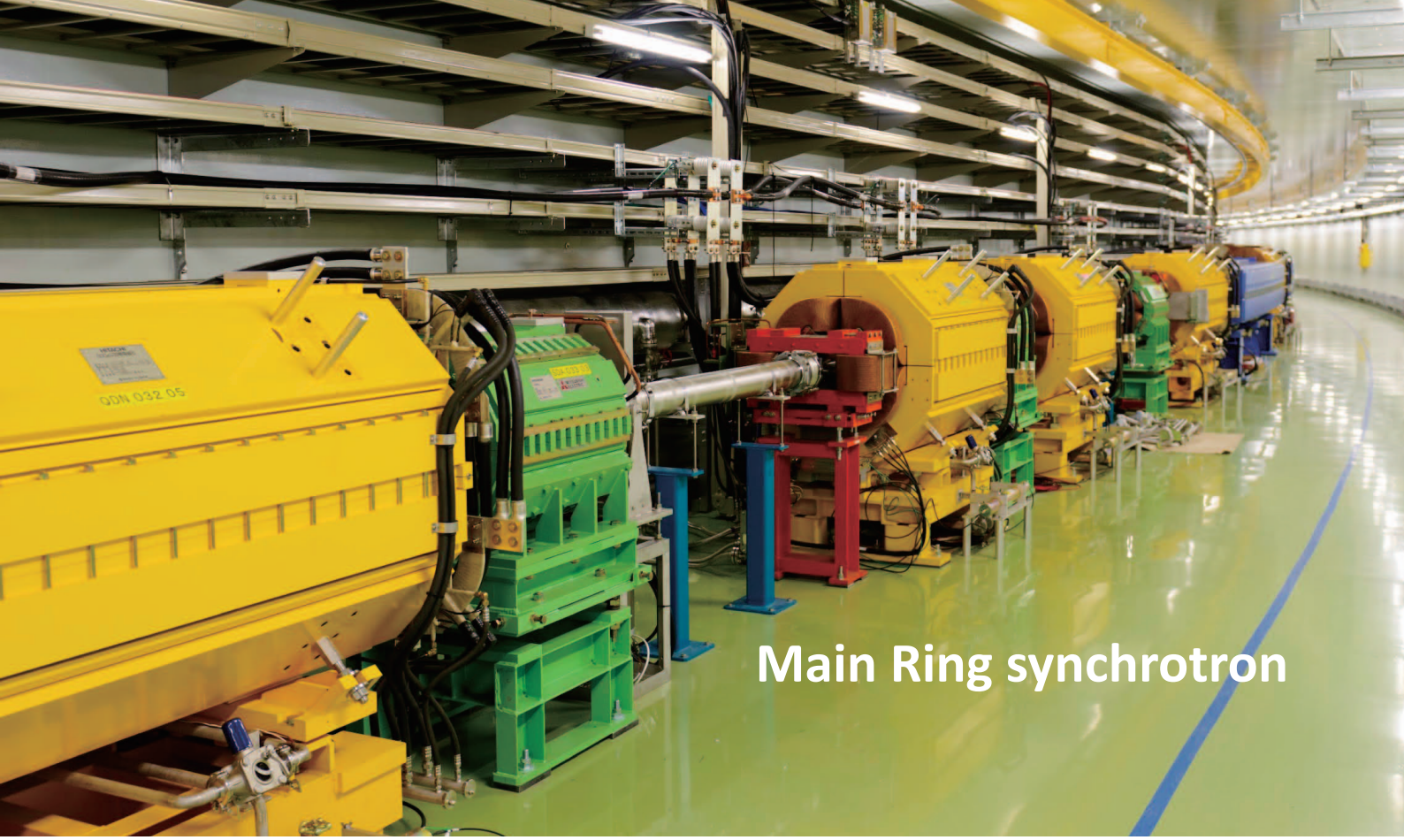

Accelerators

Overview of the Accelerator

The J-PARC accelerator complex consists of a 400 MeV linac, a 3 GeV Rapid Cycling Synchrotron (RCS) and a Main Ring Synchrotron (MR, 30 GeV). The proton beam from the RCS is delivered to the Materials and Life Science Experimental Facility (MLF) for neutron and muon experiments as well as injected to the MR. The MR has two beam extraction modes: fast extraction (FX) mode for the Neutrino experimental facility (NU) and slow extraction (SX) mode for the Hadron experimental facility (HD).

The operation in FY 2019 is illustrated in Fig. 1. The topics related to the beam operation are as follows:

(1) Operation for the MLF

After the replacement of the ion source at the end of March, we started a new Run #82. We delivered beam for the MLF user operation at a beam power of 500 kW. The user operation for the MLF ended in the morning

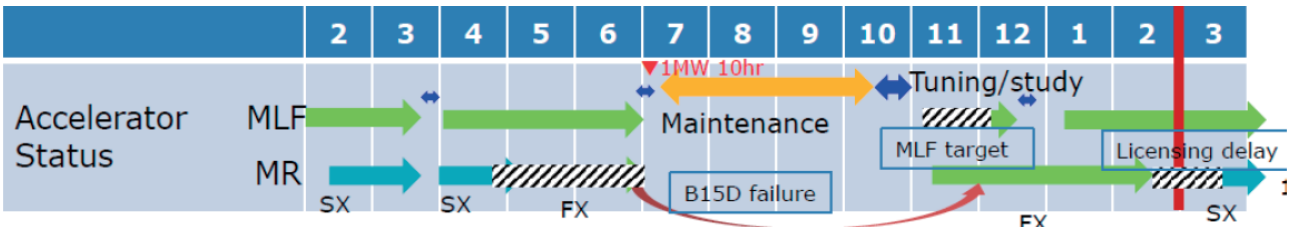

Fig. 1. Accelerator operation in FY 2019 (overlapping with the end of FY 2018).

of July 3. From April, the operation ran smoothly with a high beam availability at about 96%. We used the remaining time for accelerator study until the morning of July 8 and then the operation was stopped for the summer shutdown. In the beginning of the study time, we successfully delivered a 1-MW power beam to the MLF for more than 10 hours. The linac, the RCS, and the neutron target were very stable during this 1-MW operation. We had only three short beam stops, and the availability was as high as 99%. In the previous year, we demonstrated a 1-MW operation for 1 hour. This year, we managed to maintain a longer operation and accumulated experiences necessary to attain the design goal of continuous operation with 1-MW beam power to the MLF.

The linac peak current was kept to its nominal value of 50 mA, but was also increased to more than 60 mA during high power studies to reach a beam power of over 1.5 MW in the RCS.

We had the usual 2-week shutdown period from the end of December until the beginning of January. The linac tuning started on January 9 followed by the RCS and MR tuning. The MLF user program started on January 14 and continued until the end of March, as scheduled.

(2) Operation of the MR for the Neutrino Experiment (FX mode) and Hadron Experiment (SX mode)

The failure of the bending magnet (B51D), which occurred in March, at the beam transport of RCS to the MR, was patched up and the beam operation stopped. The beam operation for the HD resumed on April 4 with a beam power of 51 kW, the value before the suspension. But on April 24, it was observed that the field strength of the B51D has dropped by 2%, a much more severe loss than that in March. After investigation, we found insufficient insulation between conductors in coils. As a result, we concluded that maintaining a stable operation of the MR would be difficult without replacement of the failed coil. It was replaced during the summer shutdown period and the user operation of the MR was resumed in the beginning of November.

On November 4, the beam delivery to the NU was resumed at a beam power of 400 kW. After fine tuning of the MR, we delivered around 490 kW beam power, a level similar to the one in the previous operation. After the New Year's holiday, further beam loss mitigation in the MR was achieved with fine tuning of the beam. As a result, the beam power to the NU operation was increased to 515 kW. We expected a change from the NU operation to beam tuning for the HD in mid-February. But the licensing for a new target and a new beam line in the HD was delayed, so the beam operation was postponed.

The operation statistics for FY 2019 (from April 2019 to March 2020) are shown in Table 1 and Fig. 2. The total operation time amounted to 5,800 hours. It included the on-duty time of the shift leaders at the control room, as well as the startup and RF conditioning. The net user operation hours and the beam availability rate for each experimental facility were as follows: 3,488 hours (95%) for MLF; 1,295 hours (90%) for NU; and 355 hours (80%) for HD. These statistics show that the linac and the RCS operated properly. The low availability for the HD was caused by the B15D trouble in March 2019.

The downtime by components is shown in Fig. 3. There were several causes of the downtime. Over the last few years, we have taken many countermeasures against troubles at the linac: stabilization of the cooling water flow, inside cleaning of some SDTL cavities, and replacement of old bias power supplies for the klystron high voltage power supply system (HVDC). The HVDC down time was still a little long, due to a failure of the old 324-MHz klystron. This year, we also experienced a shutdown for several hours caused by an antenna failure at the ion source.

There were no serious downtime events in the RCS and the beam operation was almost stable throughout the year.

The MR had only one serious downtime event, which was the trouble of the B15D magnet included in the "Others" category.

Most of the improvement and upgrade work was carried out during the summer shutdown. Specific improvements, major downtime causes, and beam power history are described in further chapters.

Table 1. Operation statistics in hours for FY 2019. Figures in the parentheses in trouble columns show the loss time contributions as a percentage.

Facility	User Time (hours)	Trouble, Acc.only (hours)	Trouble, Faculty.only (hours)	Net Time (hours)	Availability, Total (%)
MLF	3,656	155 (4.3%)	12 (0.3%)	3,488	95.4
Neutrino (FX)	1,434	121 (8.4%)	17 (1.2%)	1,295	90.3
Hadron (SX)	445	88 (19.8%)	1 (0.3%)	355	79.8

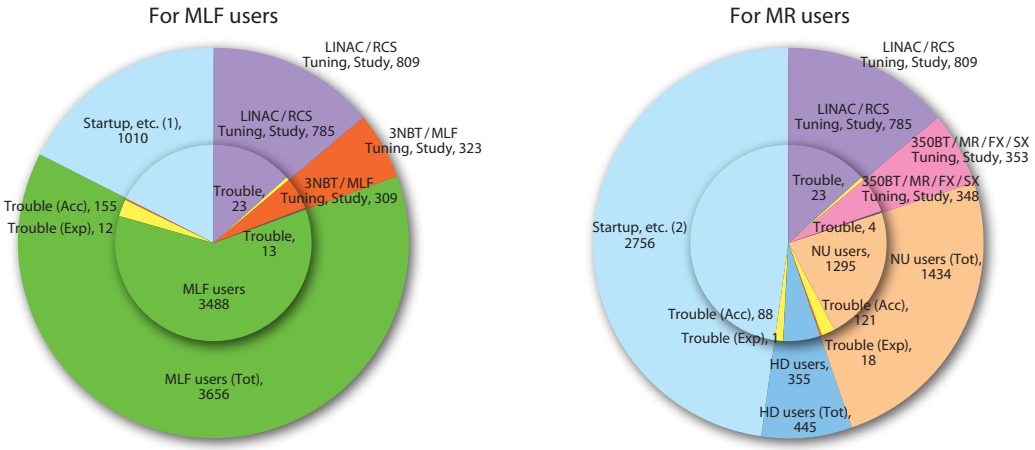

Fig. 2. Operation statistics for FY 2019. The total operation time was 5,800 hours.

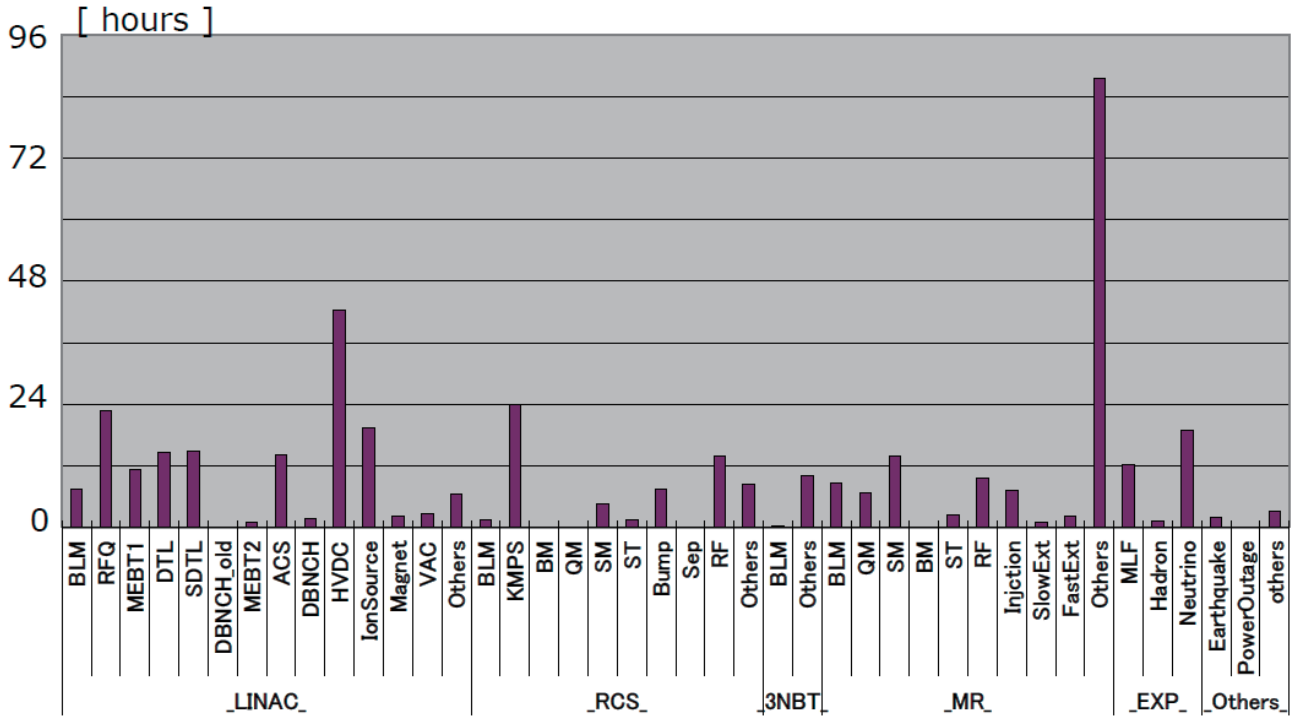

Fig. 3. Downtime by components in FY 2019.

Linac

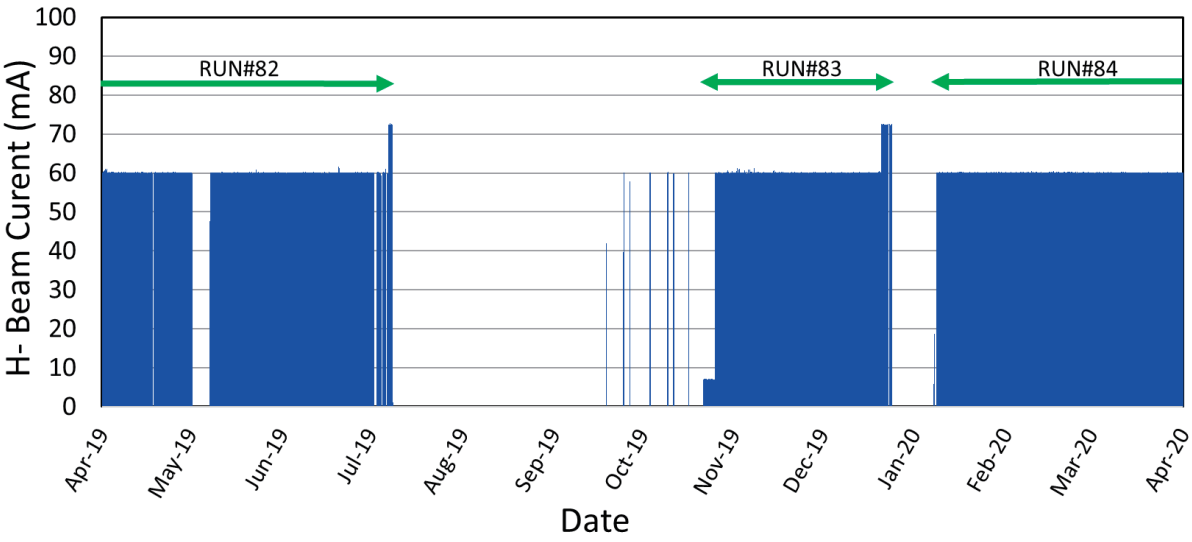

Fig. 1. Operation history of the ion source in FY2019.

Overview

The J-PARC linac has been operated with a nominal peak beam current of 50 mA. High availability of approximately more than 95% (to the MLF) was achieved during FY2019 at the linac. Two 10-hour long beam stop events occurred due to the failure of an ion source and a klystron power supply. The number of trips due to the RFQ was still higher than that of other components.

Accelerator components status

The operation history of the ion source in FY 2019 is shown in Fig.1. Presently, the ion source is being operated with a beam current of 60 mA for the user operation. At the end of RUN#82 and RUN#83, the ion source extracted stable 72 mA beams for high-intensity beam studies at the linac. in RUN#82, unscheduled ion source replacement was performed due to an antenna malfunction during the operation. An investigation established that the malfunction was most likely caused by the coating on the antenna surface breaking due to the collision of heavy ions, because a vacuum leak was detected during a vacuum fitting of the antenna feedthrough. In order to prevent a recurrence of this issue, we have decided to replace the fitting with a new one when we perform a full maintenance of the ion source.

Figure 2 shows the time variation of number of RFQ trips. The RFQ trip rate was typically 9 times per day during the 25 Hz (MLF) and 50mA beam operation in FY2019. This situation is almost the same as before. To reduce the down time of the linac due to regular RFQ trips, modifications have been done to the LLRF system. The new LLRF system can re-start the high-power RF with the next macro-pulse (40 ms) after the RFQ trip. Presently, a re-start of MPS (machine protection system) by the operator requires approximately 30 seconds. The auto-restart without activation of the MPS is planned for the next year.

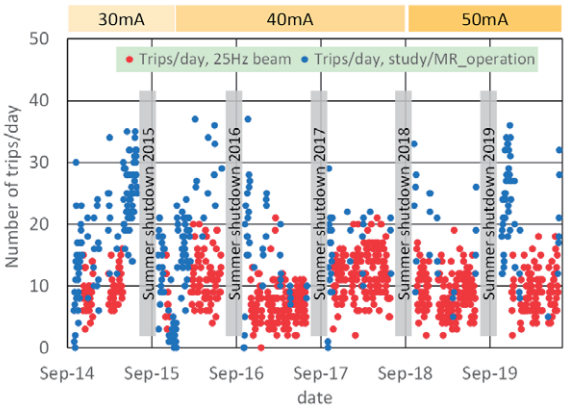

Fig. 2. Time variation of the number of RFQ RF-trips.

After the Great East Japan Earthquake in 2011, we could not input the design rf power into some SDTL cavities due to the multipactor effect. To improve this situation, since 2015, we have been wiping the inside of the cavities by using acetone during the summer

shutdown. After the treatment, the multipactor region disappeared completely, except in the SDTL05A cavity. We suppose that the SDTL05A was not cleaned up sufficiently, therefore we retried the cavity cleaning of the SDTL05A in the summer of 2019. Immediately after treatment, the region was reduced, but spread again in a few weeks. Although it is assumed that there is no serious problem in the operation, we plan to try wiping with dilute sulfuric acid in the 2020 summer shutdown.

The operation of the ACS cavities was more stable than the one of the other cavities. The number of trips of all the ACS cavities was less than once per day.

RF system status

We have been using two types of klystrons, a 324-MHz klystron and a 972-MHz one. Their operation times as of March 2020, are shown in Fig. 3. Eight out of the twenty 324-MHz klystrons exceeded 70,000 hours of operation, which has been the entire period since the linac operation was started. Most of the 972-MHz klystrons exceeded 40,000 hours of operation. In FY2019, one of each type of klystrons was replaced during the 2019 summer shutdown. The 324-MHz klystron for the SDTL09 was replaced due to its performance degradation. The 972-MHz one for the ACS17 was replaced due to slight water leak from a body cooling pipe.

In RUN#83, malfunction of the klystron power supply #6 occurred. The malfunction was caused by a defect in the control board installed at an AVR (automatic voltage regulator) in the klystron power supply system. The power supply was restored by replacing it with a spare one.

Procurement of the conditioned klystron is getting difficult from manufacturer due to busy schedule of the conditioning equipment in manufacturer's factory. A test-stand for the klystrons was assembled to perform off-line conditioning. The test-stand will be fully operational in FY2020.

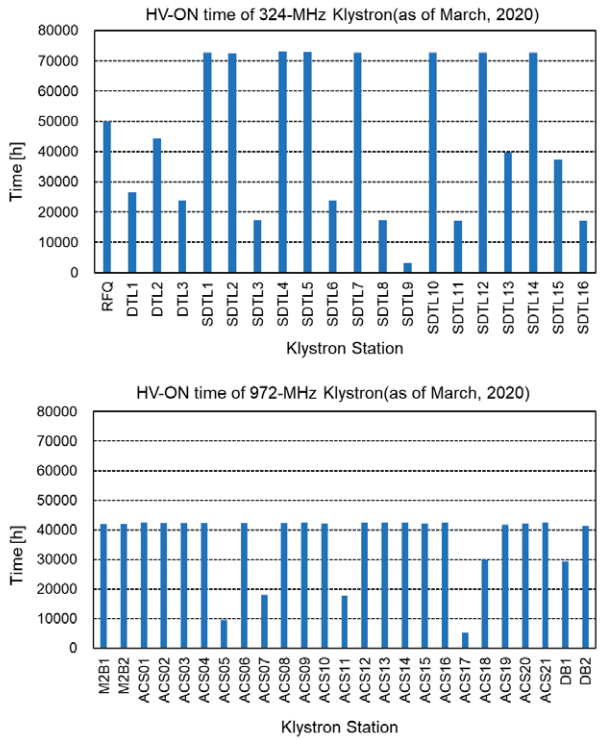

Fig. 3. The operation time of the 324-MHz klystron (upper) and the 972-MHz klystron (lower) as of March 2020.

Beam monitor development

For higher intensity beam measurement, we have developed a beam monitor with high thermal load tolerance and a non-destructive type beam profile monitor (e.g. gas sheet beam monitor).

We have developed a new wire scanner monitor (WSM) based on the CNT wire, which has high tensile strength and electric conductivity, and are sequentially replacing it with the WSM based on the carbon wire at MEBT1 (medium energy beam transport1 located between the RFQ and the DTL).

We are working to improve the beam quality of the linac by tuning the longitudinal beam profile at the MEBT1 using the bunch shape monitor (BSM). The measurement of the high-intensity and slow (3 MeV) beam of the MEBT1 was difficult with the conventional BSM using tungsten wire as a secondary-electron production target due to the limitation of the thermal-fatigue damage. Therefore, a highly oriented pyrolytic graphite (HOPG), which has high thermal load tolerance, was adopted as the target (Fig. 4). As a result of the performance evaluation test, we succeeded in detecting the secondary electrons generated by the HOPG target placed in the center of the beam. Since the HOPG was found to be useful as a secondary- electron target for

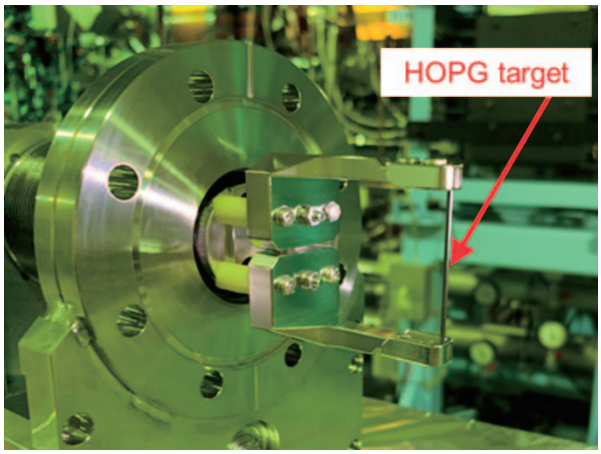

Fig. 4. Bunch shape monitor head equipped with a HOPG target.

the high-intensity and slow beam, the BSM using the HOPG will be installed in the beamline in the near future.

Beam study

Beam studies have been conducted to resolve some issues, such as the beam loss mitigation, confirmation of feasibility for the further upgrade plan, and so on.

An increase of the residual radiation at DTL1 was observed at the 50-mA operation. By local envelope correction and confirming the effect with scintillation monitor measurements, the radiation source was removed, and the residual radiation decreased significantly.

At the ACS section, the main source of beam loss was found to be IBSt (intra-beam stripping) in the H- beam. Because the loss rate by IBSt can be affected only by beam optics, some optics with different temperature ratio between transverse and longitudinal planes (Tx/Tz) were examined (The optics of Tx/Tz=1.0 is the J-PARC linac baseline design based on the equipartitioning setting). The use of Tx/Tz=0.7 optics in the operation started in April 2019. As a result, the residual radiation decreased by 40% compared with Tx/Tz=1.0. The result was in good agreement with the numerical simulation projection.

We are considering a further upgrade plan to increase the RCS beam power to 1.5 MW. To realize that plan, the beam current and the beam pulse length must increase to 60 mA and 600 μs respectively. We obtained successfully a 400-MeV and 60-mA beam at the linac exit in July 2018. In this year, we tried 60-mA and 600-μs beam injection to the RCS. Figure 5 shows the first result of the 60-mA and 600-μs beam extracted from the linac in July 2019. Although the beam current and the pulse length satisfied the upgrade requirement, the linac output emittance was large. As a result of fine beam tuning by changing the MEBT1 bunchers, the emittance was improved. Further beam study is necessary.

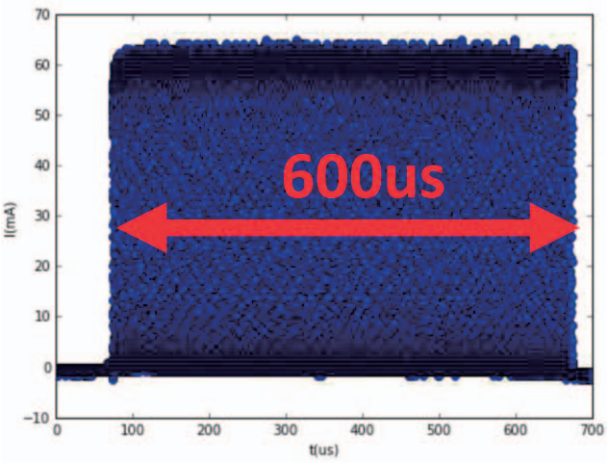

Fig. 5. First result of 400-MeV, 60-mA and 600-μs demonstration at the linac.

RCS

Operational status

The operation status of the RCS was quite stable in JFY 2019. The availability of the RCS is summarized in Table 1. The operation time for the MLF over the year was approximately 2775 h, excluding the commissioning time, and the downtime was approximately 27 h. The availability for the MLF was evaluated by these values and it was 99.0%. For the Neutrino and Hadron users, the availabilities of RCS were almost same as in the MLF case and those values were around 99%.

Table 1. Summary of the availability

Facility	User time (h)	Trouble in RCS (h)	Availability of the RCS (%)
MLF	2775:22	27:22	99.0
Neutrino	1053:32	8:28	99.2
Hadron	1089:28	3:06	99.7

Figure 1 shows the change in the RCS output power with respect to time. Throughout the JFY 2019, RCS delivered more than 500-kW beam to the MLF. Just before the summer shutdown period, we tried a 1-MW, 10-h continuous operation for the MLF.

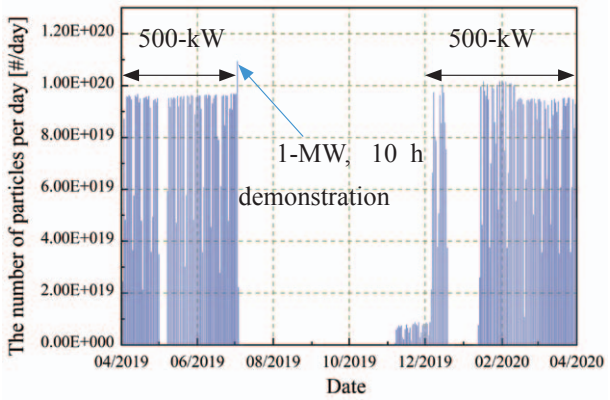

Fig. 1. Changes in the RCS output particles over time.

This year, there were no serious problems in the RCS, but a dipole magnet in the beam transport line from the RCS to MR malfunctioned. Due to this trouble, the MR operation was suspended and only the MLF accepted the RCS beam until the summer shutdown. Next, there was a trouble with the neutron target replacement process during the summer shutdown period. Due to this trouble, the MLF operation was delayed by more than a month.

Maintenance and improvements

1) Foil production

In the J-PARC RCS, The Hybrid type Boron-doped Carbon (HBC) foil produced in KEK had been used for charge exchange injection. Now it is produced at the J-PARC site and we have been using this HBC foil for the full user operation. Fig. 2 shows photographs of two foils after the user operation. Foils were used for 1-2 months with more than 500-kW beam power, and all foils maintained sufficient charge exchange efficiency under those conditions regardless of different production lots. We have also been searching for another candidate and tested a commercial carbon film developed by Kaneka corporation. This Kaneka foil also showed enough toughness and performed consistently under the 500-kW user operation condition.

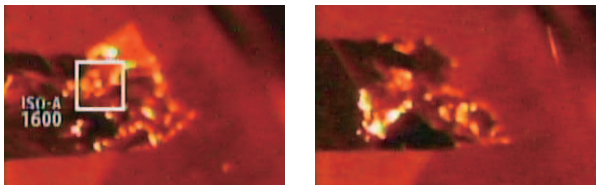

Fig. 2. Photographs of foils after irradiation. The foil on the left looked deformed, but its performance was unchanged.

2) RF feedback system

In the RCS, mitigation of the wake voltage in an accelerating cavity is a key to achieving stable acceleration of the high-intensity beam. The RF feedforward method had been employed in the original low-level rf (LLRF) control system for such purpose, but it showed performance degradation at 1-MW beam power.

Therefore, the multi-harmonic vector rf voltage control feedback implemented in the new LLRF control system was deployed in 2019. The feedback system was tested using a 1-MW equivalent beam. The test result showed that the wake voltage due to the high beam current was well minimized by the new feedback system. However, the beam loss in the RCS increased.

We investigated its reason and a numerical simulation indicated that the wake voltage was increasing the bunching factor. In the former feedforward system, the wake voltage could not be completely compensated. However, such remaining wake voltage shook the particle motion in the longitudinal phase space and led to flattening of the bunch. Therefore, the complete compensation of the wake voltage by the new feedback

system caused a decrease of the bunching factor and an increase of the beam loss. In order to rectify this situation, the duration of the second harmonic rf voltage application was extended. As a result, the beam loss was recovered to the same level as that of the feedforward system.

Residual dose distribution and exposure during maintenance

Table 2 summarizes the radiation doses received by the workers during the summer shutdown period in 2019. A total of 60 workers were exposed to doses of more than 0.01 mSv, and their collective dose was 6.6 man-mSv. The maximum dose received by any one worker was 0.42 mSv. Both the collective and maximum doses had increased compared to the previous years.

Table 2. Summary of worker radiation doses during the summer shutdown period in 2019.

Dose (mSv)	Number of workers
0.01–0.05	30
0.06–0.10	12
0.11–0.20	4
0.21–0.30	7
0.31–	7

1-MW demonstration

We demonstrated the 1-MW, 10 h continuous operation in the beginning of July 2019. Figure 3 shows the trend of some parameters during the 1-MW continuous operation.

At the first 1-MW continuous operation in 2018, we observed a vacuum pressure rise of three orders of magnitude due to a failure of the turbo molecular pump (TMP) at an arc section. In contrast, the maximum vacuum pressure of this 1-MW continuous operation was only three times larger than that of the 500-kW user operation. The lower graph in Fig. 3 shows the trend of vacuum pressure in the RCS beam line.

The other concern about the 1-MW continuous operation is the durability of the charge exchange foil. We have been carefully monitoring the foil deformation during the beam operation by a video camera, and also measuring the beam current toward the injection dump to evaluate the charge exchange efficiency. The middle graph in Fig. 3 shows the trend of the beam current. During the 1-MW operation, this beam current fluctuated about ± 5%, which corresponded to only 0.025% fluctuation of the circulating beam current. This stability was sufficient for the user operation.

The upper graph in Fig. 3 shows the temperature trend of the injection beam dump. In this situation, only three interlocks happened during 10-h continuous

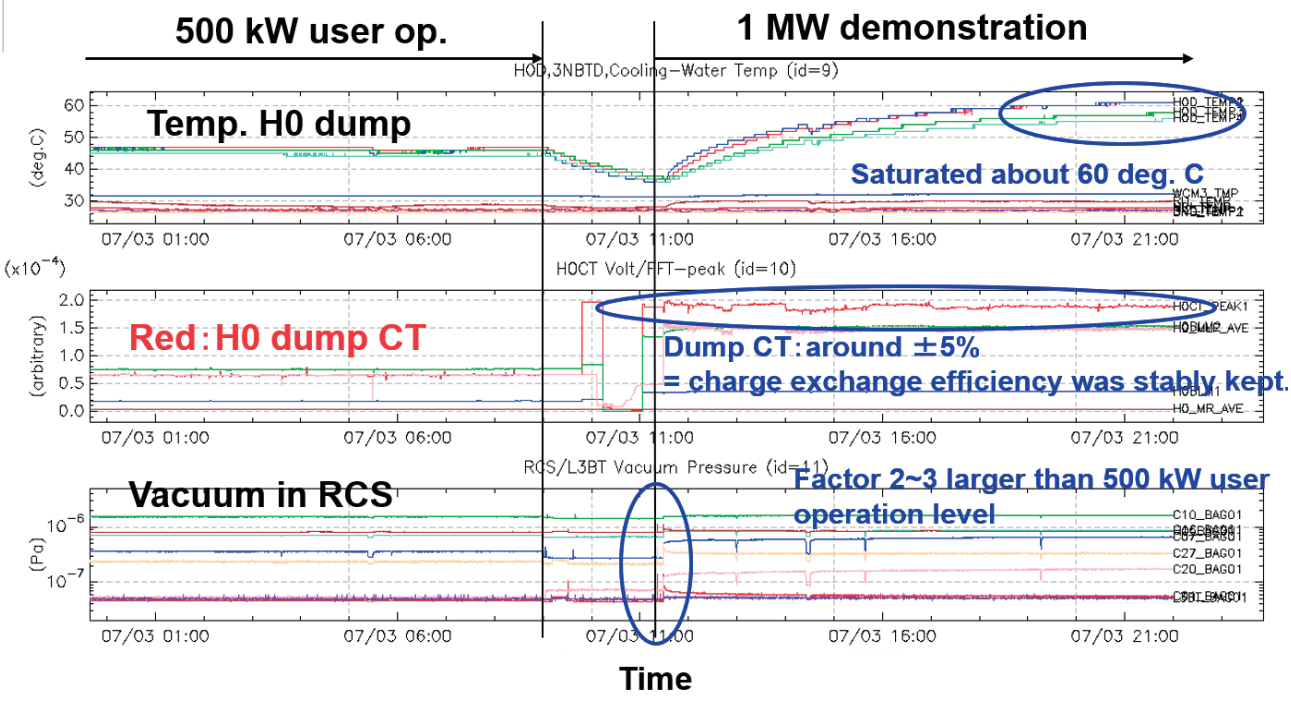

Fig. 3. Trend of parameters during the 1-MW continuous operation.

operation. Therefore, the injection dump was continuously heated up and the temperature seemed almost saturated at the end of this demonstration.

After the demonstration, we measured the residual dose values around the accelerator components and found that they were low enough to accept and the same as those in the previous year.

Beyond 1-MW: Beam study for 1.5-MW beam power

Last year, we successfully demonstrated 1.2-MW equivalent beam acceleration in the RCS. Unfortunately, the present RF system cannot accelerate stably a beam with power over 1 MW and we carried out the 1.2-MW beam trial with an acceleration energy of 1 GeV.

This year we tried for a 1.5-MW equivalent beam acceleration in the RCS. In order to establish this condition, both the peak current and macro pulse length of the injection beam were increased. For the same reason as in the previous year, we limited the acceleration energy to 0.8 GeV. In order to minimize the beam loss, the betatron tune and the transverse painting parameters were changed from those of the 1-MW operation. After fine tuning in this situation, we obtained sufficient low-loss beam condition even at 1.5-MW equivalent beam power. Figure 4 shows the circulating beam intensity measured by the slow current transformer (SCT) with various levels of beam power. We can see no signal reduction in any cases and the beam loss monitor signal indicated that the amount of a total beam loss was an order of 10^{-3} even if the 1.5-MW beam was accelerated.

In this way, we demonstrated the RCS potential to deliver more than 1-MW beam power. Nevertheless, there are some issues to limiting the acceleration of a beam over 1 MW. To begin with, reinforcement of RF system would be needed. The improvement plans of the power supply system and the cavity are under consideration. The second issue is the transverse painting area extension. To reduce the loss near the injection point, it is better to have a wider painting area. As a result, we chose the value of 200 π mm-mrad. as a 1-MW operation parameter. However, we have to reduce the painting area to 150 π mm-mrad. to minimize the total loss in the 1.5-MW case. Therefore, the residual dose near the injection point would be several times higher than that of the 1-MW operation. We have continued the study to establish a better parameter to meet both requirements.

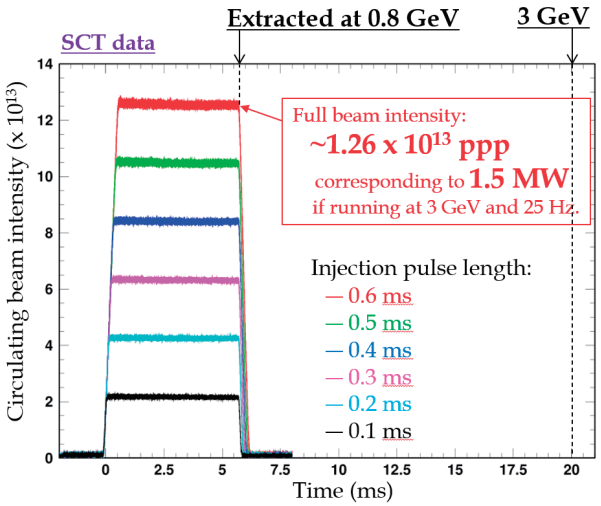

Fig. 4. Circulating beam intensity measured by the SCT for various beam intensity.

Summary

The RCS has stably delivered 4.6e13 ppp (530-kW) beam to the MLF and 6.7e13 ppp (810-kW equivalent in RCS) beam to the MR in JFY2019.

We achieved a 1-MW, 10-h continuous operation with sufficient stability of all components.

Beam studies for achieving 1.5-MW power were also carried out. Results indicated that the RCS has enough capability to accelerate a 1.5-MW beam but needs some improvements for a stable user operation. We are continuing the study to achieve more stable conditions.

MR

Overview

The 30-GeV Main Ring synchrotron (MR) of J-PARC supplies the intense 30-GeV proton beam alternatively to the neutrino experimental facility and the hadron experimental facility. The repetition rate of the MR beam operation for the former experiment is 2.48 s and 5.2 s for the latter. Thus, the 2.48-s period operation is called fast extraction (FX) mode and the 5.2-s operation is called slow extraction (SX) mode.

The design beam power for the neutrino experimental facility is 750-kW of 30-GeV proton. However, it should be increased to 1.3-MW because the Japanese government has approved the construction of a larger neutrino detector, Hyper-Kamiokande (HK), and HK needs a more intense beam. The hadron experiment requires 100-kW proton beam power at 30-GeV with extremely high stability of the magnetic fields of around 10^{-5} or less.

The MR aims to achieve the desired power and beam quality by the closed collaboration with the linac and the RCS of J-PARC. Furthermore, a stable daily beam operation for the users must be maintained regularly.

A beam availability of approximately 90% is normally demanded as the user facility. The availability at the neutrino experimental facility was 90.3% in JFY2019. However, it was 79.8% for the hadron experimental facility due to a trouble.

As mentioned in the previous annual report of J-PARC (JFY2018), the magnet in the beam transport line from the RCS to MR failed due to an interlayer short-circuit of the coil on March 18, 2019. After the temporary repair of the magnet, MR resumed the SX-mode operation for users from April 4 and a 51-kW beam was stably supplied to the hadron experiment with an efficiency of 99.5%. However, the magnet trouble recurred on April 24, 2019 and the operation was suspended. As a result, the hadron experimental period was reduced and the beam availability for the hadron experimental facility became lower.

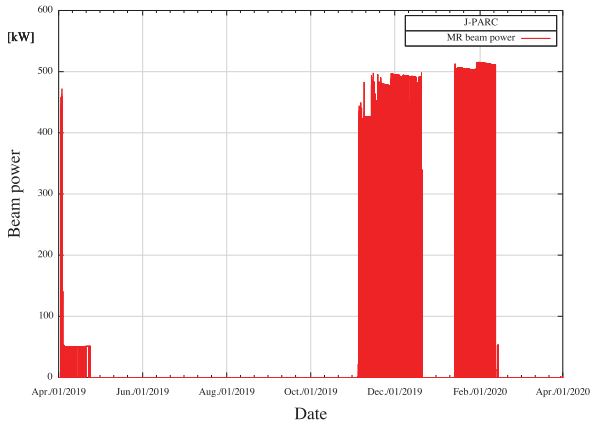

Fig. 1. MR beam power history (JFY2019)

The broken coil was replaced with a new one in September 2019. Thus, the suspended MR operation was resumed in November 2019 on schedule for the neutrino experiment. During the neutrino experiment, the stable operation of the 515-kW beam power was achieved as shown in Fig. 1.

FX-mode operation

The beam power of MR is limited mainly by the beam loss in the collimation area, where the beam losses in the ring are localized. The beam transport line from the RCS to MR and the injection area have beam collimation systems. Each system has been designed to cope with 2 kW of beam losses.

The comparison of the operation loss in JFY2018 and JFY2019 is summarized in Table 1.

Table 1. Comparison of the beam loss.

	JFY2019	JFY2018
Power	515 kW	490 kW
Repetition	2.48 sec	2.48 sec
#. of protons @ 30 GeV	2.66×10^{14} protons per pulse	2.53×10^{14} protons per pulse
Beam loss at MR	800 W [*1]	500 W
Loss at 3-50BT	100 W [*2]	50 W

[*1] Estimated by the current monitor, DCCT in the MR
[*2] Measured data of long AIC beam loss monitor (calibrated)

The operation of the 515-kW beam power with an acceptable beam loss was achieved by the tunings described below:

(1) The RCS improved the transverse emittance of the beam extracted to MR. It was done by the optimization of the beam tuning not only in the RCS but also in the linac.

(2) The renovated LLRF feedback systems suppressed the coupled bunch instabilities appearing for h=8 and h=10 effectively during acceleration as shown in Fig. 2. It has been proved that the feedback system is more effective than the feed forward one.

(3) Tune tracking during the acceleration reduced the losses in the collimation system even further.

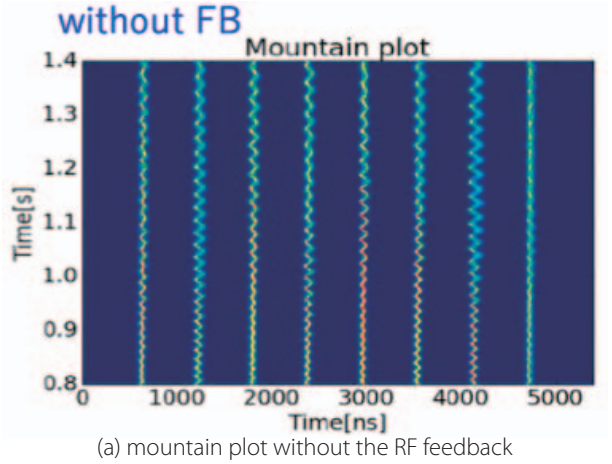

(a) mountain plot without the RF feedback

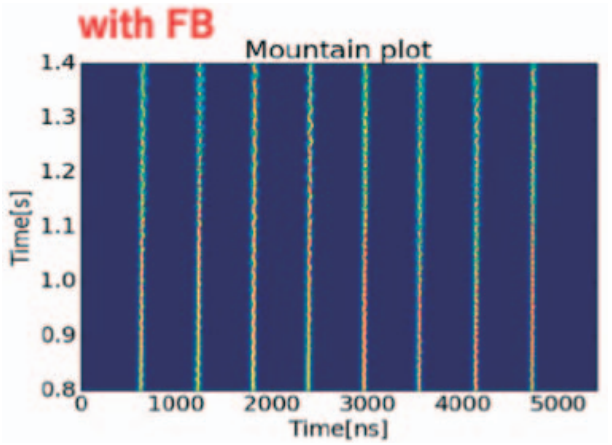

(b) mountain plot with the RF feedback

Fig. 2. Bunch oscillation of the 480-kW beam

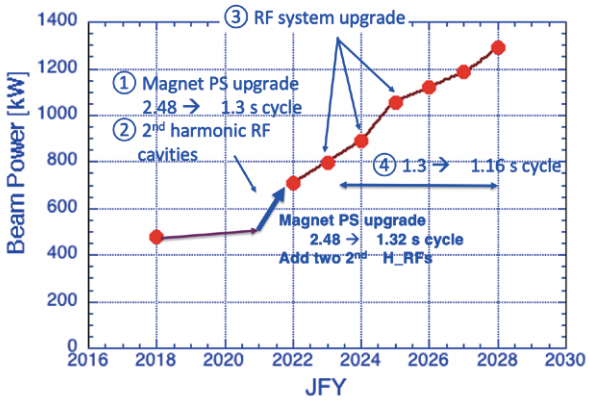

Fig. 3. MR 1.3 MW power upgrade plan

Toward the 1.3-MW operation

As mentioned above, MR is needed to accelerate the 1.3-MW beam for the HK detector. It requires not only new power converters for main dipoles and quadrupoles to increase the MR cycle of about 1.16 s, but also the improvement of the following subjects.

(1) The RF cavities of the fundamental system should be increased in number over the years from 7 to 9. Furthermore, the RF anode current must be increased by adding new power units to the existing anode power supply.

(2) Two second harmonic rf cavities are also required.

(3) The injection and extraction elements (septa and kicker) must be changed to increase their repetition rate.

(4) The collimation system in the MR injection region must be upgraded for a capacity of 3.5 kW beam loss as compared to the present 2 kW.

The revised upgrade plan for the MR beam power ramp up is shown in Fig. 3.

Summary

The magnet trouble recurred in April of JFY2019 and caused a suspension of the user operation until the fall of 2019. As a result, the beam availability of the hadron experiment dropped to almost 80%. However, the beam availability for the neutrino experiment, which was started from December 2019 after the repair of the magnet, reached more than 90%. The beam power for the FX-mode increased up to the 515 kW. The Hyper-Kamiokande project was approved by the government, so the planned beam power to be reached was increased from 750 kW to 1.3 MW. Thus, the power upgrade plan has also been revised.

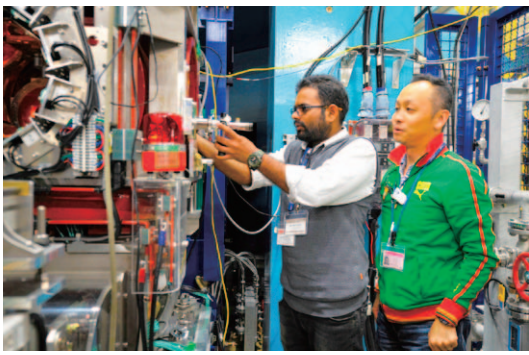

Materials and Life Science Experimental Facility

Overview

In fiscal year 2019, Materials and Life Science Experimental Facility (MLF) ran the user program for 8 months with the proton beam power of 500 kW, demonstrating the durability of the mercury target with 500 kW. Besides, the validity of the system design at the final power target was reconfirmed by a 10-hour 1-MW test on July 3. During the summer outage period, target vessel #9 was replaced with a target vessel #11 with a new design which has the coupling-free structure between the inner mercury and the surrounding outer water. The restart of the beam operation was delayed for about a month since the gas processing needed longer time than expected to reduce the radioactive gas before releasing it from the stack.

The muon rotating target system, which could suffer potential damage from a flexible joint for transferring motor rotation to the graphite disk target, served for muon production for 7 months and was replaced with a brand-new spare in the summer outage.

Due to the stable operation of the facility, the MLF was able to produce many excellent outcomes in various research fields. The construction of beam lines and development of detectors and devices advanced. However, at the end of JFY2019, the COVID-19 pandemic affected the user program mainly because the users could not travel to J-PARC. Some of those experiments were done by instrument groups and the others were carried over.

The annual meeting of industrial application at J-PARC MLF was held on July 18 and 19 at Akihabara Convention Hall. The 4th Neutron and Muon School was held from October 28 to November 2, together with the MIRAI PhD School 2019 (youngMIRAI-2019). Quantum Beam Science Festa which is an annual conference mainly for domestic users for MLF J-PARC and IMSS KEK was planned to be held in Mito on March 12

and 13, 2020, but was canceled due to COVID-19.

In the annual report, the research highlights and the technical developments in 2019 are described in detail.

Neutron Source Section

The neutron source continued its stable operation in fiscal year 2019. The beam operation of mercury target #9, which had the same design as the preceding target #8, started in late October 2018 and ended in early July 2019 with a beam power of 500 kW during almost the entire operation time. It was the first achievement to continue the user program with that high power throughout 8 months operation, which demonstrated the durability of the mercury target to be used for 500-kW power. After the user program was closed, a high-power operation study was held for 10.5 hours at 930 kW on July 3. Much operation data which need long time to reach stable value could be obtained and the validity of the system design at the power of final goal was reconfirmed.

The most important challenge to achieve 1-MW stable operation is to mitigate the pitting damages on the inner wall of the target vessel that are caused by pressure waves in mercury. This is achieved by using target vessels designed to inject micro-bubbles of helium gas into mercury for reducing the intensity of the pressure waves. The efficiency of the micro-bubble injection is monitored by measuring sound signals with a microphone. Figure 1 shows the dependency of the sound signal magnitude on the beam power. The sound signal was normalized with that in the case of 340 kW without micro-bubble injection. The broad scatterings of target #9 data from 300 kW to 600 kW are due to the change in the amount of the micro-bubble injection and proton beam profiles. All in all, the sound data of targets #8 and #9 showed a consistent trend, which confirmed the efficiency of the micro-bubble injection to reduce pressure waves.

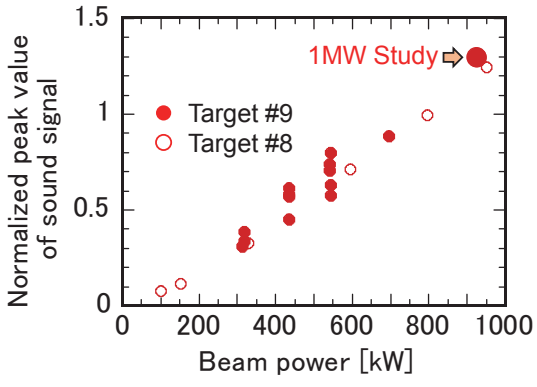

Fig. 1. Sound signal data of the target vessels at beam study.

Specimens were cut out from the forefront wall of target vessel #9 to see the inside pitting damages. As shown in Fig. 2, both the high-speed mercury flow in a narrow channel and the micro-bubbles injection into mercury are used to mitigate the pitting damages. The picture in Fig. 2 shows that the pitting damages on the outer wall that is the boundary of mercury containment were negligibly small, even after the long run of the 500-kW operation. But on the other hand, the maximum damage depth on the inner wall, which was protected by micro-bubbles, was 3.3 mm. R&D for a technology to intensify the bubbling effect to mitigate pitting damages will be continued.

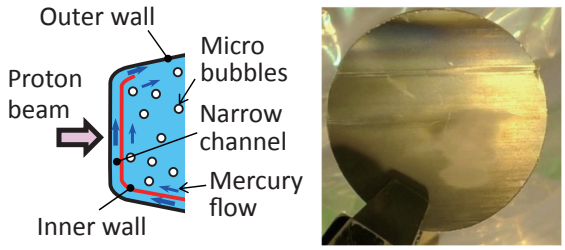

Fig. 2. Structure of the target fore-front part and the inner surface of an outer wall specimen

Target vessel #9 was replaced to a target vessel with a new design, in which the coupling-free structure between the inner mercury and the surrounding outer water shroud removes the structural cause of generating high thermal stress on the target. The stable operation of this new type of target vessel demonstrated the successful design improvement after the target vessel failure in 2015 and was one of the major milestones to achieve 1 MW power.

After the summer outage period, the restart of the beam operation was delayed for about a month since the gas processing system, which plays an important role in the target replacement procedure, needed longer time than expected for careful operation to secure the enough radiation-safety. These operation experiences will be reflected on more robust and reliable system improvements.

Neutron Science Section

1. New perspective in Neutron Science Section

Materials and Life Science Experimental Facility (MLF), one of world-leading user facilities, expands gradually its activities. Stable 500-kW beam power is being continuously supplied for the user program. And the beam test with the full power of 1 MW was performed successfully. The applied proposals have increased to a record number in 2019B. In JFY2019, the total usage by visitors reached 16,204 person-days.

To continue the constant expansion of the activities in the Neutron Science Section and the MLF, we maintain contacts not only with domestic, but also with foreign scientific facilities, such as ANSTO (Australia) and CSNS (China), in the areas of personnel, techniques, and research exchange. Also, we made efforts to communicate with the neutron scattering society through the annual meeting about industrial applications at the MLF (282 participants), the J-PARC symposium (909 participants), the 4th Neutron-Muon School (MIRAI PhD School) (41 participants), and the CROSSroads Workshop (70 participants).

2. Instrumentation kept up to date

Currently, 21 neutron instruments are operated. POLANO is the youngest instrument, which just opened for the user program. POLANO combines inelastic neutron spectroscopy with polarization analysis, and is one of the most complicated but demanded instruments, particularly for researches of systems where multiple physical degrees of freedoms are struggling or cooperating. Since the polarization devices on POLANO are still under commissioning, the proposals with unpolarized neutrons are currently available.

A brand new T0 chopper developed by the Technology Development Section debuted in the 4SEASONS spectrometer (Fig.1). A T0 chopper is a device that can eliminate unwilling gamma flash and very fast neutrons from the target source. After several years of design and development, the first prototype was installed and used for real beam experiments.

Fig. 1. Brand new T0 chopper installed into the beamline of 4SEASONS.

3. User program

In fiscal year 2019, the MLF received 326 proposals for 2019A and 444 for 2019B, of which 222 and 224 were approved, respectively. Also, 4 long-term proposals (LTP) were adjusted from 9 submissions and 17 LTPs are being executed in 2019B. Due to a one-month interruption of the beam delivery after the summer maintenance, all experiments scheduled for this term were carried over to 2020A. At the end of JFY2019, the COVID-19 pandemic affected the user program mainly because the users could not travel to J-PARC. Some of those experiments were conducted by instrument groups and the rest were carried over.

4. Scientific outcome

The research activities in neutron science at the MLF resulted in more than 150 papers and 12 press releases. Inelastic and quasielastic neutron scattering measurements using AMATERAS revealed pressure-induced large entropy changes associated with the molecular order-disorder phase transition in plastic crystals (Bing Li et al., Nature 567 (2019) 506.). These findings can be applied to novel refrigeration technology.

Y. Kawakita[1], T. Yokoo[1,2], M. Nakamura[1], S. Itoh[1,2], K. Nakajima[1] and T. Otomo[1,2]

[1]*Neutron Science Section, Materials and Life Science Division, J-PARC Center;* [2]*Institute of Materials Structure Science, High Energy Accelerator Research Organization, KEK*

Neutron Device

As one of the activities at the Neutron Instrumentation Section of the MLF Division, research and development of a scintillation neutron detector has been in progress for the neutron diffraction imaging experiments at the MLF. A two-dimensional neutron detector with a spatial resolution of about 200 μm and with a neutron-sensitive area of more than 20 × 20 mm is required for the experiment.

We introduce here our solution to provide such detectors with scintillator / wavelength shifting (WLS) fiber detector technology. To meet the requirements, the neutron-detecting head was made by using WLS fibers with a diameter of 100 μm [1]. Figure 1 shows a photograph of the prototype detector. The WLS fibers were aligned in a flat without air gap between them. Two of these fiber arrays were produced and each contained 224 fibers. They were arranged diagonally in contact with each other, creating fiber channels for the x and y directions. On top of the crossed fiber arrays, a single ^{6}Li:ZnS scintillator screen was implemented. The scintillator screen was grinded down to 0.17 mm to lower the light spread within the scintillator. It ensured a high spatial resolution of the detector. The spatial resolution, neutron detection efficiency, and gamma-ray sensitivity were estimated to be about 200 μm, 7% at 1.8Å-neutrons, and 10^{-6} at gamma-ray energy of 1.17 MeV and 1.33 MeV of a ^{60}Co source, respectively, in other experiments. The detector specifications are summarized in Table 1.

Figure 2 shows one of the time-of-flight neutron diffraction images measured at BL10 of the J-PARC MLF. Details of the experiments can be found in Ref. [2]. The coarse-grained electromagnetic steel plate was set as a sample at the distance of 13.4 m from the pulsed neutron source. The detector was located close to the sample at a distance of 7 cm from it at 90 degrees. Many diffraction spots were traced clearly in the measured images, confirming the feasibility of the detector.

In summary, a high-resolution neutron detector was developed by using scintillator / WLS fiber detector technology. The developed detector was implemented successfully into the demonstration experiment for time-of-flight neutron diffraction imaging in the J-PARC MLF. In the future, the detection efficiency will be improved by adjusting the ^{6}Li content in the scintillator and/or by equipping multiple scintillator / WLS detecting heads.

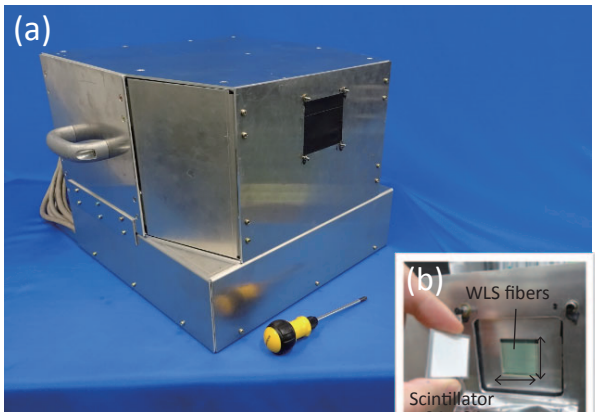

Fig. 1. (a) Photograph of the 200-μm spatial resolution scintillation detector. (b) Inside view of the neutron detecting head.

Table 1. Detector specifications

Neutron sensitive area	: 24 x 24 mm
Pixel size	: 107 x 107 μm
Number of pixels	: 50176
Spatial resolution	: 200 μm
Neutron detection efficiency	: ~ 7% @1.8Å
Gamma-ray sensitivity	: ~10^{-6} @ ^{60}Co
Physical size	: 40^{w} x 45^{d} x 30^{h} cm
Weight	: 25 kg

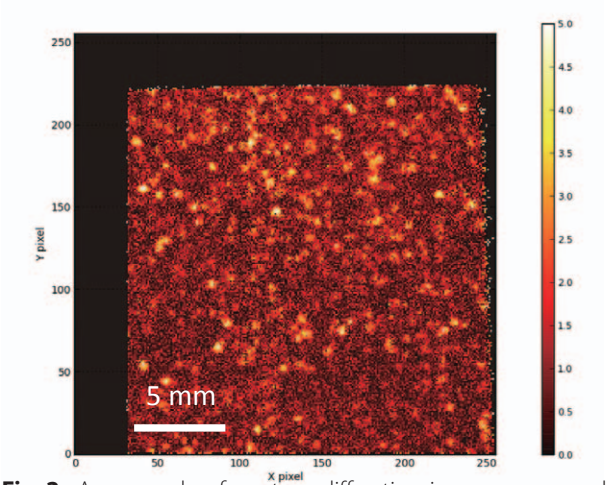

Fig. 2. An example of neutron diffraction images measured with the detector [2].

References

[1] T. Nakamura, *et al.*, 2018 IEEE NSS/MIC Conference Records, pp. 1-3, doi: 10.1109/NSSMIC.2018.8824447.

[2] T. Kawasaki, *et al.*, Physica B: Condensed Matter 551 (2018) 460.

Muon Section

Construction of electric power substation for the H-line completed

Among the muon beamlines envisioned in the original plan of the MLF, the H-line in experimental hall No. 1 has been delayed for years due to lack of funding from MEXT. Considering the situation, the J-PARC headquarters decided to provide partial support for realization of the plan. The support was primarily for the construction of a new electric power substation to cover the huge demand for electricity expected when the H-line becomes fully operational. Following the installation of cable racks, pitting of the MLF building wall, and outdoor structures in FY2017, the major civil engineering work for the substation site near the MLF building was completed by the end of March 2019 (see Fig. 1). Meanwhile, the work continued to ensure access to electricity at the substation site. During the last summer shutdown, a power panel was installed in hall No.1 at the MLF. The scaffoldings around the main carry-in door (where power cables pass through) was removed after the completion of cabling work from the new power substation to the interior of the MLF. Those who plan experiments on the H-line are now hoping to have electricity available sometime in FY2020.

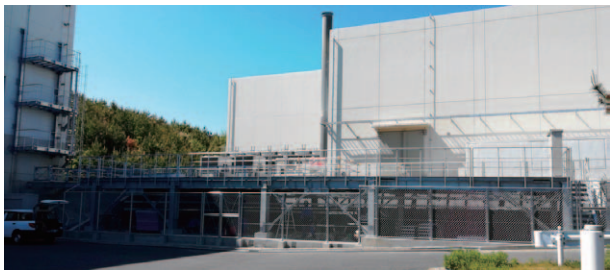

Fig. 1. Electric power substation constructed on the east side of the MLF building (left). The white wall in the back is that of the NU2 building. (Photo taken in May 2019)

Muon rotating target replaced

As reported a year ago, potential damage of a flexible joint within the muon rotating target system was suspected during the summer maintenance in FY2018. After careful assessment of the risk expected in case of joint breakdown, a multitude of safety measures were imposed to allow for restricted operation of the target until the next summer shutdown. Fortunately, the target served for muon production without trouble for about seven months, and was finally replaced with a brand-new spare during the last summer shutdown. Actually, this was an unprecedented occasion for the muon target team to replace the whole system after high-proton power operation, and utmost care was taken to minimize the risk of radiation hazard during the replacement work (Fig. 2). Now, the new target seems ready to be exposed to a 1-MW proton beam in the years to come.

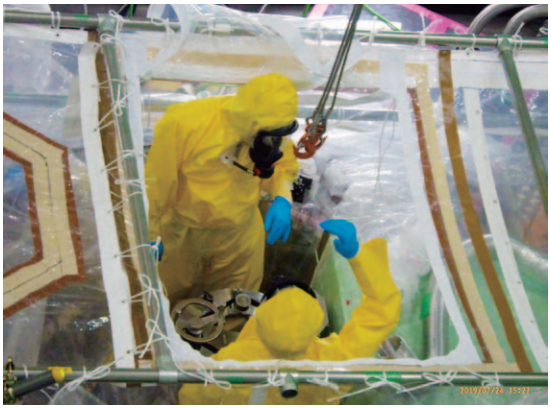

Fig. 2. A snapshot of the MUSE target team working on the target replacement assembly, where the radiation workers wearing airtight suites are in a temporary greenhouse to contain radioactive contaminants.

New forum for non-destructive element analysis with negative muons

A negative muon beam with variable incident beam energy available at the D2 area is a powerful tool for depth-resolved non-destructive element analysis by muonic X-ray emitted on negative muon capture, which is applicable to variety of objects, from industrial goods, meteorites, to archeological relics. In FY2019, some extra funding was granted from MEXT for promoting this promising technique by creating a new interdisciplinary community that unifies historians and quantum beam scientists. To exchange ideas, two workshops were held in Tokyo and Osaka with some 170 attendants, including the general public (Fig. 3). Results

Fig. 3. Group photo at the workshop on application of quantum beams in archelogy and history at the National Museum of Nature and Science, Tokyo.

of several element analysis measurements, including old Japanese coins from the end of the Muromachi period and contents of medicine bottles from the end of Edo period, were presented.

Updates from S & U-lines

The Okayama University group received a JSPS Kakenhi grant for their research project "Precision test of electroweak theory and search for new physics beyond the Standard Model by laser spectroscopy of purely leptonic atoms". This led to the application of a new S1-type research proposal to use a high-flux surface muon beam provided by MUSE, which was approved at the recent PAC meeting. As a result of discussion with the MUSE staff on how to complete this project within the limited term of the grant, it was agreed that Okayama University group was going to assume full support for the construction of a new experimental area S2 in FY2020, so that they can secure a major portion of the beamtime without affecting other user programs.

At the U-Line, continued efforts for increasing ultra-slow muon intensity were in progress. For a muonium ionization laser system, a new crystal (YSAG) for amplification of 212 nm light was successfully fabricated and its implementation in the existing system started. At U1B, a dedicated interference experimental setup was prepared as a part of the S1-type research project "Transmission Muon Microscopy" to verify the wave-particle duality of the muon.

Technology Development Section

Development of ^{3}He spin filters

We have been developing ^{3}He neutron spin filters (^{3}He-NSFs), which can polarize neutrons in a wide energy range and cover a large solid angle, in order to apply them to the neutron beamlines of J-PARC MLF. A gas-filling station to fabricate the ^{3}He-NSF cells has been constructed in 2018. The high-quality cells composed of ^{3}He-gas, potassium, and rubidium with a long relaxation time of the ^{3}He polarization were fabricated in 2019 (Fig.1). Also, a new ^{3}He pumping system using a 110 W fiber laser setup has been constructed at the J-PARC research building in 2019. The build-up time of the ^{3}He polarization with the new pumping system is about 20 hrs., which is 3 times shorter than in the systems made before the gas filling station and the new pumping system were ready.

Fig. 1. The ^{3}He spin filter cell fabricated at J-PARC.

The ^{3}He-NSF polarized by the new pumping system was installed on neutron beamline BL10 of the MLF. The neutron transmission experiment proved that a very high ^{3}He polarization of 85% could be achieved. The relaxation time of ^{3}He polarization was ~170 h at the beamline. The neutron polarization and transmission passing through the ^{3}He-NSF is shown in Fig.2. We can see that high neutron polarization is obtained for neutrons in the wide energy range.

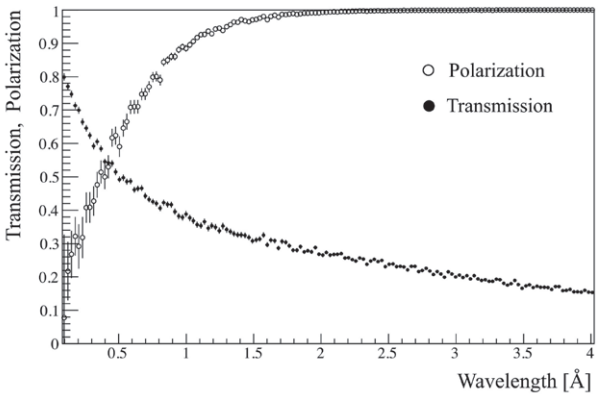

Fig. 2. The neutron wavelength dependence of the neutron polarization and transmission obtained by using the ^{3}He-NSF at BL10.

Application of ^{3}He spin filters at the MLF

The ^{3}He-NSF was first applied to a user experiment at the MLF in 2017. In 2018, no user experiment using the ^{3}He-NSF was planned. In 2019, four user experiments and a demonstration study were performed at

BL04, BL10, and BL06, respectively. The ^{3}He-NSFs were used as neutron polarizers for the experiments to study nuclear reactions at BL04 and to measure the neutron holography at BL10. Furthermore, our ^{3}He spin filter was applied to the MITZE experiment as a spin analyzer to study the dynamics of a ferrofluid at BL06 (Fig.3). In this experiment, a high ^{3}He polarization of 75% and long relaxation time of 130 h were achieved at the beamline.

Experiments with the ^{3}He-NSFs at BL15 and BL21 are also planned to experimentally determine the incoherent scattering intensity from hydrogen atoms and the magnetic scattering one from a magnetic sample. A Helmholtz coil equipped with a sample changer to keep ^{3}He polarization at the neutron beam lines has been prepared for BL15. Also, a coil, which can be installed to the vacuum chamber of BL21, is under development. The experiments are planned for JFY 2020.

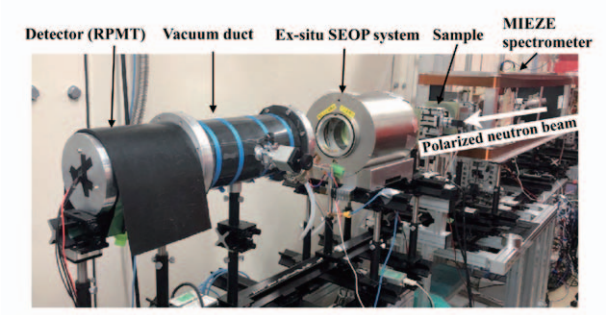

Fig. 3. The experimental setup at BL06. The ^{3}He-NSF, which was installed after the sample to analyze the scattered neutrons.

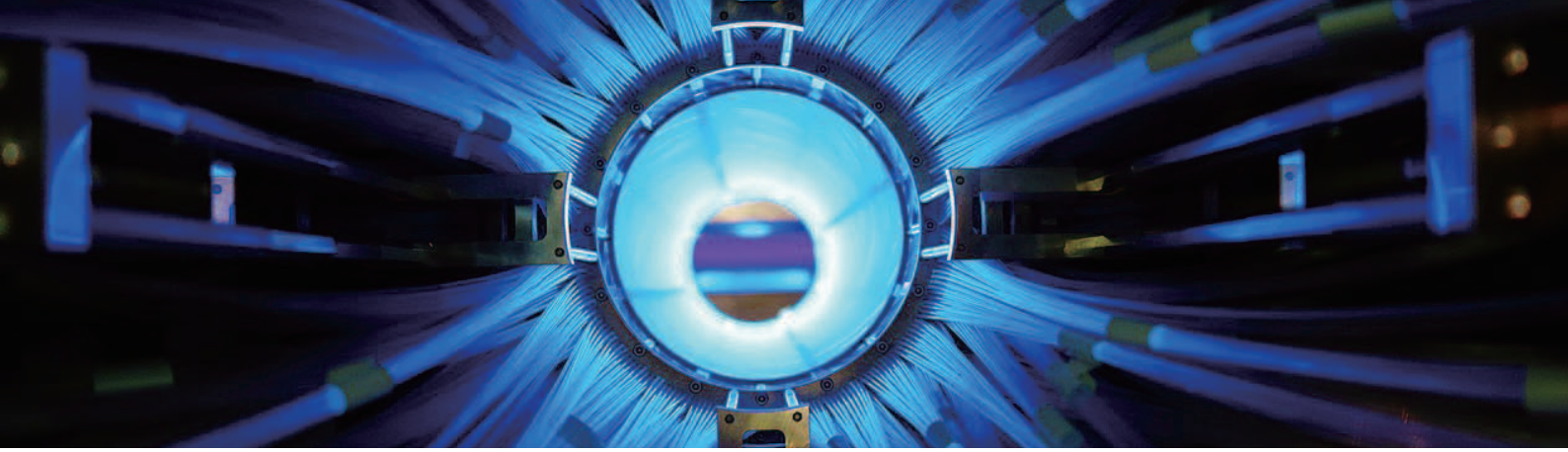

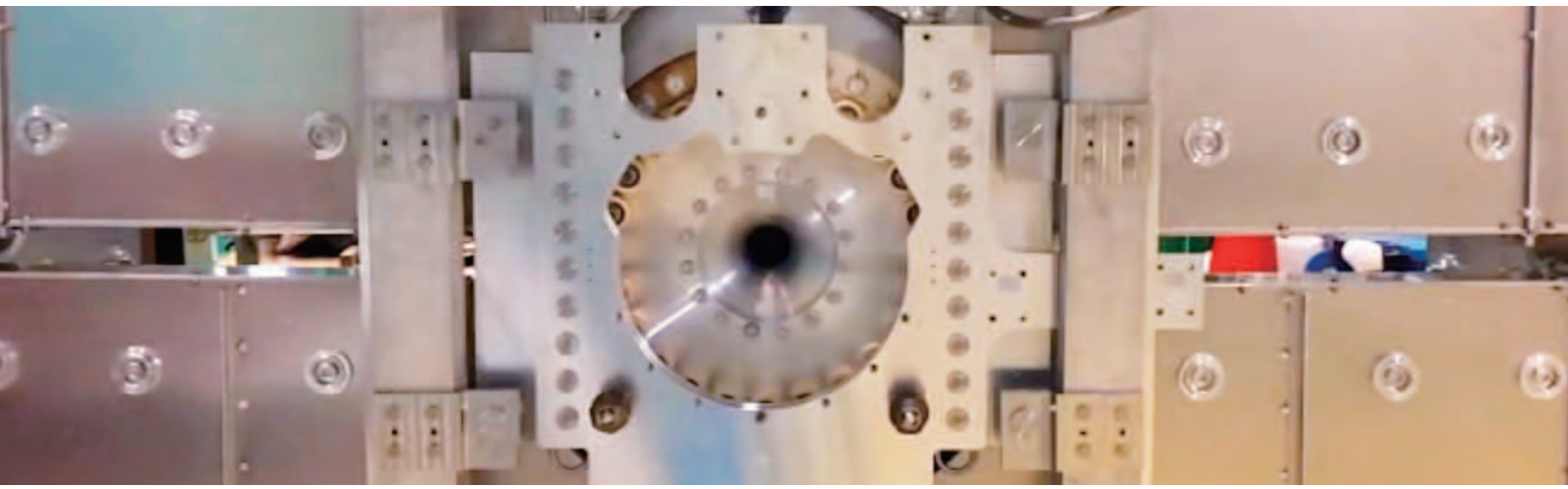

Particle and Nuclear Physics

Neutrino Experiment

The T2K run in JFY 2019 began in neutrino mode on November 5 after a shutdown lasting longer than a year and ended on February 12, 2020. The history of the accumulated protons on the target (POT) and beam power is plotted in Fig. 1. Stable operation with a beam power of 515 kW was successfully achieved. As of February 12, since the beginning of the experiment, T2K accumulated 19.9×10^{20} POT in neutrino mode in addition to the accumulation of 16.5×10^{20} POT in anti-neutrino mode.

On October 9, T2K submitted new analysis results regarding CP violation. The details of this study are described in the Research Highlight of this report. T2K published six papers in JFY 2019, including papers on neutrino-nucleus interaction cross-section measurements. Knowledge regarding such interactions is essential for reducing the systematic uncertainty of neutrino oscillation analysis.

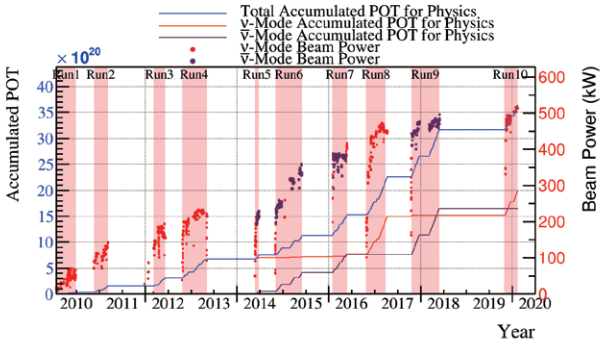

Fig. 1. History of accumulated POT and beam power since the beginning of T2K.

To improve the performance of the on-site neutrino detector ND280 and achieve beam power beyond 1 MW, extensive work has been conducted. These activities were further boosted by the approval from the government for the Hyper-Kamiokande project in January. For high-power operation, a new proton beam profile monitor is required and a detector using beam-induced gas fluorescence is under development. A prototype monitor was installed in the proton beam transport line and the signal of the beam was clearly observed, as shown in Fig. 2.

The E71 Ninja experiment, which aimed to precisely study neutrino-nucleus interactions using a hybrid emulsion detector at the near-detector hall, yielded its first data. The development of emulsion films has been completed and combined analysis using downstream detectors is underway.

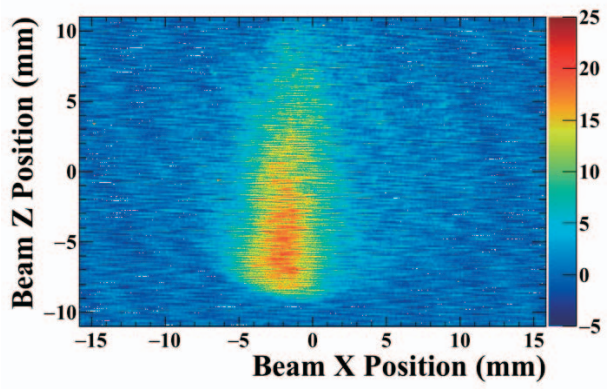

Fig. 2. Fluorescence light image generated by the proton beam passing through nitrogen gas injected into the beamline. The vertical axis is the beam direction, while the horizontal axis is the horizontal beam position

Hadron Experimental Facility

The Hadron Experimental Facility (HEF) of J-PARC was developed for fixed-target particle and nuclear physics experiments with secondary hadron beams produced by a slowly extracted (SX) 30-GeV proton beam from the Main Ring (MR) accelerator. In JFY 2019, the SX beam operation began in April with a beam power of 51 kW and a repetition cycle of 5.20 s. The operation was stopped abruptly after only 356 hours by a water leak in a magnet in the transport line from the RCS to the MR, marking the start of an unforeseen long shutdown.

To utilize this shutdown, the beamlines were upgraded earlier than planned with the goal of resuming beam operation in the spring of 2020. A new production target for secondary particles was installed in November 2019 (Figs. 3 and 4). This target has a cooling structure similar to that of the previous target, but the cooling efficiency is improved by doubling the number of copper cooling blocks. This should make it possible to receive a primary proton beam power as high as 95 kW on the target with a 5.2 s repetition cycle.

The construction of a new primary beamline (B-line) was completed in January of 2020 (Fig. 5). This beamline transports a small fraction of the primary protons to the hall, where 30 GeV protons can be used in experiments. In the near future, this beamline will also deliver 8 GeV beams for the COMET experiment.

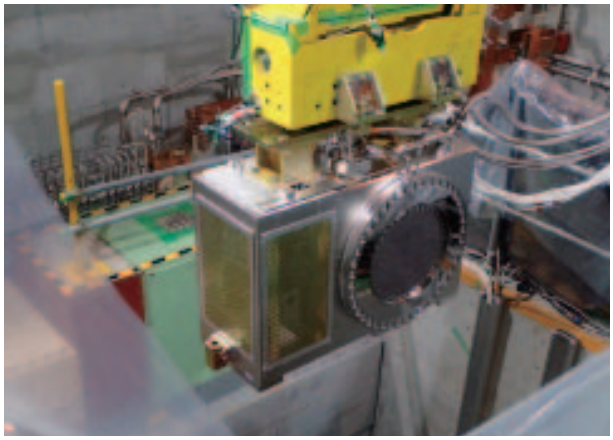

Fig. 3. A He-filled chamber containing the new production target, which is being lifted for installation.

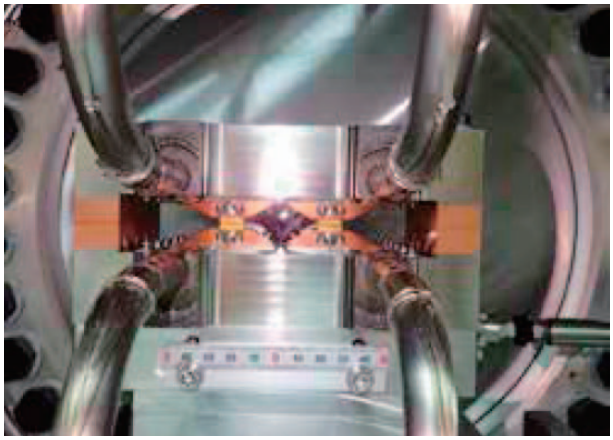

Fig. 4. A new production target in the chamber with two sets of gold targets cooled by rectangular copper blocks from the top and bottom.

Fig. 5. The newly constructed B-line and a spectrometer (left end) for the new E16 experiment.

Strangeness/Hadron Physics Experiments

With a short beam time in April, the E40 experiment at the K1.8 beamline, which is the key experiment to understanding the origin of the repulsive core of the nuclear force, collected approximately half of the planned Σ^+ p scattering data. Pilot data on kaonic hydrogen atom X-ray were also collected by the E57 experiment at the K1.8BR beamline in order to test the feasibility of the measurement for the kaonic deuterium atom.

A new experiment (E16) was designed to measure the mass spectra of di-electron pairs around the mass region of the ϕ vector meson in proton-nucleus interactions. A novel spectrometer system for the corresponding "Run-0" was constructed at the B-line and made ready for commissioning.

A review paper that describes the results of the strangeness/hadron physics experiments, as well as the physics goals of the ongoing and approved experiments, has been published.

Kaon Decay Experiment

The KOTO experiment was designed to study the decay of a long-lived neutral kaon into a neutral π meson (π^0) and a pair of neutrinos. This decay breaks the CP symmetry directly and the branching ratio can be accurately predicted by the SM as $(3.0 \pm 0.3) \times 10^{-11}$. The detection of this decay is so challenging because only two photons from π^0 are observable and nobody has succeeded in the observation. By examining this type of ultra-rare decay, a new source of CP symmetry breaking that can explain the matter–antimatter asymmetry in the universe may be revealed.

In JFY 2019, the KOTO experiment continued to accumulate more physics data and confirmed the upgrades to the calorimeter readout. Analysis of the data collected from JFY 2016 to JFY 2018 was reported at the International Conference on Kaon Physics 2019 (Perugia, Italy, September 2019). Four candidate events were observed in the signal region and their properties and origins are currently under investigation.

Muon Experiments

COMET, which is a J-PARC E21 experiment, aims to identify muon-to-electron conversion with a sensitivity better than 10^{-14}. Intensive research and development were conducted in 2019. A cylindrical drift chamber was successfully tested using cosmic-ray muons with a full setup of readout electronics, including a parallel readout scheme. The construction of a straw tube tracker and the mass production of lutetium yttrium orthosilicate for the electron calorimeter are ongoing.

The construction of a capture solenoid (CS), which

will be used to collect and transport pions/muons produced by the COMET primary proton target, as well as the preparation of a cryogenic system, is progressing according to schedule. The superconducting wire winding of all necessary coils for the CS was completed in 2019. The assembly and installation of these coils into a cryostat will occur in 2020. The COMET collaboration has published a detailed design for this experiment.

The E34 collaboration is preparing for precision measurements of the anomalous magnetic moment and EDM of muons. This collaboration has published the technical design of their experiment. A task force for the H-line building extension was formed and has planned to proceed with construction. Experimental technology and components have also been developed. Important achievements in the development of a silicon strip detector module, a buncher cavity, diagnostic tools for muon accelerators, and an NMR probes for absolute magnetic field measurements have been published in various journals.

Highlight: T2K data place the strongest constraint on the leptonic CP violating phase in neutrino oscillation

The matter-antimatter imbalance of the observable universe is one of the biggest mysteries in physics. Violation of the charge-conjugation and parity-reversal (CP) symmetry is required to explain the imbalance. Although the CP violation has been observed in the quark sector, it is too small to ex- plain the observed imbalance in the universe [1]. However, the CP violation in the neutrino sector may be up to three orders of magnitude larger and could therefore help solve the mystery.

The neutrino is an elementary particle that interacts only via the weak and gravitational forces. There are three types of neutrinos - electron, muon, and tau neutrinos; they are named for their charged partners. Neutrinos have an interesting property: as they travel, they can change from one type to another in a phenomenon known as neutrino oscillation. The oscillation probability is expressed by the three mixing angles (θ_{12}, θ_{23}, θ_{13}), two mass differences (Δm^2_{21}, Δm^2_{32}), and the CP phase (δ_{CP}) in the standard parameterization.

The Tokai-to-Kamioka (T2K) experiment [2] is a long baseline neutrino experiment built to reveal the nature of neutrino oscillations. Figure 1 shows the experimental setup for T2K. A high-intensity beam of 30 GeV protons is produced in J-PARC, Tokai.

The beam is exposed to a graphite target to produce charged pions and kaons, which decay in flight mostly to muon neutrinos after focusing by three magnetic horns. The beam can be switched between neutrino and antineutrino modes by changing the polarity of the horn current. The unoscillated neutrino flux is measured by the near detectors placed at 280 m from the target. Neutrino oscillation effects are measured at the far detector, Super-Kamiokande, with a 295 km baseline. The T2K experiment began data-taking in January 2010, and discovered electron neutrino appearance in muon neutrino beam in 2013 [3], which enabled us to measure the δ_{CP} in the neutrino oscillation. The parameter δ_{CP} can take any values between -180° and 180°. If it equals 0° or 180°, the neutrinos and antineutrinos change their types in the same way during oscillation in a vacuum. Otherwise, the δ_{CP} parameter has a value that enhances or suppresses the oscillations of neutrinos or antineutrinos, breaking the CP symmetry. Currently, the T2K experiment is aiming to measure the unknown δ_{CP}. Measurements of the neutrino CP phase provide new

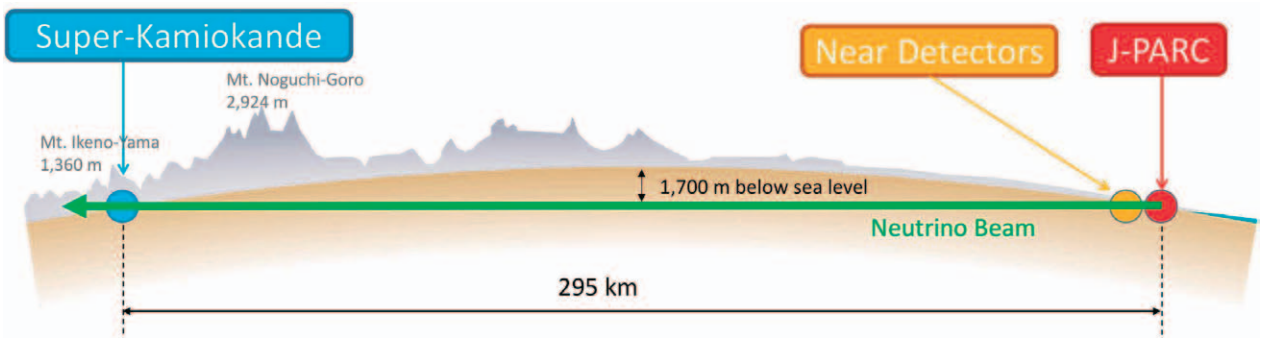

Fig. 1. Experimental setup of T2K

knowledge on the nature of neutrinos as well as a hint of matter-antimatter imbalance of the universe.

The T2K collaboration released new results [4], analyzing data with 1.49×10^{21} and 1.64×10^{21} pro- tons from the accelerator for neutrino and antineutrino modes, respectively. The observed number of electron (anti)neutrino events as a function of reconstructed neutrino energy is shown in Fig. 2. T2K observed 90 electron neutrino candidates and 15 electron antineutrino candidates. T2K is expected to observe 82 electron neutrino events compared to 17 electron antineutrino events for maximal neutrino enhancement at δ_{CP} = -90˚, and 56 electron neutrino events compared to 22 electron antineutrino events for maximal antineutrino enhancement at $\delta_{CP} = 90$˚.

The T2K data are most compatible with a value close to $\delta_{CP} = -90$˚ which significantly enhances the oscillation probability of neutrinos in the T2K experiment. Using this data, T2K evaluates confidence intervals for the δ_{CP}. The disfavored region at the 99.7% (3σ) confidence level is -2˚ to 165˚ as illustrated in Fig. 3. This result represents the strongest constraint on δ_{CP} to date and an important step toward knowing whether or not neutrinos and antineutrinos behave differently. The values of 0˚ and 180˚ are disfavored at the 95% confidence level, which is consistent with previous results in 2018 [5], indicating that CP symmetry may be violated in neutrino oscillations. This result has been published in the journal, Nature in April 2020 [6]. While this result shows a strong preference for enhancement of the neutrino rate in T2K, it is not yet clear whether the CP symmetry is violated or not. To further improve the experimental sensitivity, we will upgrade the near detector to reduce systematic errors, and J-PARC will increase the beam intensity by upgrading the accelerator and beamline. T2K will then continue to take high-quality data with the upgraded detector and beamline.

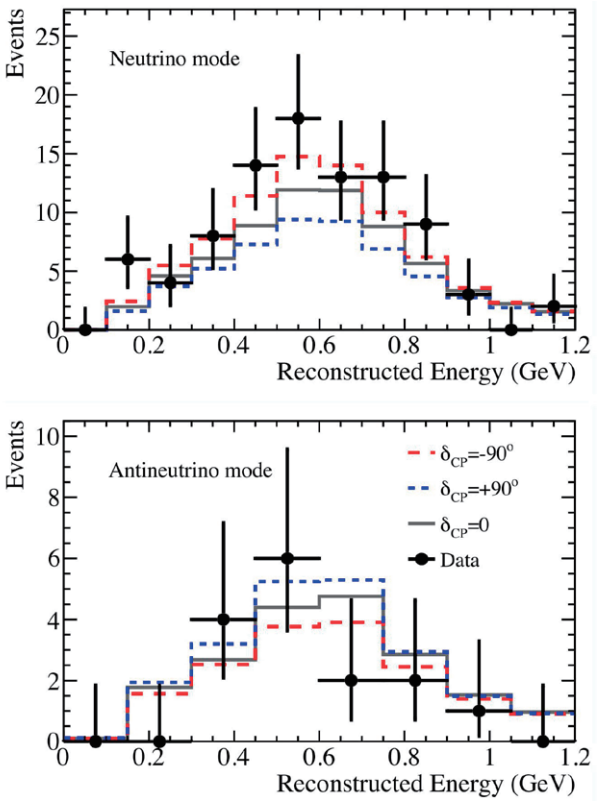

Fig. 2. Observed electron (anti) neutrino candidate events with predictions for different δ_{CP} values. T2K data is most compatible with a value close to δ_{CP} = -90˚ (red, long dashed).

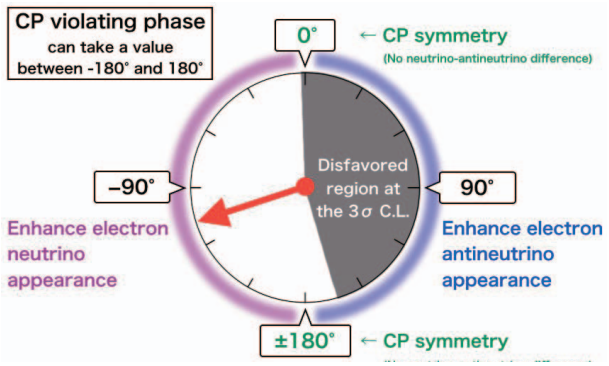

Fig. 3. Constraint on the neutrino CP phase. About half of the possible values are disfavored at the 99.7% (3σ) confidence level.

Reference

[1] M. Tanabashi *et al*. (Particle Data Group), Phys. Rev. D **98**, 030001 (2018).

[2] K. Abe *et al*. (T2K Collaboration), Nucl. In- strum. Meth. A **659**, 106 (2011).

[3] K. Abe *et al*. (T2K Collaboration), Phys. Rev. Lett. **112**, 061802 (2013).

[4] K. Abe *et al*. (T2K Collaboration), arXiv:1910.03887 (2019).

[5] K. Abe *et al*. (T2K Collaboration), Phys. Rev.Lett. **121**, 171802 (2018).

[6] K. Abe *et al*. (T2K Collaboration), Nature **580**, 339 (2020).

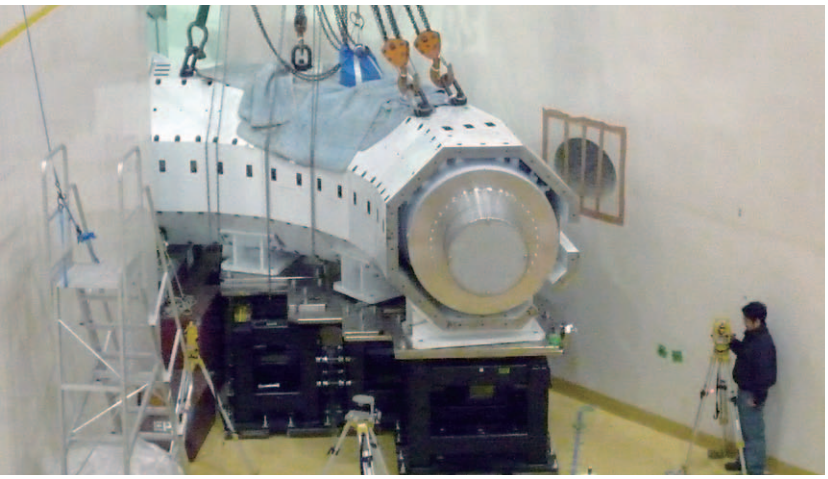

Cryogenics Section

Overview

The Cryogenics Section supports scientific activities in applied superconductivity and cryogenic engineering, carried out at J-PARC. It also supplies cryogen of liquid helium and liquid nitrogen. The support work includes maintainance and operation of the superconducting magnet systems for the T2K neutrino beamline and the muon beamlines at the Materials and Life Science Experimental Facility (MLF) and construction of the magnet systems at the Hadron Experimental Facility (HEF). It also actively conducts R&D works for future projects at J-PARC.

Cryogen Supply and Technical Support

The Cryogenics Section provides liquid helium cryogen for physics experiments at J-PARC. The used helium is recycled by the helium gas recovery facility at the Cryogenics Section. Figure 1 summarizes the liquid helium supply in FY2019.

Liquid nitrogen was also supplied to the users for their convenience. Its amount in FY2019 is summarized in Fig. 2. Liquid nitrogen has been regularly provided to the Radiation Safety Section for operation of a gas chromatograph. It was also supplied to the users in the MLF and the HEF.

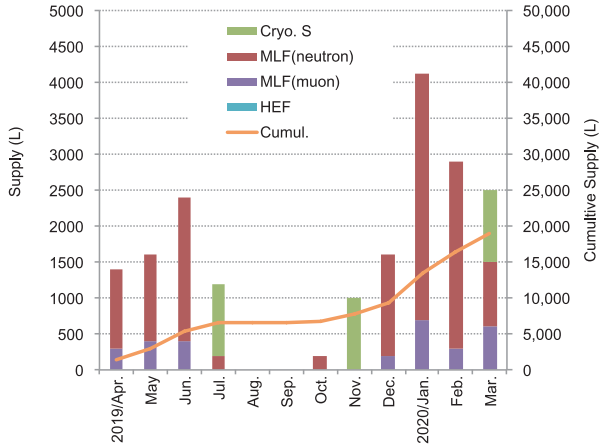

Fig. 1. Liquid helium supply at J-PARC from April 2019 to March 2020.

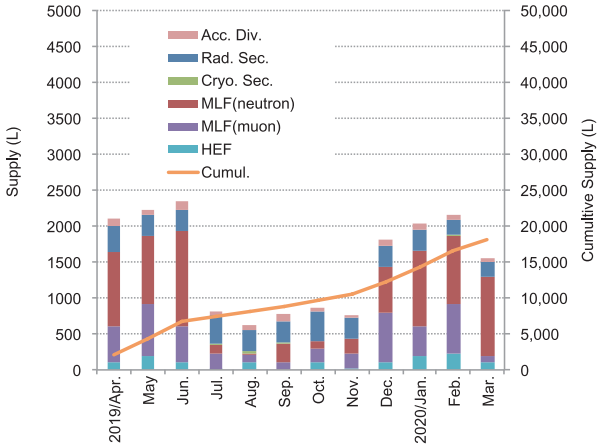

Fig. 2. Liquid nitrogen supply at J-PARC from April 2019 to March 2020.

Superconducting Magnet System for T2K

The superconducting magnet system for the T2K experiment operated during the periods shown in Table 1. The system worked well without disturbing the beam time. The operation time was only 3 months in the winter and regular maintenance works were carried out in the summer. Figure 3 summarizes the incidents in the refrigeration system from FY2009 on. The system was suspended only in its early period due to problems in the hardware and control parameters. Although a few problems with hardware parts occurred in the recent years, the troubles had been resolved without interrupting the operation. The system was very stable in FY2019 as well.

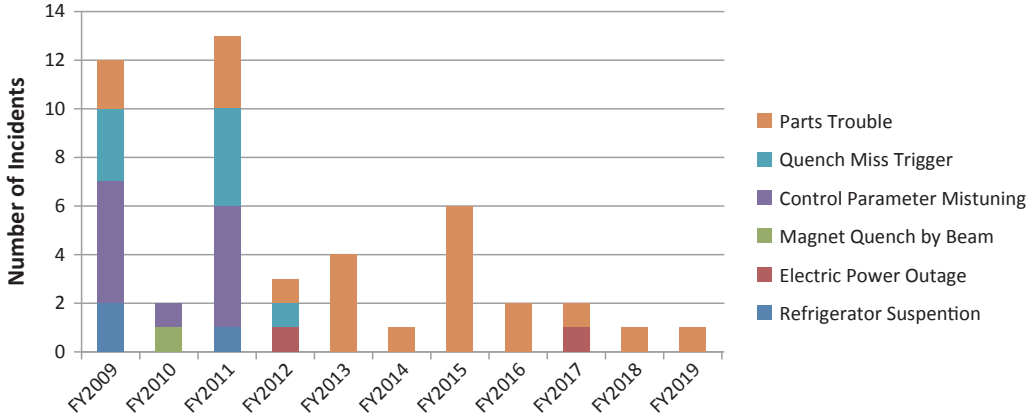

Fig. 3. Summary of incidents in the Refrigerator System for T2K.

Table 1. Operation history of the T2K superconducting magnet system.

	2019 Apr.	May	June	Jul.	Aug.	Sep.	Oct.	Nov.	Dec.	2020 Jan.	Feb.	Mar.
Operation							10/18-12/21			1/13-2/12		
Maintenance					←	→						

Superconducting Magnet Systems at the MLF

The Cryogenic Section contributes to the operation and maintenance of the superconducting magnet systems at the Muon Science Facility (MUSE) in the MLF. The superconducting solenoid in the Decay Muon Line (D-line) was operated from January to the end of June 2019. Annual maintenance, such as exchange of the oil separation filter, safety valve maintenance and so on, was performed from July to October. The cryogenic operation was restarted on December 2. This was significantly behind the schedule since the exchange work of the mercury target took longer than expected. It was stopped on December 19 for the New Year holidays. After the update of the computers for the cryogenic control system, it resumed on January 10. There was no serious problem in the cryogenic system for D-line magnets in FY2019.

A reused superconducting solenoid (Fig. 4), which had originally been developed for a cosmic ray observation, was operated in BL05 for measurement of neutron life time. The Cryogenic Section prepared equipment for cooling with liquid helium and for supplying excitation current. The first beam operation was carried out for two weeks and the solenoid magnet system worked well. Improved equipment must be developed for the future long-term operation.

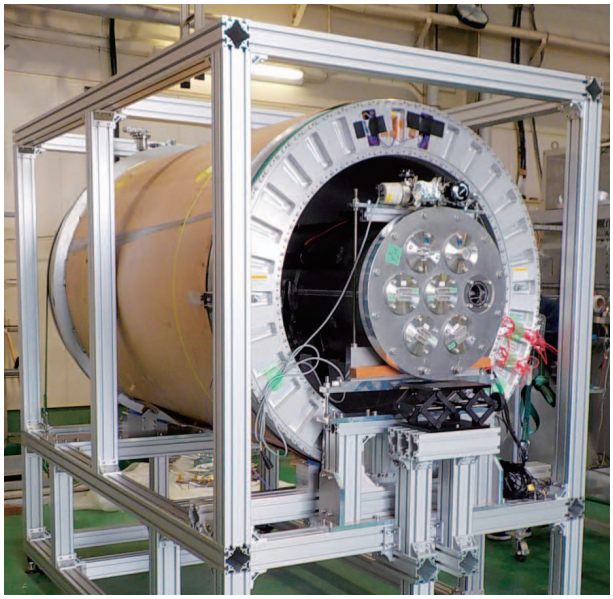

Fig. 4. Superconducting solenoid magnet developed for cosmic ray observation, reused at MLF BL5.

Superconducting Magnet Systems at the HEF

The COMET experiment is under construction in the Hadron South Experimental Hall (HDS) of the Hadron Experimental Facility (HEF). The Cryogenics Section was involved in the construction of the cryogenic system and superconducting magnets. Production of the superconducting solenoid magnet for the muon source is in progress. Superconducting coils of the Pion Capture Solenoid (PCS) have been manufactured using radiation-resistant material and the detailed design to assemble the cryostat was improved.

The magnets are designed to be cooled by a two-phase flow of liquid helium which is supplied by a helium refrigeration system built in HDS. The cooling capacity of the helium refrigerator has been measured to be 140 W at 4.5 K in the case of 500 W heat load on shield gas. Currently, transfer lines connecting the magnets to the refrigerator and the power supply are under construction.

The transfer line from the current lead system to the Muon Transport Solenoid (MTS) was installed in the HDS in FY2018. The cooling pipe in the transfer line is made of stainless steel. The transfer line was connected

to the small cryostat for protection diodes, which is separated from the cryostat of MTS magnet. Since the cooling port of MTS has an aluminum cooling pipe, an aluminum pipe should be connected from the diode to the magnet. Connecting the aluminum pipe, which ensures leak-free conditions in cryogenic temperature with thermal shocks and thermal cycles, requires a great deal of skill. Therefore, an automatic welding machine is under development (Fig. 5) to perform welding with high reliability and high yield, while optimizing welding conditions for manual welding. Construction of the control system and tuning the control parameters will be performed.

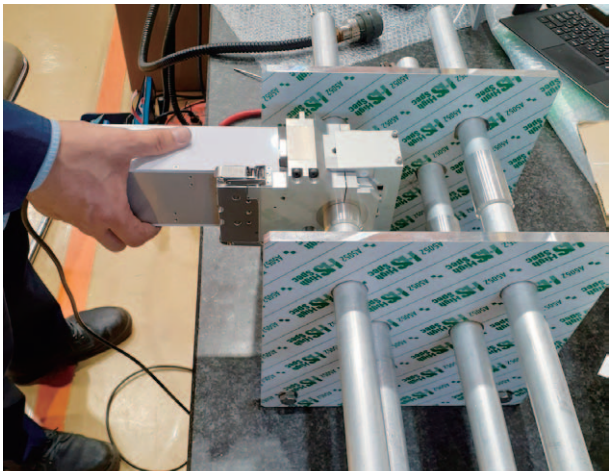

Fig. 5. Automatic welding machine developed for welding cooling pipes.

R&D for the Future Projects at J-PARC

The g-2/EDM project aims for the precise measurement of the anomalous magnetic moment and the electric dipole moment of muons. This experiment was proposed at the MUSE H-Line. A superconducting solenoid with a high field homogeneity, better than 1 ppm locally, plays a very important role as a muon storage ring. The temperature effect of iron yoke on the error field was evaluated in detail. Thermal expansion and magnetization change due to temperature change of 1 K causes an error field of about 1 ppm, which is larger than the expectation obtained with primitive calculation of less than 0.1 ppm. The simulation study shows that the error field could be reduced to 0.2 ppm/K by applying a bypass circuit. It means that the temperature needs to be controlled within 0.5 K, which is an acceptable value.

A muonium hyperfine structure measurement, called MuSEUM experiment, has been proposed for the same beam line as the g-2/EDM project. In the experiment, the energy state transition in muonium will be observed under a static magnetic field with local homogeneity of 1 ppm. A standard NMR probe to determine the absolute magnetic field is being developed to calibrate other probes. Cross-calibration tests in the collaborative framework between the USA and Japan have been in progress since 2017. The analyses of the tests at 1.45 T and 1.7 T, which were conducted in January and February 2019, are still in progress. The new probe for 3.0 T was tested at the ANL in February 2020 (Fig. 6) to verify the performance, but the cross calibration test was postponed due to the COVID-19 situation.

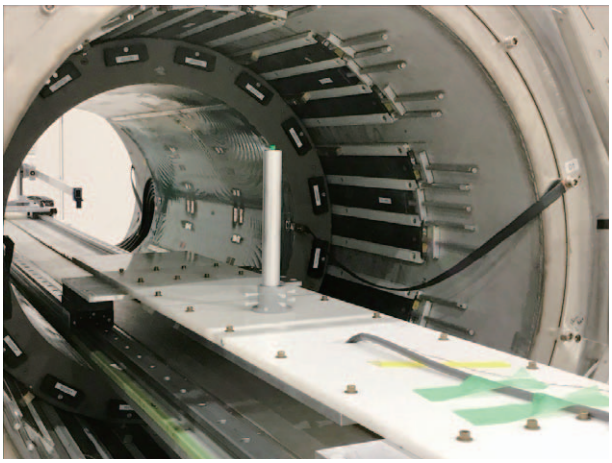

Fig. 6. Newly developed probe for 3.0 T tested at the ANL.

Information System

Overview

The Information System Section plans, designs, manages and operates the network infrastructure of J-PARC and also provides support to ensure its information security. In terms of computing, until now, J-PARC has owed its major computer resource for analyzing and storing data from neutrinos, nuclear physics and MLF experiments to the KEK central computer system. The section connects the J-PARC network to the KEK central computing system directory and helps the users to utilize the system effectively.

Status of Networking

Since 2002, the J-PARC network infrastructure, called JLAN, has been operated independently from KEK LAN and JAEA LAN in terms of logical structure and operational policy. In 2019, the total number of hosts on JLAN exceeded 5,000 and the number has decreased to 99.8% from the last year. The growth curve of edge switches, wireless LAN access points and hosts (servers and PCs) connected to JLAN are shown in Fig. 1.

In April 2016, the National Institute of Informatics (NII) upgraded SINET (Japan Science Information Network https://www.sinet.ad.jp) from version 4 to 5. SINET is not only a gateway from JLAN to the internet but also an important connection between Tokai and KEK Tsukuba site in J-PARC.

Figures 2 and 3 show the network utilization of the internet from/to JLAN. Since the bandwidth capacity for the internet through the SINET is 10 Gbps, it is clear that there is enough space for additional activity. Figures 4 and 5 show the statistics of data transfer between the Tokai site and the Tsukuba site. The network bandwidth capacity between the two sites is 10 Gbps. This shows that the usage level has been approaching a half of it, especially during the period when the Hadron facility was running. In addition to the current bandwidth, the upgrade offers a future option of 20 Gbps for both of internet and Tokai-Tsukuba connections, if J-PARC network can be adapted.

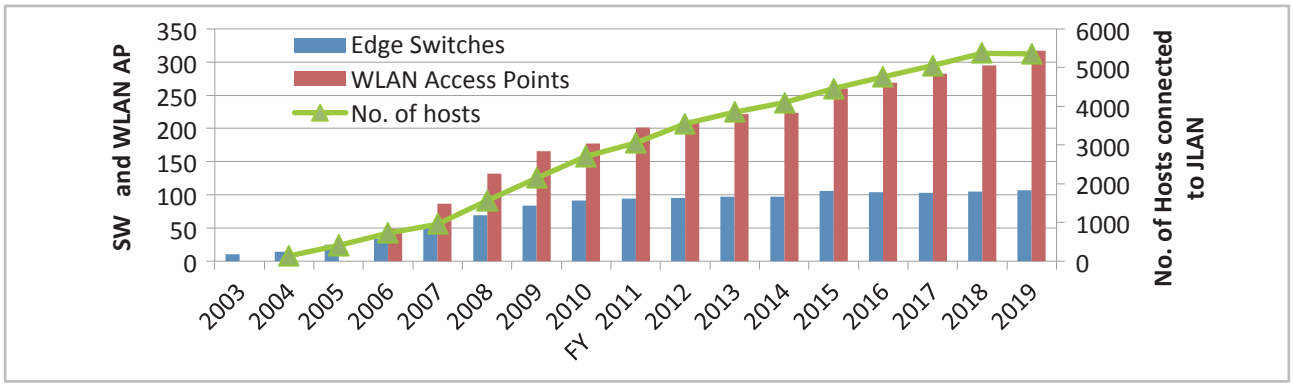

Fig. 1. Number of hosts, edge SW and wireless AP on JLAN.

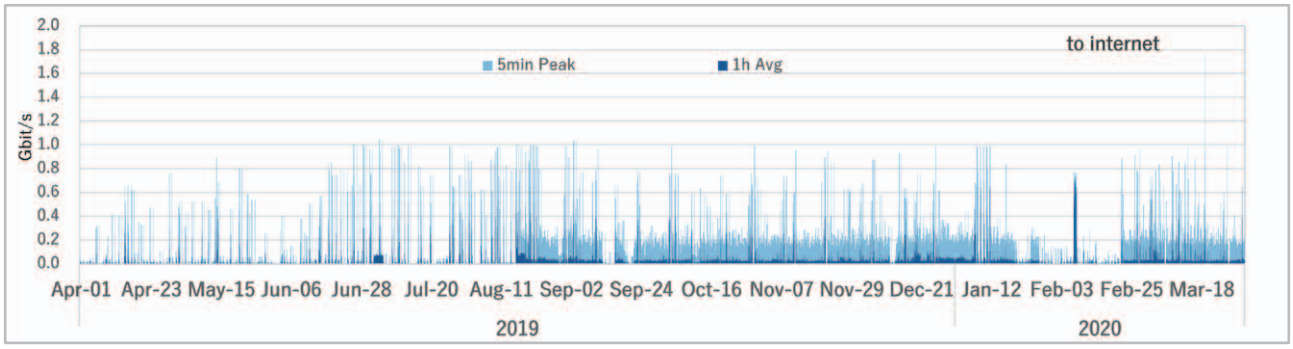

Fig. 2. Network traffic from JLAN to the internet.
(1 hour average and 5 minutes peak value)

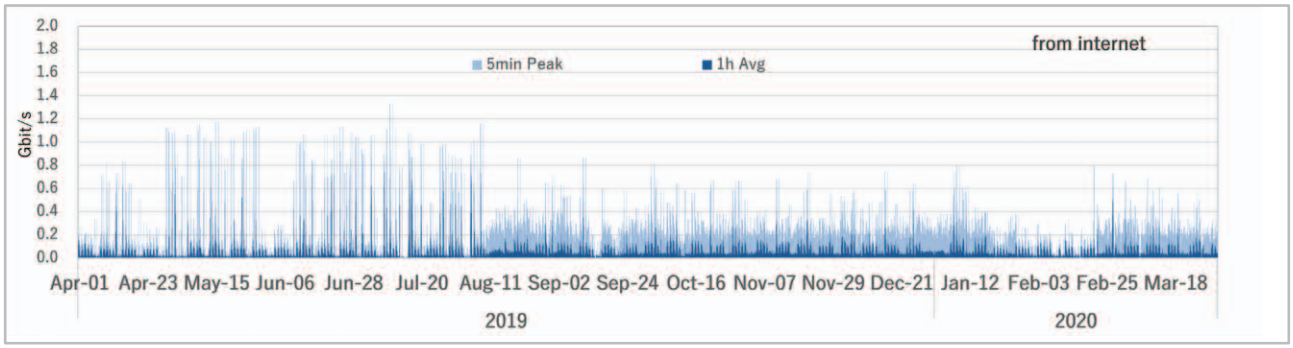

Fig. 3. Network traffic from the internet to JLAN.

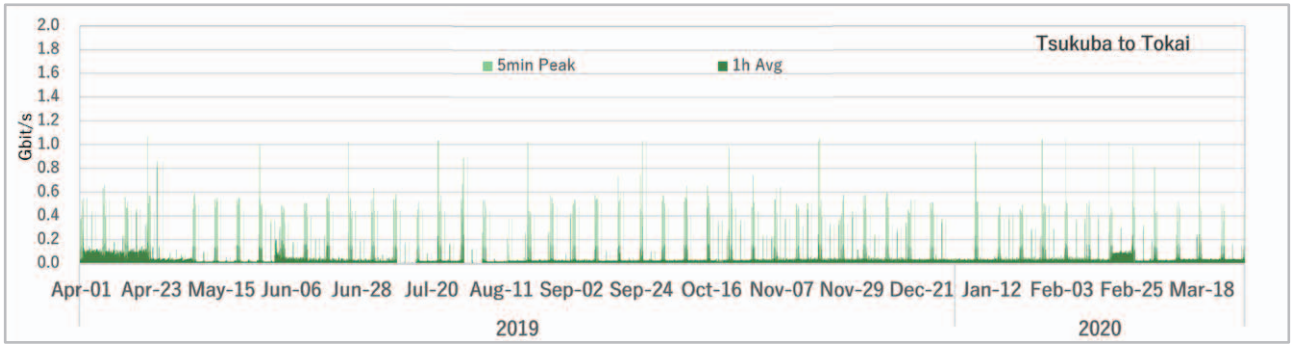

Fig. 4. Network traffic from the Tsukuba site to the Tokai site.

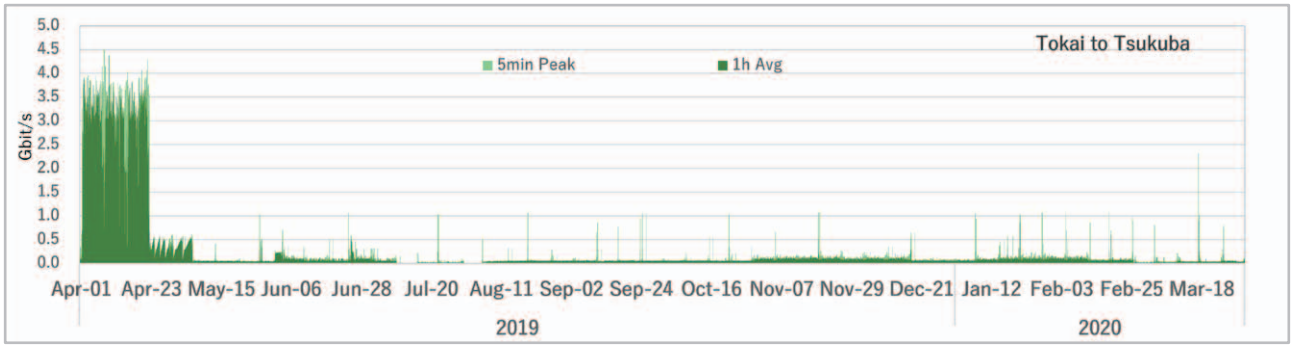

Fig. 5. Network traffic from the Tokai site to the Tsukuba site.

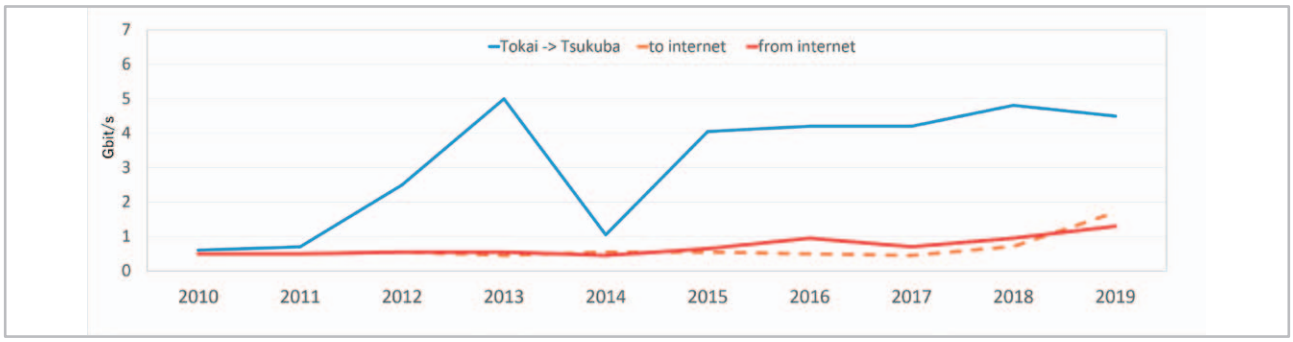

Fig. 6. Peak network traffic for the recent years.

Internet Connection Services for Visitors and Public Users of J-PARC

Since 2009, J-PARC has offered a Guest network (GWLAN) service, which is a wireless internet connection service for short-term visitors, available in almost all J-PARC buildings. In the end of 2014, additional network service called User LAN has started. To use the GWLAN, users are required to receive a password at the J-PARC Users Office beforehand, while in the User LAN they are authenticated by the same ID and password for the User Support System, which is also used for dormitory reservation and so on. From March 2016, a new service called "eduroam" has been started. The eduroam (https://www.eduroam.org/) is a secure roaming access service developed for the international research and education community and mutually used among a huge number of research institutes, universities, and other institutions around the world. The eduroam service will be a convenient third option of internet connection service for J-PARC visitors. Figure 7 shows this FY usage statistics of GWLAN, User LAN and the newly introduced eduroam service.

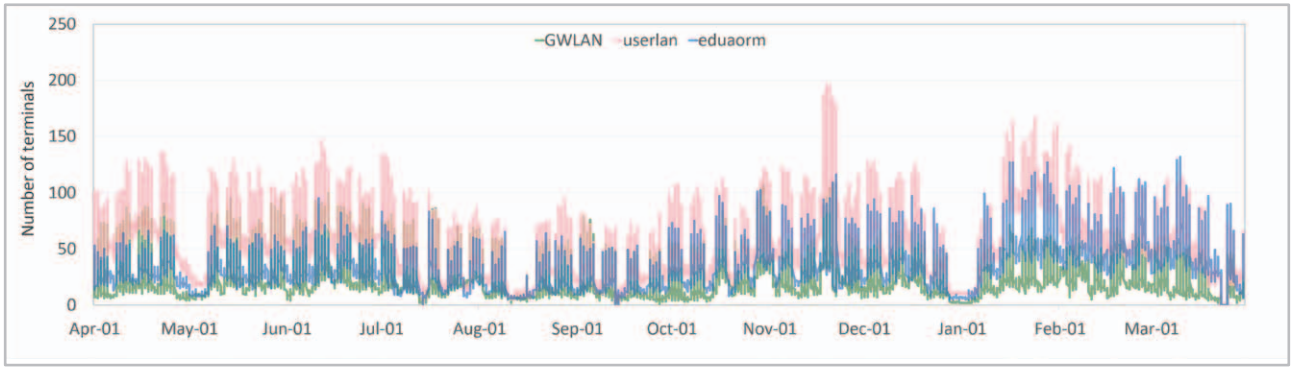

Fig. 7. Usage trends of GWLAN, User LAN and eduroam.

Status of Computing

Since J-PARC does not have computing resources for physics analysis, starting from 2009, the KEK central computing system (KEKCC) at the KEK Tsukuba campus has been mainly used for that purpose. At the Neutrino (T2K), Hadron and Neutron (MLF) experiments, the data taken in J-PARC are temporarily saved at their facilities and then promptly transferred, stored, and analyzed at the system in Tsukuba. The storage of the system is also be utilized as a permanent data archive for their data.

The second upgrade of the system was completed in 2016, and the computing resources assigned to J-PARC are shown in Table 1. The system will be upgraded in 2020. Figure 8-10 show the utilization statistics of the computing resources in FY2019. The main users who used the CPU and storage constantly were from the Hadron experiment and the Neutrino groups. The MLF group also started to store data to tapes on the system.

Table 1. Assigned computing resources to J-PARC activities in the KEKCC.

CPU (Intel Xeon E5-2697v3)	4700 cores
RAID Disk (GPFS)	4.5 Peta Bytes
Tape (HSM)	27 Peta Bytes

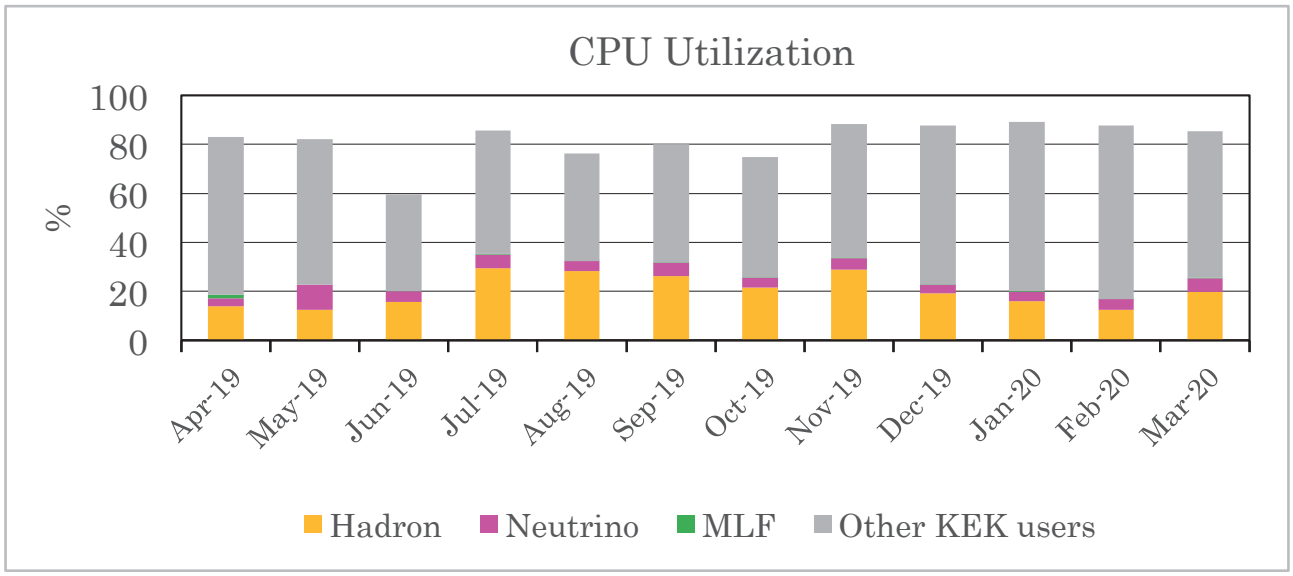

Fig. 8. CPU usage statistics of KEKCC in FY2019.

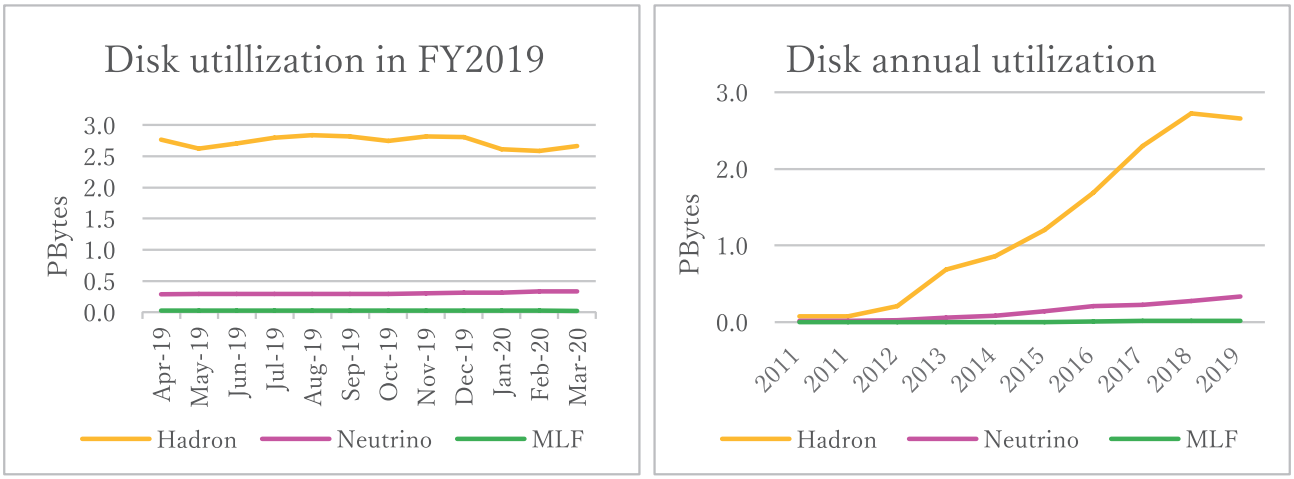

Fig. 9. Disk usage statistics (Left: trend for this FY year; Right: annual trend).

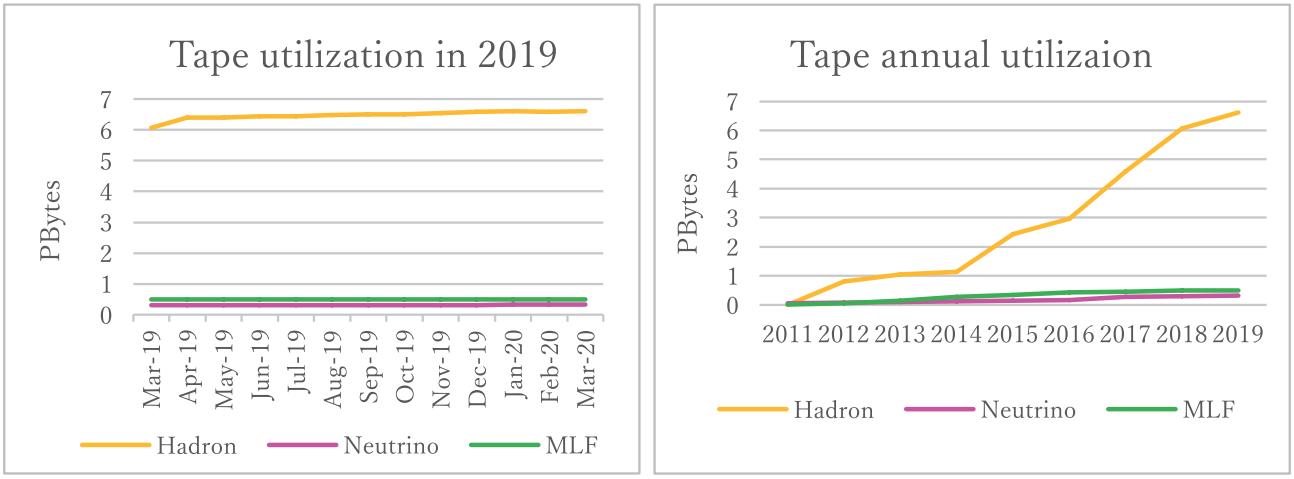

Fig. 10. Tape library usage statistics (Left: trend for this FY year; Right: annual trend).

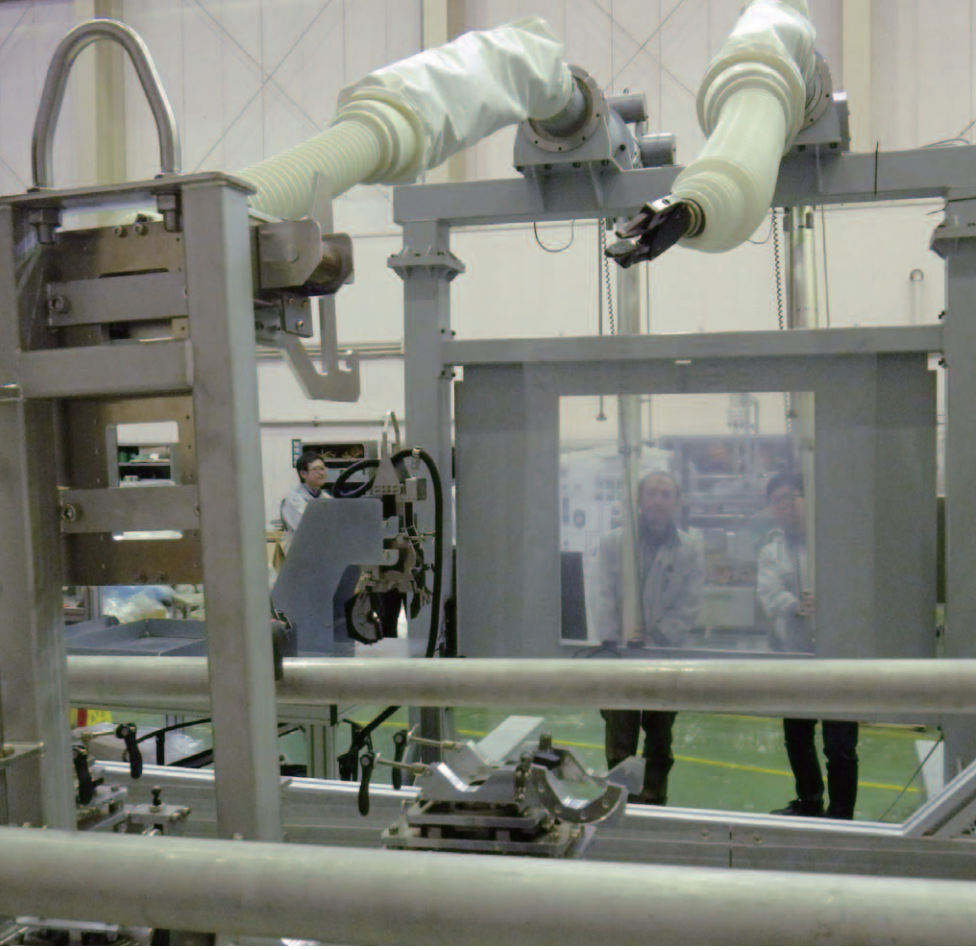

Transmutation Studies

Overview

We are developing nuclear transmutation technology with accelerator-driven systems (ADS) using the J-PARC's research resources and expertise in high-power accelerator and target technologies. The ADS is an effective nuclear system for volume reduction and mitigation of harmfulness of high-level radioactive waste produced in nuclear reactors. We believe that the ADS is one of the most beneficial applications of high-power accelerators that contribute to society.

The baseline design of the J-PARC Transmutation Experimental Facility (TEF) was completed in FY2017 (JAEA-Technology 2017-003 and 2017-033). To make the facility more attractive and effective by introducing leading edge knowledge to its purpose and specifications, we are transforming the concept of the TEF to a new one. The main purpose of the new facility is to acquire irradiation damage data of ADS's beam window materials by impinging a proton beam to a lead-bismuth eutectic target, in which the sample materials are located. In addition, it is under consideration to irradiate directly the beam window and target materials used in high-power accelerator facilities, such as J-PARC, with the proton beam to acquire irradiation data of the materials and ensure a safe and efficient operation of those facilities. We also plan to equip the new facility with a hot laboratory for efficient post-irradiation examination (PIE). Accordingly, it is expected that the new facility would contribute not only to the development of ADS but also to the upgrade of J-PARC's existing facilities.

We have continued our R&D activities to support the design of the experimental facility and ADS. We are developing LBE target technologies applicable in thermal-hydraulics, materials corrosion, instrumentation, including oxygen concentration control, and are acquiring operation experience by using two large LBE circulation loops, and so on. We have continued our work on other projects, such as measurement of nuclear data needed for ADS designs, development of proton beam monitors, which can withstand a high-power proton beam, design of an accelerator for ADS and prototyping of a super-conducting cavity. We have also continued our reactor physics experiments by using critical assemblies. Details of these R&D activities are described in this chapter.

On February 14 and 15, 2020, the sixth TEF Technical Advisory Committee (T-TAC), one of the technical advisory committees under the J-PARC International Advisory Committee, was held (Fig. 1). In addition to the usual reports on our progress in the R&D activities, in this T-TAC, we described specifically our future R&D plans. The T-TAC gave us the following consideration: "this planning is feasible provided that particular attention is given to the alignment between the deliverables to be provided by the Target Technology developments and the needs of the design works for the Irradiation Facility."

Fig. 1. T-TAC members and attendees.

Research and development

Studies for the spallation target for ADS

The experimental studies to establish the lead-bismuth eutectic (LBE) spallation target for ADS development have been progressing. Within the LBE loop experiment, a heat exchange experiment has been performed by using IMMORTAL (Integrated Multi-functional MOckup Real-scale TArget loop). Regarding the material properties study, oxygen concentration (OC) control tests in OLLOCHI (Oxygen-controlled LBE LOop Corrosion tests in HIgh-temperature) started. The developments of a laminated thin plate (LTP) type oxygen sensor and an electro-magnetic (EM) flow velocity probe are progressing. The development of a remote handling technology for target maintenance is also advancing. The results are described in detail below.

IMMORTAL

In the IMMORTAL loop, LBE is heated by a module heater and cooled by a heat exchanger (PHX), which utilizes pressurized water. A heat transfer performance between the heated LBE and pressurized water was observed to measure the prediction accuracy of system analysis programs for the LBE system. To improve the simulation further, a more precise flow controller was installed to the secondary system of IMMORTAL. In near future, more detailed experimental data will be provided by modifying the instrumentation to increase the calculation accuracy of the safety analysis programs.

OLLOCHI

Since the last year, the dissolved OC control tests in LBE have been carried out to obtain loop-specific parameters necessary for the automatic OC controlled operation. The automatic OC control tests started in January 2020. We managed to maintain the OC automatically within a certain range by mixing inlet gases. We will continue to carry out automatic control tests assuming actual corrosion test conditions, and then start long-term corrosion tests in FY2020.

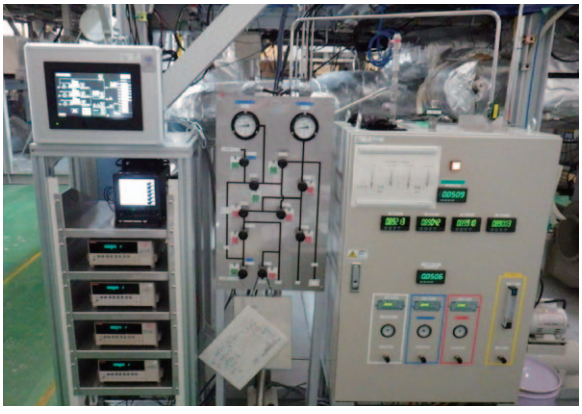

Fig. 2. Outline of the automatic OC control system for OLLOCHI.

Oxygen sensor development

Although a developed oxygen sensor worked well under the LBE flow environment, a conventional sensor cannot eliminate the possibility of ceramic tube's breakage. To provide a more robust one, development of "Laminated Thin Plate (LTP)" type oxygen sensor shown in Fig. 3 (a) was performed in cooperation with a sensor production company.

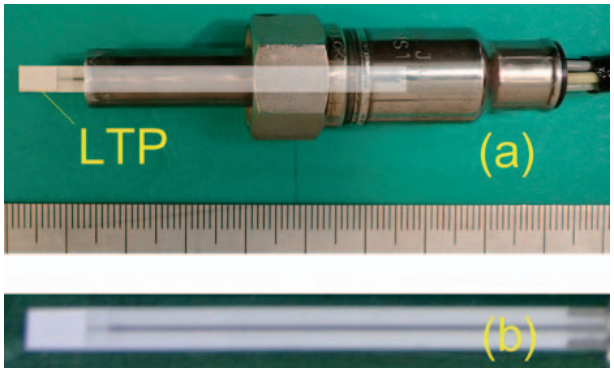

Fig. 3. Photograph of the LTP type of oxygen sensor (a) Exterior of the sensor, (b) Exterior of the LTP element

Several plates having different functions, such as an electrode and a guide spacer for reference materials, are laminated to the small single LTP element shown in Fig. 3 (b) (66 mm in length, 4.2 mm in width and 1.65 mm in height). This structure drastically improves the robustness. Furthermore, the necessary space for handling is reduced significantly and it may have a possibility to detect local oxygen potential because of the small sensing area of LTP. Experimental results of the LTP type showed sufficient performance above 250˚C under saturated OC condition. The output error was estimated below 1%, which satisfied sufficiently the design requirements. After specific modification to improve stability and wettability, the LTP sensor will be installed in several LBE test loops to perform OC control test and to confirm the durability of the sensor under flowing LBE condition.

EM flow velocity probe development

Measurement of local flow velocity in LBE under operation condition of LBE spallation target or ADS is important to verify the existing CFD codes. In order to measure local LBE flow velocity, development of electro-magnetic (EM) probe for flow velocity measurement has been started. The probe works on the basis of Faraday's law. Normally, the probe consists of a permanent magnet, electrodes and an outer tube. However, if the LBE temperature changes, attenuation of the magnetic flux density of the permanent magnet occurs, which disturbs the precise detection of local flow velocity due to linearity loss of the probe. To overcome the issue, a miniature electromagnet was manufactured and adopted to the probe as a source of constant magnetic flux density. Figure 4 shows the originally manufactured electromagnet type EM probe with 6 mm of outer diameter and 155 mm of length.

Before applying the EM probe to a high-temperature LBE, preliminary experiments were carried out in a mercury test loop. As a result, the manufactured probe was successfully calibrated and the local flow velocity distributions in the square flow channel were measured successfully. As a next step, the manufactured EM probe will be tested under a high-temperature LBE flow up to 500 ˚C in FY2020.

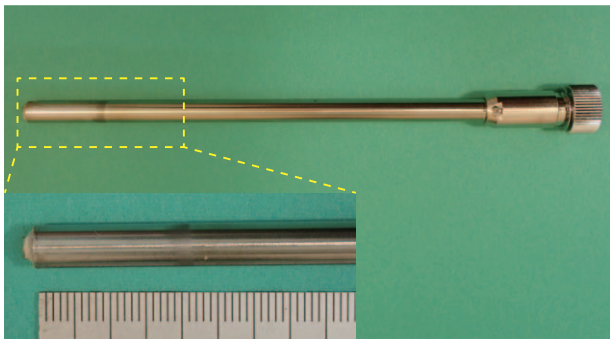

Fig. 4. The originally manufactured EM flow velocity probe.

Remote handling technology

To establish the exchange method of LBE spallation target components, a remote handling technology based on cutting / welding the system piping has been developed. In order to perform a series of planned remote operation procedures, prototype devices based on commercially available equipment have been developed. To figure out the issues in the planned remote operation procedure, demonstrative tests were performed using a mock-up of the target vessel with

Fig. 5. Outline of the remote handling test device.

piping and prototypical remote devices, as shown in Fig. 5. As a result of the mock-up tests, the procedure was completed without significant failures. To make the work more efficient and reliable, improvement of the tools and jigs is underway.

Experimental program on nuclear data for ADS using FFAG accelerator

An experimental program on nuclear data for research and development of ADS was launched in October 2019, entrusted by the ministry of Education, Culture, Sports, Science and Technology of Japan (MEXT). This program consists of two subprograms: neutron energy spectrum measurement and high-energy fission measurement. It will continue until fiscal year 2022. The experiment of the first subprogram will be conducted in the middle of fiscal year 2020, and the second experiment will start from fiscal year 2021. This program focuses on nuclear data at incident energies from several tens of MeV to 100 MeV, which is the most difficult area to predict by theoretical nuclear models. To this end, we will use proton beams produced by the Fixed-Field Alternating Gradient (FFAG) accelerator at Kyoto University.

In the first subprogram, energy spectra of neutrons produced from the proton-induced nuclear reaction will be measured with the time-of-flight (TOF) technique using liquid organic scintillation spectrometers. To meet the requirements of the TOF experiment, this subprogram includes an improvement of the FFAG accelerator, in which the pulse width will be reduced from the present specification of ~10 ns by the bunch rotation technique. Lead, bismuth, and iron, which are major constituent materials of the ADS, will be used as target materials. Furthermore, the fission rate of ^{237}Np at the produced neutron field will be measured. In the second subprogram, the mass number distribution of fission fragments produced from heavy target materials, such as lead and bismuth, will be measured with the combined use of micro-channel plates and multi-wire proportional counters. Moreover, fission neutrons will be also measured by the neutron detectors.

Measurement of nuclide production cross sections by high-energy protons at J-PARC

In the high-energy accelerator facilities such as ADS, radioisotopes are produced by high-energy nuclear reactions. In such facilities, production yields of radioisotopes must be predicted for the shielding design and dose assessment. To estimate the production yields of radioisotopes, nuclide production cross section data are required for various target materials. We have systematically measured the nuclide production cross sections for various target materials induced by GeV-order protons.

The radioisotopes produced in an irradiated sample foil can be derived by measuring a γ-ray energy spectrum. In the spectrum, some sharp peaks are observed, which correspond to γ-ray energies emitted from each production nuclide. Figure 6 shows examples of nuclide production cross sections for Ni and Zr targets. Theoretical calculations and cross section data taken from nuclear data library are also shown. Among the nuclides shown in Fig. 6, ^{51}Cr, ^{54}Mn, and ^{58}Co, which have a relatively long half-lives and high activities, are particularly important for dose assessment in the accelerator facilities. For the Zr target, the experimental data were much scarcer than for the Ni target. The cross section of Zr(p,X)^{81}Rb was successfully obtained for proton energy higher than 1 GeV as the first experimental data. It was observed that the calculations and the nuclear data library underestimated the cross sections for these nuclides, which will be improved in future work.

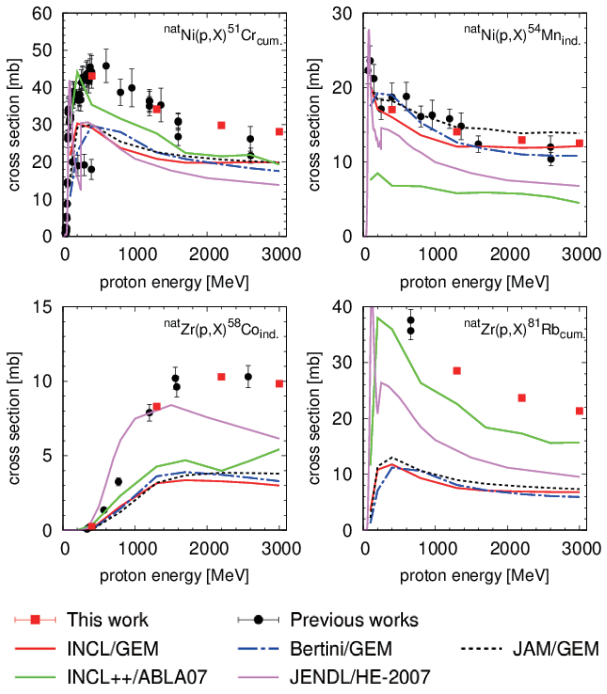

Fig. 6. Present experimental production cross-sections of Ni and Zr irradiated with protons.

Displacement cross-section measurement

As an index of radiation damage to materials, displacement per atom (dpa) is widely used in many fields, such as fission and fusion reactors, and accelerator

facilities. The dpa is evaluated by integrating a particle flux by the displacement cross-section. Since the experimental displacement cross section data for the protons with energies used in the ADS were scarce, the experiment was conducted in J-PARC, as a program entrusted by the MEXT. The displacement cross-section could be delivered from an electric resistivity increase of a sample by proton irradiation. To prevent the defect from recovering by the thermal motion of atoms, the sample was cooled less than 4 K by using a cryocooler. The experimental instruments were installed at the beam channel extracted from the RCS and Main Ring (MR) in J-PARC.

The first experimental data [1] of iron were successfully obtained for the protons with the kinetic energy utilized in the ADS. The present result of the displacement cross-section of iron is compared in Fig. 7 with the experimental data carried out in the lower energy region and the calculation. PHITS with the improved model with athermal recombination correction (arc) model showed remarkably good agreement with the experimental data. From the present experimental campaign, the displacement cross-section data of Al, Fe, Cu and W were successfully obtained. The program entrusted by the MEXT was successfully completed by the end of fiscal year 2019.

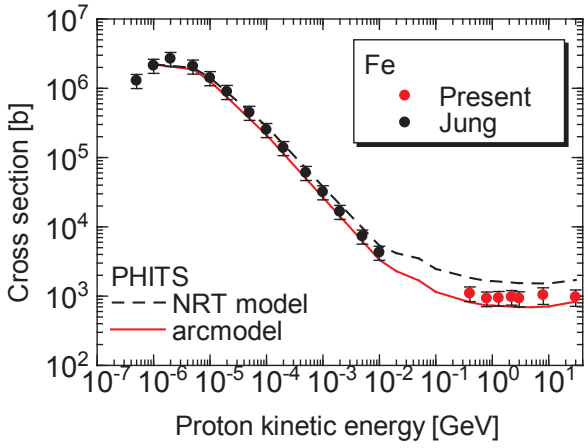

Fig. 7. Displacement cross-section of iron obtained by the present experiment.

Proton accelerator for ADS

One of the biggest challenges for the high-intensity proton linac for ADS is to operate the accelerator with a beam loss level lower than 1 W/m, to allow hands-on maintenance. The beam halo, the particles which are the outermost region of the distribution, is the main source of particle loss, and the beam halo is associated with the emittance growth. As a result, by controlling the emittance growth, it is possible to reduce the beam halo; consequently, decrease the beam loss [2].

The robustness of the lattice was tested by multiparticle tracking using a large number of particles, about $1x10^7$, to achieve an accurate description of the beam behavior. Figure 8 presents a smooth evolution of the horizontal beam size and the maximum beam envelope, which corresponds to the beam fraction lower than 10^{-6}, remains below the aperture. The beam dynamics results, of the JAEA-ADS linac, showed a proper control of the emittance growth and the beam halo, which confirmed the absence of beam loss along the lattice.

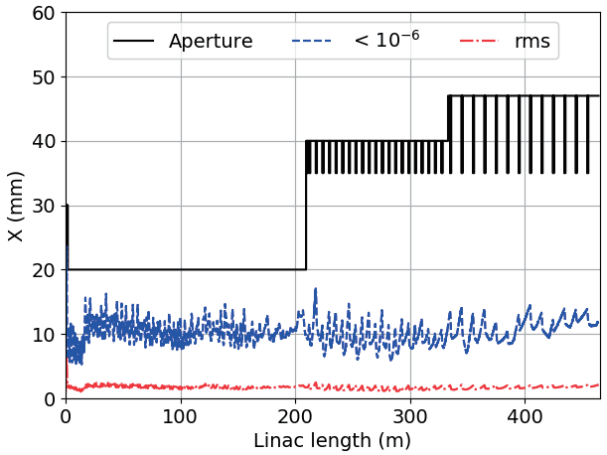

Fig. 8. The Horizontal evolution of the root-mean-square (red dashed-dotted line) and the maximum envelope for beam fraction < 10^{-6} (blue dashed line).

MA irradiation experiments

To develop an accelerator-driven system (ADS), it is necessary to verify the nuclear data of minor actinides (MAs) in a fast neutron core, such as the transmutation physics experimental facility (TEF-P) designed in J-PARC. As planned in TEF-P, one of the verifications is to use fission chambers containing MA as fissionable material and a well-known material such as ^{235}U as reference in critical or sub-critical core, where neutron spectrum in ADS core can be simulated. To achieve high-accuracy verification, precise fabrication of the chamber (e.g. accountancy and purity of MA, uniformity of MA layer, and hermeticity) is important, but the fabrication itself requires R&D because the preparation of pure raw MA and its treatment are possible in a very limited number of facilities. We have recently fabricated several chambers containing ^{237}Np, ^{241}Am, ^{243}Am or ^{244}Cm in NUCEF in JAEA and measured the ratio of the ^{243}Am and ^{235}U fission reaction rates at the Kyoto University Critical Assembly (KUCA).

The irradiation experiment of ^{243}Am and ^{235}U was conducted at A-core in KUCA shown in Fig. 9. Fission reaction rates were measured by using the JAEA single fission chamber shown in Fig. 10, which has a foil, such as ^{235}U (10 μg) or ^{243}Am (12 μg). The simultaneous measurement of ^{243}Am and ^{235}U fission reaction rates was conducted at the center voided region. The pulse height distributions from the fission chambers were acquired under the condition of critical core corresponding to a reactor power of 3.5 W. The irradiation time was 1 hour.

The distributions of pulse height of ^{243}Am and ^{235}U fission reactions were observed, as shown in Fig. 11. The fission reaction signals need to be separated from noises due to α and γ rays in a small pulse height. The fission reaction events of ^{243}Am and ^{235}U in Fig. 11 were determined by integrating the counts at voltages greater than 0.589 and 0.592, respectively. As a result, the effective total fission counts of ^{243}Am and ^{235}U were estimated to be 5,208 and 118,664, respectively. Finally, the fission reaction rate ratio of ^{243}Am and ^{235}U was obtained by the total counts and the number of atoms, and a detection efficiency of the fission chamber was 0.042 ± 0.002. These experimental data will be usable for verification of evaluated nuclear data by conducting detailed analyses [3].

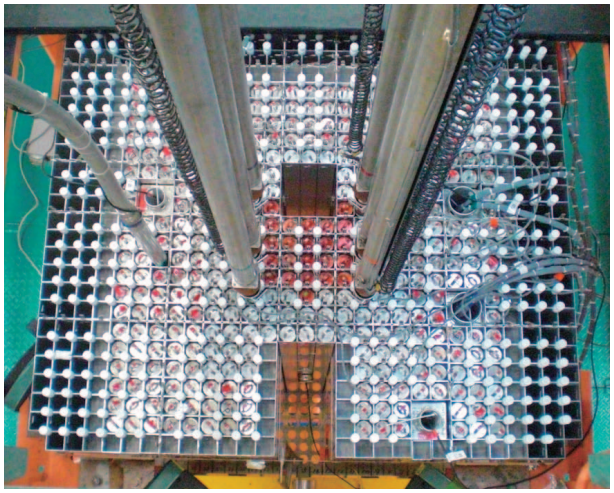

Fig. 9. Photograph of A-core in KUCA facility.

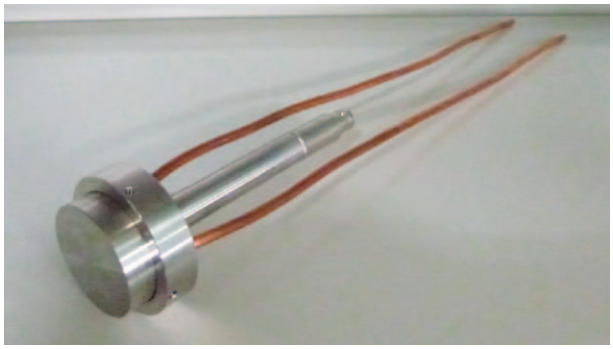

Fig. 10. Photograph of the JAEA single fission chamber.

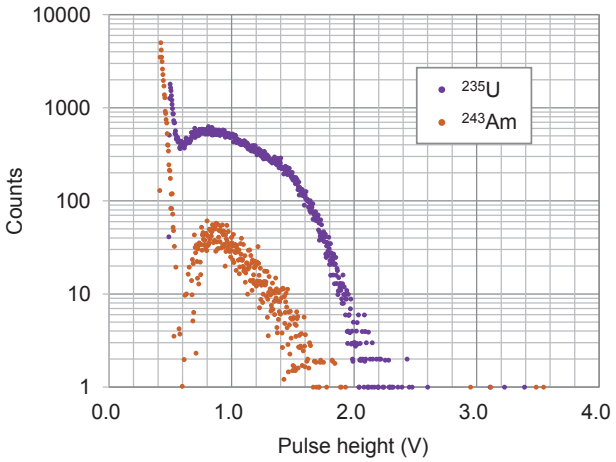

Fig. 11. Fission signals of the ^{243}Am and ^{235}U fission chambers [3].

International cooperation

We are collaborating closely with the Belgian Nuclear Research Centre (SCK CEN) for the ADS development under the collaboration arrangement between SCK CEN and JAEA. SCK CEN is promoting the MYRRHA (Multi-purpose hYbrid Research Reactor for High-tech Application) project, which is the world's first large scale ADS project at power levels scalable to industrial systems.

On April 4 and 5, 2019, four members of the J-PARC staff visited the MYRRHA accelerator team for information exchange on the development of a superconducting linac for ADS. One of the important topics discussed was how to achieve considerably high operation reliability needed for ADS's accelerators to drive subcritical reactor cores. One of J-PARC's representatives, Dr. Jun Tamura, joined the MYRRHA accelerator team for a year from January 2020 to enhance mutual collaboration.

On November 27, 2019, we welcomed seven SCK CEN's delegates including Dr. Eric van Walle, who was the Director-General of SCK CEN, to discuss future collaboration between SCK CEN and JAEA (Fig. 12). At the meeting, we agreed to enhance the mutual collaboration in the field of ADS development, including

LBE technology, materials irradiation, and accelerator technology.

On February 4 and 5, 2020, three SCK CEN's scientists visited JAEA to hold a technical meeting under the Collaboration Arrangement. The meeting was attended by many JAEA staff including J-PARC Center who were involved in the development of ADS. Recent progress and future collaboration items on two main topics, LBE technology and neutronics, were discussed.

In addition, JAEA and the Karlsruhe Institute of Technology in Germany decided to sign an arrangement for research collaboration in the ADS development, especially in the field of high-power LBE target technology, which was one of the important themes studied at the J-PARC Center.

Fig. 12. Visit of SCK CEN's delegates.

Reference

[1] H. Matsuda, *et al*, J. Nucl. Sci. Technol. Doi: 10.1080/00223131.2020.1771453.

[2] B. Yee-Rendon, *et al*, J. Phys. Conf. Ser. **3501**, 12120 (2019).

[3] A. Oizumi *et al*., KURNS Progress Report 2019, (in printing).

Safety

Safety

1. Major events on safety culture and safety activities at the J-PARC Center

The major events on safety culture and safety activities at the J-PARC Center are listed in Table 1.

Every year since 2014, the J-PARC Center has held workshop 5.23 for fostering safety culture to keep fresh the lessons of the radioactive material leak incident at the Hadron Experimental Facility on May 23, 2013. A "Safety Day" was launched two years ago, which, in addition to workshop 5.23, also includes a discussion of the safety culture. The safety day took place on May 24. In the morning, we held a meeting between the sections to exchange information on the safety efforts. The number of participants was 104. The director of the J-PARC Center gave away three "Safety Awards for good examples". The neutron science section/technology development section/CROSS received one because they reported more good examples of safety in their daily works than the other sections. Another was given to accelerator section 1 and the hadron section, because they reported creative good examples. The third was given to the neutron science section/technology development section/CROSS, because they reported good examples with consideration for hygiene.

Mr. Fumihiro Saito from the radiation control section gave a scientific talk with the title "If the beam operation is done with the worker in the accelerator tunnel… -Study on quick and simple estimation method of exposure dose". Dr. Hidetaka Kinoshita from the neutron source section introduced the safety work of the MLF facility under the title "On-site transportation of used mercury target container". Also, Dr. Kazuo Gorai from the information system section introduced the safety work under the title "Response and countermeasures against the fire of the temporary generator".

In the afternoon part of the Safety Day, workshop 5.23 for fostering safety culture was held at the auditorium of the Nuclear Science Research Institute with 278 attendees. Dr. Yayoi Ngai, representative of the Office Style Road was invited this year; she spoke about "the power of people necessary" for a strong and safe organization.

The emergency drill was carried out on January 9, 2020. It assumed an abnormal release of radioactive materials into the MLF facility environment during the operation of the accelerator. The main purpose of the drill this year was to practice the appropriate response from the initial reaction until the event was contained.

Fig. 1. Emergency drill

The J-PARC Safety Audit in FY2019 was conducted by two external auditors (Prof. Akira Tose from Niigata University and Dr. Katsumi Hayashi from the Institution of Professional Engineers) on December 16. After completing their observations, the auditors recommended that all stakeholders involved in J-PARC foster a safety culture by safe and stable use of the equipment, which will lead to achieving excellent research results.

2. Radiological license update and facility inspection

Applications to update the radiological license were submitted to the Nuclear Regulation Authority on May 30 and December 6. The major application items are listed in Table 2. The permits for the applications were issued on June 12 and on April 28, 2020, respectively. There were no cases requiring a facility inspection in FY2019.

3. Meeting of the committee on the radiation safety matter

The basic policies on radiation safety in the J-PARC are supposed to be discussed by the J-PARC Radiation Safety Committee (RSC). Meanwhile, the J-PARC Radiation Safety Review Committee (RSRC) is expected to discuss specific subjects of radiation safety in the J-PARC. The RSC held one meeting and the RSRC met three times during FY2019. The RSC meeting scheduled for March 2020 was postponed due to the coronavirus. The major issues are summarized in Table 3.

4. Radiation exposure of radiation workers

In FY2019, 3254 persons were registered as radiation workers. In the last five years, the numbers of

workers fluctuated between 3000 and 3500.

The distribution of annual exposed doses is summarized in Table 4 for each category of workers: in-house staff, users, and contractors. The exposed doses of gamma-rays and of neutrons were measured with an optically stimulated luminescence (OSL) dosimeter and with a plastic solid-state track detector, respectively. The exposure of all users and almost all of the in-house staff and contractors were below the detection limit (Not Detected, expressed as "ND" in the table). The maximum exposed dose was 1.1 mSv. Though it was less than the administrative dose limit at the J-PARC (7 mSv/year), we should continue to make efforts to reduce the exposed doses of all workers.

Table 1. List of major events on safety in FY2019.

Day	Events
May 24, 2019	Safety Day (Meeting to exchange safety information between all sections, Workshop for fostering safety culture)
June 26, 2019	Liaison committee on safety and health for contractors
September 3, October 4, 17, November 6, 8, 2019	Refresher course on radiation safety for the in-house staff
December 16, 2019	FY2019 J-PARC Safety Audit
January 9, 2020	Emergency drill assuming an abnormal release of radioactive materials into the MLF facility environment during the operation of the accelerator
January 23 - 24, 2020	7th Symposium on Safety in Accelerator Facilities

Table 2. Major application items of the radiological license

Facility	Items of an application
Li	• Change of the installation position of the particle count monitor
RCS	• Change of the safety interlock structure
MR	• Addition to the purpose of use (research of the material science) • Addition of description concerning the proton beam irradiation experiment • Change of beam loss • Construction of a new primary beam line (B-line)
HD	• Beam intensity: $4.3 \times 10^{16} \rightarrow 7.1 \times 1016$ protons/hour • Construction of a new primary beam line (B-line) • Addition of a storage facility for induced radioactive materials
NU	• Expansion of the controlled area
All	• Optimization of the application document

Table 3. Radiation Safety Committee (RSC) and Radiation Safety Review Committee (RSRC) in FY2019

No.	Date	Major Issues
The Radiation Safety Committee		
34th	July 31, 2019	• Nomination of committee chair and deputy chair • Materialization of deliberation matter concerning safety at J-PARC • Report of radiation exposure status in FY2018 • Report of radioactive waste emission (exhaust air and drain water) in FY2018
The Radiation Safety Review Committee		
24th	May 31, 2019	• Report of radiation exposure status in FY2018 • Update of the radiological license for the HD and NU facilities • Decision of assumed events requiring emergency responses
25th	October 8, 2019	• Report of correction of the dose evaluation value at the J-PARC site boundary • Report of preparation of the interlock handling guide • Revision of the Detailed Rule of Local Radiation Protection Rule for J-PARC • Revision of the RSRC Rule • Decision of emergency responses for assumed events described in the operation guides
26st	February 7, 2020	• Revision of the accident-response activity guide • Revision policy of the operation guide for the HD facility • Use of the X-ray generator at the JRB facility

Table 4. Annual exposed doses in FY2019

	# of workers	Dose range x (mSv)				Collective dose (person · mSv)	Maximum dose (mSv)
		ND	0.1≤ x ≤1.0	1.0< x ≤5.0	5.0< x		
In-house staff	695	666	28	1	0	12.4	1.1
Users	1,197	1,197	0	0	0	0	0
Contractors	1,367	1,294	73	0	0	21.5	0.8
Total	3,254	3,152	101	1	0	33.9	1.1

User Service

Users Office (UO)

Outline

The J-PARC Users Office (UO) was established in 2007. It opened an office on the first floor of the IBARAKI Quantum Beam Research Center in Tokai-mura, in December 2008. UO maintains the Tokai Dormitory for the J-PARC users. UO provides on-site and WEB support with one-stop service for the utilization of the J-PARC. As of March 31, 2019, UO had 13 staffs and 4 WEB Support SE staffs in the Users Affairs Section. The J-PARC Users, after the approval of their experiment, follow the administrative procedures outlined on the Users Office (UO) WEB Portal Site, related to the registration as a J-PARC User, radiation worker registration, safety education, accommodation, invitation letter for visa and other requirements. Then, the UO staffs provide them with support by e-mail. After their arrival at the J-PARC, UO gives on-site assistance to the J-PARC Users, like receiving the J-PARC ID, glass badge, and safety education. Since 2015, UO had been doing its part to improve the J-PARC on-line experiment system and make it more user-friendly

After the experiments. UO may return the experiment samples at User's cost after radioactivity cools down.

Map to J-PARC Users Office

Activities of UO

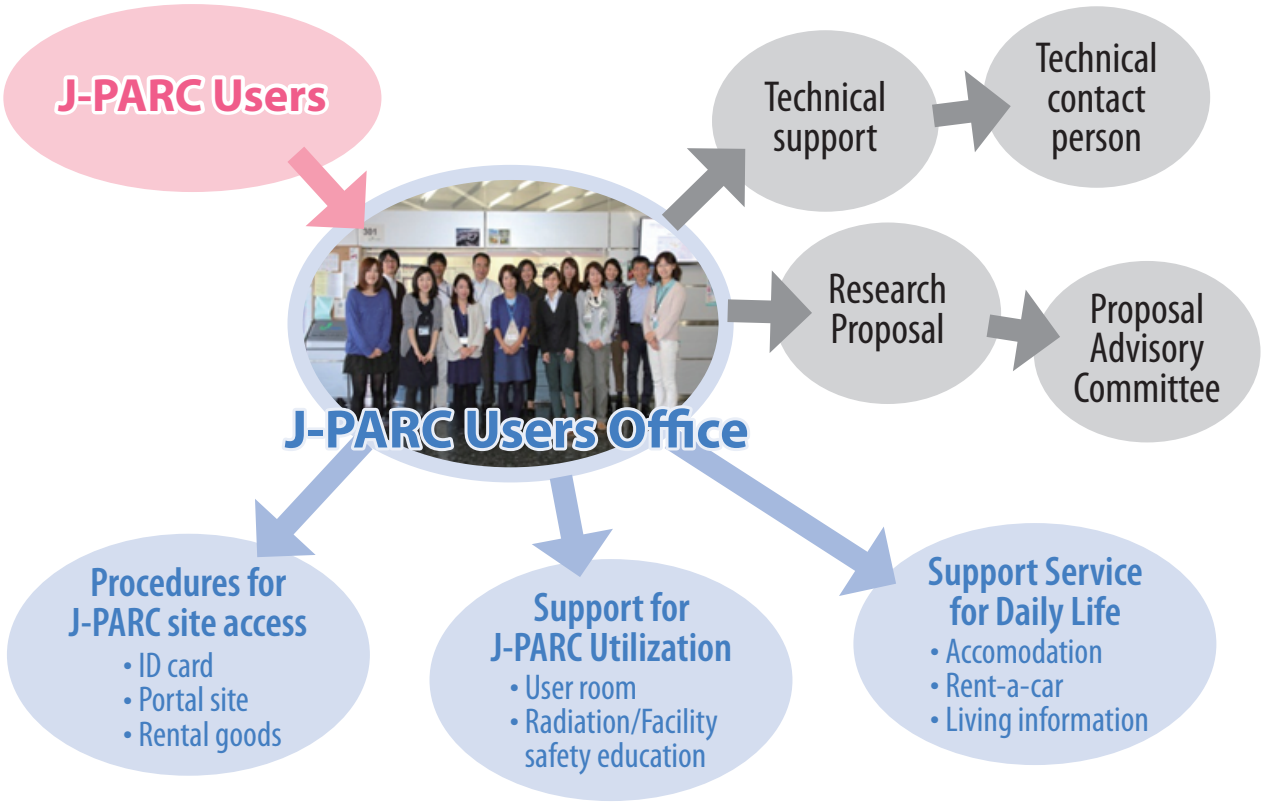

One stop service for J-PARC users

on the web

Step 1 User registration

New user
Getting user ID

Registered user
Annual registration, specifying of the visit

Approval of UO

Step 2-1 Obligatory application

Application form to visit J-PARC
Visit proposal (foreign nationality)
Reservation of safety training
On-line education video

Step 2-2 Optional application

J-PARC Card for facility access
Network registration
Radiation worker registration
Reservation of Dormitory
Invitation letter for Visa

on-site support

Step 3

Procedures upon arrival at the first day

Recieve J-Parc User ID card

Vehicle Permission pass

Safety education and dosimeter

Rental goods
Bicyle
PHS
Cafeteria card
Locker key
Office key

Step 4 J-PARC Experiment and meeting

Step 5 Leaving procedures

Retern all cards, keys, rental goods UO (office hours) or return box!

Users Office at IQBRC
Office hours(9:00-17:00, Mon.-Fri.)

Rental bicycle

Return box at IQBRC

User Statistics

Users in 2019 (Japanese/Foreigners, person-days)

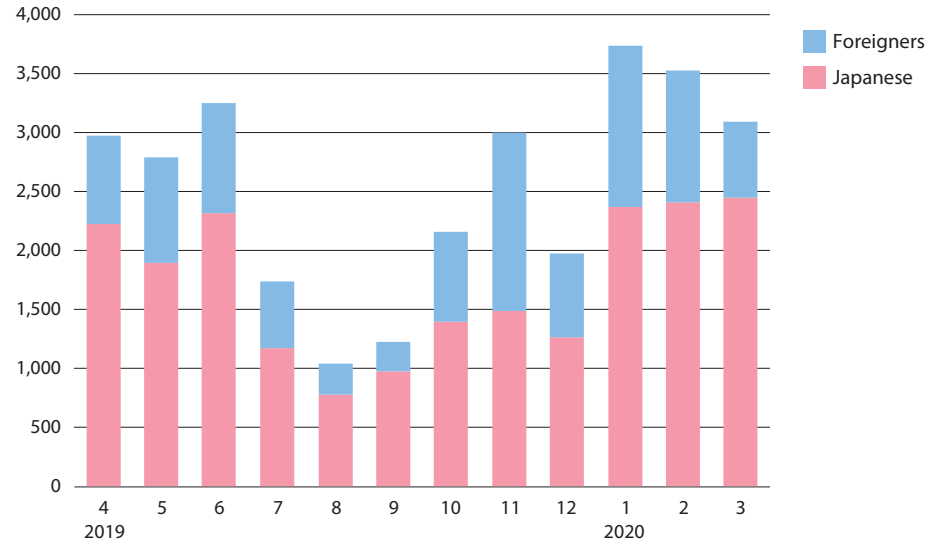

Users in 2019 (according to facilities, person-days)

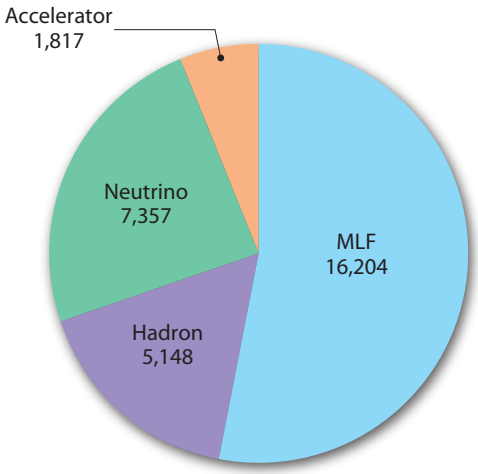

Users in 2019 (according to organizations, person-days)

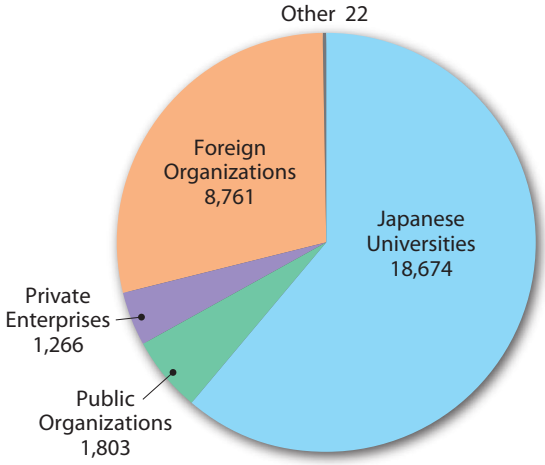

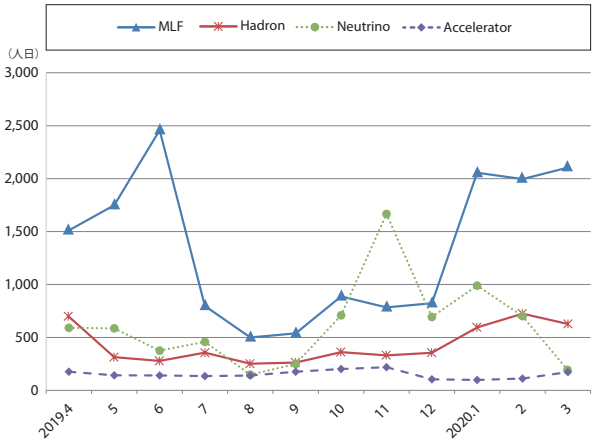

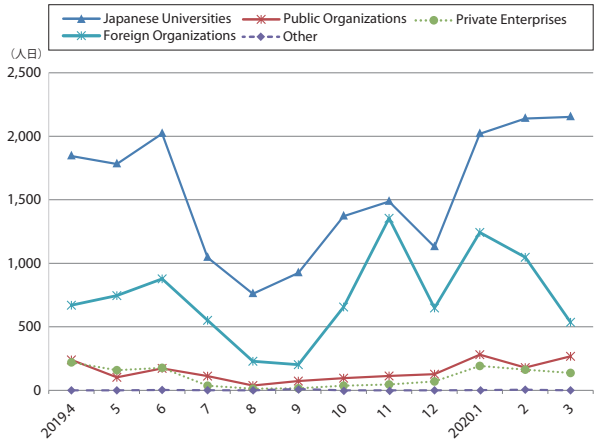

MLF Proposals Summary - FY2019

Table 1. Breakdown of Proposals Numbers for the 2019 Rounds

Beam-line	Instrument		2019A		2019B		Full Year			
			Submitted	Approved	Submitted	Approved	Submitted		Approved	
			GU	GU	GU	GU	PU/S	IU	PU/S	IU
BL01	4D-Space Access Neutron Spectrometer - ***4SEASONS***		16(0)	13(0)	26(1)	12(1)	1	1	1	1
BL02	Biomolecular Dynamics Spectrometer - ***DNA***		12(0)	8(0)	29(3)	10(3)	2	2	2	2
BL03	Ibaraki Biological Crystal Diffractometer - ***iBIX***	(100-β)‡	1	0	1	1	0	0	0	0
		(β)†	0	0	0	0	43※	0	43※	0
BL04	Accurate Neutron-Nucleus Reaction Measurement Instrument - ***ANNRI***		10	4	11	4	1	1	1	1
BL05	Neutron Optics and Physics - ***NOP***		5	5	5	5	1	0	1	0
BL06	Neutron Resonance Spin Echo Spectrometers - ***VIN ROSE***		4	3	4	2	1	0	1	0
BL08	Super High Resolution Powder Diffractometer - ***S-HRPD***		14	10	17	12	1	0	1	0
BL09	Special Environment Neutron Power Diffractometer - ***SPICA***		6	3	4	4	1	0	1	0
BL10	Neutron Beamline for Observation and Research Use - ***NOBORU***		8	8	13	7	3	1	3	1
BL11	High-Pressure Neutron Diffractometer - ***PLANET***		9(0)	9(0)	15(0)	10(0)	0	1	0	1
BL12	High Resolution Chopper Spectrometer - ***HRC***		5	5	10	5	1	0	1	0
BL14	Cold-neutron Disk-chopper Spectrometer - ***AMATERAS***		27	11	37	10	3	1	3	1
BL15	Small and Wide Angle Neutron Scattering Instrument - ***TAIKAN***		38(2)	14(2)	59(0)	13(0)	3	3	3	3
BL16	High-Performance Neutron Reflectometer with a horizontal Sample Geometry - ***SOFIA***		21	18	21	20	0	1	0	1
BL17	Polarized Neutron Reflectometer - ***SHARAKU***		19(2)	16(2)	27(2)	13(2)	1	3	1	3
BL18	Extreme Environment Single Crystal Neutron Diffractometer - ***SENJU***		13(0)	8(0)	25(1)	5(1)	1	1	1	1
BL19	Engineering Diffractometer - ***TAKUMI***		16	12	24	14	1	1	1	1
BL20	Ibaraki Materials Design Diffractometer - ***iMATERIA***	(100-β)‡	10	5	14	8	0	0	0	0
		(β)†	42	42	25	25	25	0	25	0
BL21	High Intensity Total Diffractometer - ***NOVA***		22	20	25	19	1	0	1	0
BL22	Energy Resolved Neutron Imaging System - ***RADEN***		17(0)	13(0)	21(0)	11(0)	1	2	1	2
BL23	Polarization Analysis Neutron Spectrometer - ***POLANO***		2	2	2	2	1	0	1	0
D1	Muon Spectrometer for Materials and Life Science Experiments - ***D1***		17(0)	8(0)	18(1)	8(1)	0	1	0	1
D2	Muon Spectrometer for Basic Science Experiments - ***D2***		8(1)	4(0)	12(4)	6(2)	0	1	0	1
S1	General purpose μSR spectrometer - ***ARTEMIS***		30(2)	25(1)	29(3)	23(3)	1	1	1	1
UA	Muon U		0	0	0	0	0	1	0	1
Total			***369***	***265***	***473***	***253***	***86***	***22***	***86***	***22***

GU : General Use **PU** : Project Use or Ibaraki Pref. Project Use **S** : S-type Proposals
IU : Instrument Group Use
† : Ibaraki Pref. Exclusive Use Beamtime (β = 80% in FY2019)
‡ : J-PARC Center General Use Beamtime (100-β = 20% in FY2019)
( ) : Proposal Numbers under the New User Promotion (BL01, BL02, BL11, BL15, BL17, BL18, BL22) or P-type proposals (D1,D2, S1) in GU

※ Proposal rounds are held twice per year (for each of the A and B periods), with only the yearly total shown above. The actual total number of proposals in each beamline named in the table does not match the number shown in the "Total" cell, because some proposals are submitted or approved across multiple beamlines.

Table 2. Proposals Numbers of Long Term Proposal for the 2019 Rounds

Application FY	Submitted	Approved
2017	24	8
2018	9	5
2019	9	4

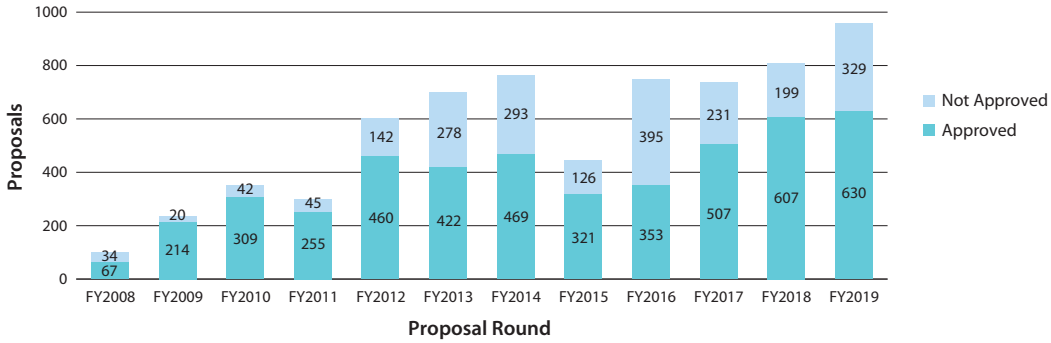

Fig. 1. MLF Proposal Numbers over Time

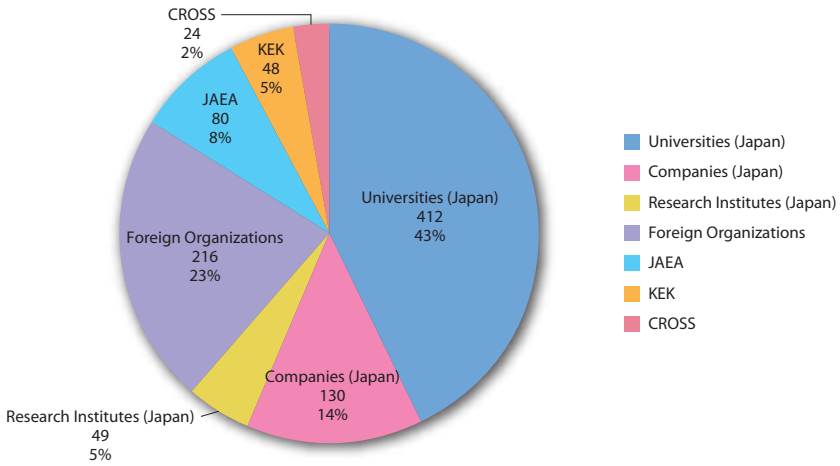

Fig. 2. Origin of Submitted Proposals by affiliation - FY2019

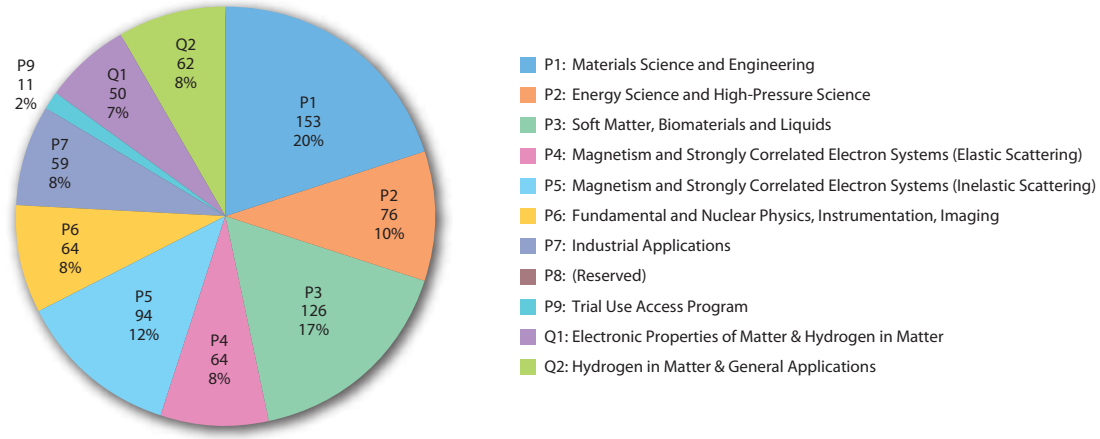

Fig. 3. Submitted Proposals by Sub-committee/Expert Panel – FY2019

J-PARC PAC Approval Summary for the 2019 Rounds

	(Co-) Spokespersons	Affiliation	Title of the experiment	Approval status (PAC recommendation)	Beamline	Status
E03	K.Tanida	JAEA	Measurement of X rays from Ξ^- Atom	Stage 2	K1.8	In preparation
P04	J.C.Peng; S.Sawada	U of Illinois at Urbana-Champaign; KEK	Measurement of High-Mass Dimuon Production at the 50-GeV Proton Synchrotron	Deferred	Primary	
E05	T.Nagae	Kyoto U	Spectroscopic Study of Ξ-Hypernucleus, $^{12}_{\Xi}$Be, via the ^{12}C(K^-, K^+) Reaction	Stage 2 New experiment E70 based on the S-2S spectrometer	K1.8	Finished
E06	J.Imazato	KEK	Measurement of T-violating Transverse Muon Polarization in $K^+ \to \pi^0 \mu^+ \nu$ Decays	E36 as the first step	K1.1BR	
E07	K.Imai, K.Nakazawa, H.Tamura	JAEA, Gifu U, Tohoku U	Systematic Study of Double Strangeness System with an Emulsion-counter Hybrid Method	Stage 2	K1.8	Finished Data analysis
E08	A.Krutenkova	ITEP	Pion double charge exchange on oxygen at J-PARC	Stage 1	K1.8	
E10	A.Sakaguchi, T.Fukuda	Osaka U, Osaka EC U	Production of Neutron-Rich Lambda-Hypernuclei with the Double Charge-Exchange Reaction (Revised from Initial P10)	Stage 2	K1.8	Li run finished, Be target run with S-2S
E11	T. Nakaya, M. Wascho	KEK	Tokai-to-Kamioka (T2K) Long Baseline Neutrino Oscillation Experimental Proposal	Stage 2	neutrino	Data taking
E13	H.Tamura	Tohoku U	Gamma-ray spectroscopy of light hypernuclei	Stage 2	K1.8	Finished
E14	T.Yamanaka	Osaka U	Proposal for $K_L \to \pi^0 \nu \bar{\nu}$ Experiment at J-PARC	Stage 2	KL	Data taking
E15	M.Iwasaki, T.Nagae	RIKEN, Kyoto U	A Search for deeply-bound kaonic nuclear states by in-flight 3He(K-, n) reaction	Stage 2	K1.8BR	Finished
E16	S.Yokkaichi	RIKEN	Measurements of spectral change of vector mesons in nuclei (previously "Electron pair spectrometer at the J-PARC 50-GeV PS to explore the chiral symmetry in QCD")	Stage 2 for Run 0	High p	
E17	R.Hayano, H.Outa	U Tokyo, RIKEN	Precision spectroscopy of Kaonic ^{3}He 3d->2p X-rays	Registered as E62 with an updated proposal	K1.8BR	
E18	H.Bhang, H.Outa, H.Park	SNU, RIKEN, KRISS	Coincidence Measurement of the Weak Decay of $^{12}_{\Lambda}$C and the three-body weak interaction process	Stage 2	K1.8	
E19	M.Naruki	KEK	High-resolution Search for Θ^+ Pentaquark in $\pi^- p \to K^- X$ Reactions	Stage 2	K1.8	Finished
E21	Y.Kuno	Osaka U	An Experimental Search for $\mu - e$ Conversion at a Sensitivity of 10^{-16} with a Slow-Extracted Bunched Beam	Phase-I Stage 2 PAC recommends producing a more detailed schedule to ensure a timely start.	COMET	
E22	S.Ajimura, A.Sakaguchi	Osaka U	Exclusive Study on the Lambda-N Weak Interaction in A=4 Lambda-Hypernuclei	Stage 1	K1.8	
T25	S.Mihara	KEK	Extinction Measurement of J-PARC Proton Beam at K1.8BR	Test Experiment	K1.8BR	Finished
E26	K.Ozawa	KEK	Search for ω-meson nuclear bound states in the $\pi^- + {}^A Z \to n + {}^{(A-1)}\omega(Z-1)$ reaction, and for ω mass modification in the in-medium $\omega \to \pi^0 \gamma$ decay	Stage 1	K1.8	
E27	T.Nagae	Kyoto U	Search for a nuclear Kbar bound state K^-pp in the d(π^+, K^+) reaction	Stage 2	K1.8	Fisnished
E29	H.Ohnishi	RIKEN	Search for ϕ-meson nuclear bound states in the pbar + $^A Z \to \phi + {}^{(A-1)}\phi(Z-1)$ reaction	Stage 1	K1.1	
E31	H.Noumi	Osaka U	Spectroscopic study of hyperon resonances below KN threshold via the (K^-n) reaction on Deuteron	Stage 2	K1.8BR	Finished Data analysis
T32	A.Rubbia	ETH, Zurich	Towards a Long Baseline Neutrino and Nucleon Decay Experiment with a next-generation 100 kton Liquid Argon TPC	Test Experiment	K1.1BR	Finished
P33	H.M.Shimizu	Nagoya U	Measurement of Neutron Electric Dipole Moment	Deferred	Linac	
E34	T. Mibe	KEK, RIKEN	An Experimental Proposal on a New Measurement of the Muon Anomalous Magnetic Moment g-2 and Electric Dipole Moment at J-PARC	Stage 2	MLF	
E36	M.Kohl, S.Shimizu	Hampton U, Osaka U	Measurement of $\Gamma(K^+ \to e^+ \nu)/\Gamma(K^+ \to \mu^+ \nu)$ and Search for heavy sterile neutrinos using the TREK detector system	Stage 2	K1.1BR	Finished Data analysis
E40	K.Miwa	Tohoku U	Measurement of the cross sections of Σp scatterings	Stage 2	K1.8	Data taking
P41	M.Aoki	Osaka U	An Experimental Search for $\mu - e$ Conversion in Nuclear Field at a Sensitivity of 10^{-14} with Pulsed Proton Beam from RCS	Deferred	MLF	Reviewed in MLF/IMSS
E42	J.K.Ahn	Pusan National U	Search for H-Dibaryon with a Large Acceptance Hyperon Spectrometer	Stage 2	K1.8	
E45	K.H.Hicks, H.Sako	Ohio U, JAEA	3-Body Hadronic Reactions for New Aspects of Baryon Spectroscopy	Stage 2 PAC requests that the group further examine ways to reduce the total beam time requested and to find an efficient running scheme, including quick but careful beam tuning.	K1.8	
T46	K.Ozawa	KEK	EDIT2013 beam test program	Test Experiment	K1.1BR	Abandonded
T49	T.Maruyama	KEK	Test for 250L Liquid Argon TPC	Test Experiment	K1.1BR	Withdrawn

	(Co-) Spokespersons	Affiliation	Title of the experiment	Approval status (PAC recommendation)	Beamline	Status
E50	H.Noumi	Osaka U	Charmed Baryon Spectroscopy via the (π,D^{*-}) reaction	Stage 1 The FIFC, IPNS, and E50 should investigate the beam-line feasibility	High p	
T51	S.Mihara	KEK	Research Proposal for COMET(E21) Calorimeter Prototype Beam Test	Test Experiment	K1.1BR	had to be stopped
T52	Y.Sugimoto	KEK	Test of fine pixel CCDs for ILC vertex detector	Test Experiment	K1.1BR	not performed yet
T53	D.Kawama	RIKEN	Test of GEM Tracker, Hadron Blind Detector and Lead-glass EMC for the J-PARC E16 experiment	Test Experiment	K1.1BR	not performed yet
T54	K.Miwa	Tohoku U	Test experiment for a performance evaluation of a scattered proton detector system for the Σp scattering experiment E40	Test Experiment	K1.1BR	not performed yet
T55	A.Toyoda	KEK	Second Test of Aerogel Cherenkov counter for the J-PARC E36 experiment	Test Experiment	K1.1BR	had to be stopped
E56	T.Maruyama	KEK	A Search for Sterile Neutrino at J-PARC Materials and Life Science Experimental Facility	Stage 2	MLF	
E57	J. Zmeskal	Stefan Meyer Institute for Subatomic Physics	Measurement of the strong interaction induced shift and width of the 1s state of kaonic deuterium at J-PARC	Stage 1	K1.8BR	in preparation
P58	M. Yokoyama	U. Tokyo	A Long Baseline Neutrino Oscillation Experiment Using J-PARC Neutrino Beam and Hyper-Kamiokande	Deferred	neutrino	
T59	A. Minamino	Kyoto U	A test experiment to measure neutrino cross sections using a 3D grid-like neutrino detector with a water target at the near detector hall of J-PARC neutrino beam-line	To be arranged by IPNS and KEK-T2K	neutrino monitor bld	Finished
T60	T. Fukuda	Toho U	Proposal of an emulsion-based test experiment at J-PARC	Arranged by IPNS and KEK-T2K	neutrino monitor bld	Finished
E61	M. Wilking	Stony Brook U	NuPRISM/TITUS	Stage 1 PAC encourages to refine the scientific and placement arguments in preparation for a new review committee for IWCD (one of near detectors of Hyper-Kamiokande)	neutrino	
E62	R. Hayano, S. Okada, H. Outa	U. Tokyo, RIKEN	Precision Spectroscopy of kaonic atom X-rays with TES	Stage 2	K1.8BR	Finished
E63	H. Tamura	Tohoku U	Gamma-ray spectroscopy of light hypernuclei II	Stage 2	K1.1	BL not ready yet. Exp. in
T64	Y. Koshio	Okayama U	Measurement of the gamma-ray and neutron background from the T2k neutrino/anti-neutrino at J-PARC B2 Hall	Arranged by IPNS and KEK-T2K	neutrino	
E65	T. Nakaya	Kyoto U	Proposal for T2K Extended Run	Stage 1	neutrino	
T66	T. Fukuda	Nagoya U	Proposal of an emulsion-based test experiment at J-PARC	Test Experiment	neutrino	
P67	I. Meigo	JAEA	Measurement of displacement cross section of proton in energy region between 3 and 30 GeV for high-intensity proton accelerator facility	Carry out the experiment within the framework of facility development	MR	
T68	T. Fukuda	Nagoya U	Extension of T60/T66 Experiment: Proposal for the Run from 2017 Autumn	Test Experiment	neutrino	
E69	A. Minamino	Yokohama National U	Study of neutrino-nucleus ineraction at around 1GeV using cuboid lattice neutrino detector, WAGASHI, muon range detectors and magnetized spectrometer, Baby MIND, at J- PARC neutrino monitor hall	Stage 2	neutrino	
E70	T. Nagae	Kyoto U	Proposal for the next E05 run with the S-2S spectrometer	Stage 2	K1.8	
E71	T. Fukuda	Nagoya U	Proposal for precise measurement of neutrinop-water cross- section in NINJA physics run	Stage-2	neutrino	
E72	K. Tanida	JAEA	Search for a Narrow Λ^* Resonance using the p(K-, Λ)η Reaction with the hypTPC Detector	Stage-2	K1.8BR	
P73	Yue Ma	RIKEN	$^{3}_{\Lambda}$H and $^{4}_{\Lambda}$H mesonic weak decay lifetime measurement with ^{3,4}He(K^-, π^0)$^{3,4}_{\Lambda}$H reaction	Deferred Submitted a test experiment proposal (P77)	K1.8BR	
P74	A.Feliciello	INFN, Torino	Direct measurement of the 3ΛH and 4ΛH lifetimes using the 3,4He(π-, K0)3,4ΛH reactions	Deferred Decision of P74 proposal is after P73 pilot run.	K1.1	
P75	H.Fujioka	Tokyo Inst. Tech,	Decay Pion Spectroscopy of 5$\Lambda\Lambda$H Produced by Ξ-hypernuclear Decay	PAC recommends stage-1 approval for the Phase-1 run. The requested 7 days of running for this measurement is appropriate.	K1.8	
P76	H.M.Shimizu	Nagoya U	Searches for the Breaking of the Time Reversal Invariance in Polarized Epithermal Neutron Optics	Defferred PAC would be prepared for an evaluation when appropriate material is made available.	MLF	
T77	Yue Ma	RIKEN	Feasibility study for 3ΛH mesonic weak decay lifetime measurement with 3,4He(K-,π0)3,4ΛH reaction	Test Experiment	K1.8BR	

Organization and Committees

Organization Structure

J-PARC Center Management System Chart

as of April 1, 2019

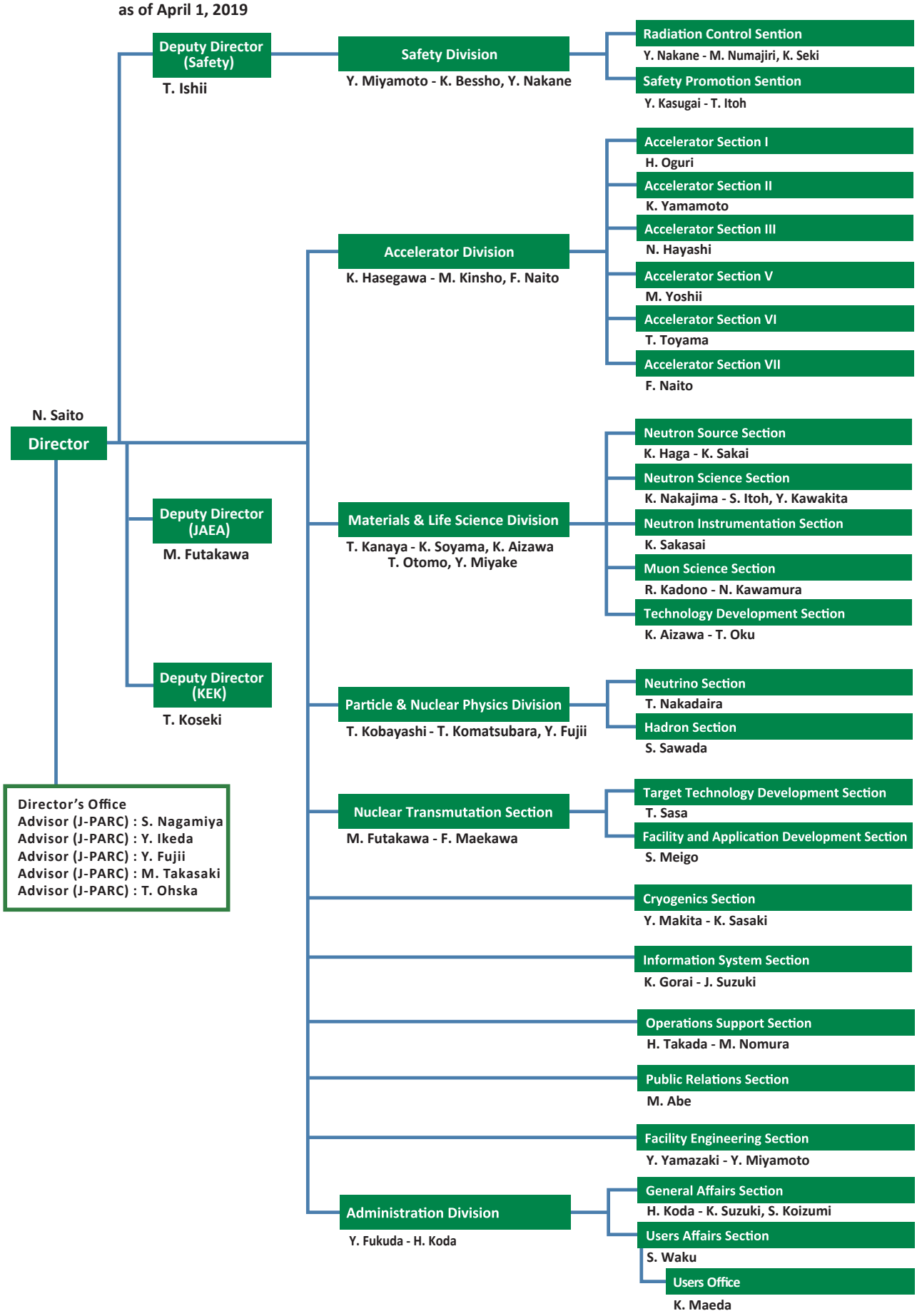

Members of the Committees Organized for J-PARC

(as of March, 2020)

1) Steering Committee

Kenji Sudo	Japan Atomic Energy Agency (JAEA), Japan
Masayasu Takeda	Japan Atomic Energy Agency (JAEA), Japan
Junji Haba	High Energy Accelerator Research Organization (KEK), Japan
Toshiyuki Momma	Japan Atomic Energy Agency (JAEA), Japan
Yukitoshi Miura	Japan Atomic Energy Agency (JAEA), Japan
Naohito Saito	J-PARC Center, Japan
Hiroyuki Oigawa	Japan Atomic Energy Agency (JAEA), Japan
Koki Uchimaru	High Energy Accelerator Research Organization (KEK), Japan
Katsuo Tokushuku	High Energy Accelerator Research Organization (KEK), Japan
Nobuhiro Kosugi	High Energy Accelerator Research Organization (KEK), Japan
Seiya Yamaguchi	High Energy Accelerator Research Organization (KEK), Japan

2) International Advisory Committee

Jean-Michel Poutissou	TRIUMF, Canada
Thomas Prokscha	The Paul Scherrer Institute (PSI), Switzerland
Jun Sugiyama	Comprehensive Research Organization for Science and Society (CROSS), Japan
Jie Wei	Michigan State University, USA
Roland Garoby	European Spallation Source, Sweden
Eckhard Elsen	European Organization for Nuclear Research (CERN), Switzerland
Patricia McBride	Fermi National Accelerator Laboratory (FNAL), USA
Robert Tribble	Brookhaven National Laboratory (BNL), USA
Donald F. Geesaman	Argonne National Laboratory, USA
Paolo Giubellino	GSI Helmholzzentrum für Schwerionenforschung, Germany
Hamid Aït Abderrahim	SCK • CEN, Belgium
Akira Hasegawa	Tohoku University, Japan
Paul Langan	Oak Ridge National Laboratory (ORNL), USA
Hidetoshi Fukuyama	Tokyo University of Science, Japan
Dan Alan Neumann	National Institute of Standards and Technology (NIST), USA
Andrew Dawson Taylor	Science and Technology Facilities Council (STFC), UK
Helmut Schober	Institut Laue–Langevin, France

3) User Consultative Committee for J-PARC

Tsuyoshi Nakaya	Kyoto University, Japan
Taku Yamanaka	Osaka University, Japan
Hiroaki Aihara	University of Tokyo, Japan
Takashi Kobayashi	High Energy Accelerator Research Organization (KEK), Japan
Hirokazu Tamura	Tohoku University, Japan
Tomofumi Nagae	Kyoto University, Japan
Hiroyuki Noumi	Osaka University, Japan

Shinya Sawada	High Energy Accelerator Research Organization (KEK), Japan
Fuminori Sakuma	RIKEN, Japan
Masaki Fujita	Tohoku University, Japan
Naoya Torikai	Mie University, Japan
Osamu Yamamuro	University of Tokyo, Japan
Yasushi Idemoto	Tokyo University of Science, Japan
Kazuhisa Kakurai	Comprehensive Research Organization for Science and Society (CROSS), Japan
Tosiji Kanaya	High Energy Accelerator Research Organization (KEK), Japan
Jun Akimitsu	Okayama University/Hiroshima University, Japan
Tadashi Adachi	Sophia University, Japan
Yasuhiro Miyake	High Energy Accelerator Research Organization (KEK), Japan
Jun Sugiyama	Comprehensive Research Organization for Science and Society (CROSS), Japan
Hiroyuki Kishimoto	Sumitomo Rubber Industries, Ltd.
Masaaki Hibi	Nippon Steel Corporation
Kenya Kubo	International Christian University, Japan
Hironori Kodama	Ibaraki Prefecture
Satoru Yamashita	University of Tokyo, Japan
Cheol-Ho Pyeon	Kyoto University, Japan
Yoshiyuki Kaji	Japan Atomic Energy Agency (JAEA), Japan

4) Accelerator Technical Advisory Committee

Wolfram Fischer	Brookhaven National Laboratory (BNL), USA
Mats Lindroos	European Spallation Source, Sweden
John Thomason	Science and Technology Facilities Council (STFC), UK
Sheng Wang	Institute of High Energy Physics (IHEP), China
Toshiyuki Shirai	National Institutes for Quantum and Radiological Science and Technology (QST),Japan
Alexander V Aleksandrov	Oak Ridge National Laboratory (ORNL), USA
Jie Wei	Michigan State Univ., USA
Robert Zwaska	Fermi National Accelerator Laboratory (FNAL), USA
Simone Gilardoni	European Organization for Nuclear Research (CERN), Switzerland

5) Neutron Advisory Committee

Robert McGreevy	Science and Technology Facilities Council (STFC), UK
Bertrand Blau	Paul Scherrer Institut (PSI), Switzerland
Michael Dayton	Oak Ridge National Laboratory (ORNL), USA
Yoshiaki Kiyanagi	Nagoya University, Japan
Christiane Alba-Simionesco	The Laboratoire Leon Brilloin (LLB), France
Jamie Schulz	Australian Nuclear Science and Technology Organization(ANSTO), Australia
Andreas Schreyer	European Spallation Source, Sweden
Sung-Min Choi	Korea Advanced Institute of Science and Technology, Korea
Yoshie Otake	RIKEN, Japan
Masaaki Sugiyama	Kyoto University, Japan
Christian Rüegg	The Paul Scherrer Institute (PSI), Switzerland

6) Muon Advisory Committee

Martin Månsson	KTH Royal Institute of Technology, Sweden
Thomas Prokscha	Paul Scherrer Institut (PSI), Switzerland
Andrew MacFarlane	University of British Columbia, Canada
Klaus Kirch	Paul Scherrer Institut (PSI), Switzerland
Kenya Kubo	International Chiristian University, Japan
Tadayuki Takahashi	University of Tokyo, Japan
Takashi Nakano	Osaka University, Japan
Hiroshi Amitsuka	Hokkaido University, Japan

7) Radiation Safety Committee

Yoshitomo Uwamino	RIKEN, Japan
Yoshihiro Asano	University of Hyogo, Japan
Hiroshi Watabe	Tohoku University, Japan
Takeshi Iimoto	University of Tokyo, Japan
Takeshi Murakami	National Institute of Radiological Science, Japan
Hitoshi Kobayashi	High Energy Accelerator Research Organization (KEK), Japan
Yoshihito Namito	High Energy Accelerator Research Organization (KEK), Japan
Shinichi Sasaki	High Energy Accelerator Research Organization (KEK), Japan
Hiroyuki Oigawa	Japan Atomic Energy Agency (JAEA), Japan
Michio Yoshizawa	Japan Atomic Energy Agency (JAEA), Japan
Nobuyuki Kinouchi	Japan Atomic Energy Agency (JAEA), Japan

8) Radiation Safety Review Committee

Tetsuro Ishii	Japan Atomic Energy Agency (JAEA), Japan
Yukihiro Miyamoto	Japan Atomic Energy Agency (JAEA), Japan
Masaharu Numajiri	High Energy Accelerator Researchi Organization (KEK), Japan
Hidetoshi Kikunaga	Tohoku University, Japan
Hiroshi Yashima	Kyoto Univaersity, Japan
Kanenobu Tanaka	Institute of Physical and Chemical Research (RIKEN), Japan
Nobuyuki Chiga	National Institute for Quantum and Radiological Science and Technoloty (QST), Japan
Toshiro Itoga	Japan Synchrotron Radiation Research Institute (JASRI), Japan
Yasuhiro Yamaguchi	Comprehensive Reserch Organization for Science and Society (CROSS), Japan
Akira Hirose	Japan Atomic Energy Agency (JAEA), Japan
Makoto Kobayashi	Japan Atomic Energy Agency (JAEA), Japan
Nobukazu Toge	High Energy Accelerator Researchi Organization (KEK), Japan
Kazuyoshi Masumoto	High Energy Accelerator Researchi Organization (KEK), Japan
Kazuo Hasegawa	Japan Atomic Energy Agency (JAEA), Japan
Yoshiaki Fujii	High Energy Accelerator Researchi Organization (KEK), Japan
Takeshi Komatsubara	High Energy Accelerator Researchi Organization (KEK), Japan
Kazuhiko Soyama	Japan Atomic Energy Agency (JAEA), Japan

9) MLF Advisory Board

Takamitsu Kohzuma	Ibaraki University, Japan
Takahisa Arima	The University of Tokyo, Japan
Taku J Sato	Tohoku University, Japan
Mitsuhiro Shibayama	The University of Tokyo, Japan
Yoji Koike	Tohoku University, Japan
Masaaki Sugiyama	Kyoto University, Japan
Yoshiharu Sakurai	Japan Synchrotron Radiation Research Institute(JASRI), Japan
Jun Takahara	Kyusyu University, Japan
Takashi Kamiyama	Hokkaido University, Japan
Toshio Yamaguchi	Fukuoka University, Japan
Hiroshi Amitsuka	Hokkaido University, Japan
Kenya Kubo	International Christian University, Japan
Toshiji Kanaya	High Energy Accelerator Research Organization (KEK), Japan
Hideki Seto	High Energy Accelerator Research Organization (KEK), Japan
Takashi Kamiyama	High Energy Accelerator Research Organization (KEK), Japan
Toshiya Otomo	High Energy Accelerator Research Organization (KEK), Japan
Yasuhiro Miyake	High Energy Accelerator Research Organization (KEK), Japan
Ryosuke Kadono	High Energy Accelerator Research Organization (KEK), Japan
Kazuhisa Kakurai	Comprehensive Research Organization for Science and Society (CROSS), Japan
Kazuya Aizawa	Japan Atomic Energy Agency (JAEA), Japan
Masayasu Takeda	Japan Atomic Energy Agency (JAEA), Japan
Kazuhiko Soyama	Japan Atomic Energy Agency (JAEA), Japan
Kenji Nakajima	Japan Atomic Energy Agency (JAEA), Japan
Yukinobu Kawakita	Japan Atomic Energy Agency (JAEA), Japan
Jun-ichi Suzuki	Comprehensive Research Organization for Science and Society (CROSS), Japan

10) Program Advisory Committee (PAC) for Nuclear and Particle Physics Experiments at the J-PARC 50Gev Proton Synchrotron

Nori Aoi	Osaka University, Japan
Ryuichiro Kitano	High Energy Accelerator Research Organization (KEK), Japan
Masahiro Kuze	Tokyo Institute of Technology, Japan
Hirokazu Tamura	Tohoku University, Japan
Ichiro Adachi	High Energy Accelerator Research Organization (KEK), Japan
Yoshitaka Itow	Nagoya University, Japan
Akira Ohnishi	Kyoto University, Japan
Deborah Harris	Fermi National Accelerator Laboratory (FNAL), USA
Steven Kettell	Brookhaven National Laboratory (BNL), USA
Josef Pochodzalla	University of Mainz, Germany
Monika Blanke	Karlsruhe Institute of Technology, Germany
Francois Le Diberder	The French National Institute of Nuclear and Particle Physics (IN2P3), France
Anthony William Thomas	University of Adelaide, Australia
Nu Xu	Lawrence Berkeley National Laboratory, USA
Rikutaro Yoshida	Thomas Jefferson National Accelerator Facility, USA
Kam-Biu Luk	University of California at Berkley, USA

11) TEF Technical Advisory Committee

Marc Schyns	SCK • CEN, Belgium
Michael Butzek	Forschungszentrum Jülich, Germany
Michael Wohlmuther	Paul Scherrer Institut (PSI), Switzerland
Yoshiaki Kiyanagi	Nagoya University, Japan
Keishi Sakamoto	National Institutes for Quantum and Radiological Science and Technology (QST), Japan
Georg Müller	Karlsruhe Institute of Technology, Germany
Masatoshi Kondo	Tokyo Institute of Technology, Japan

Main Parameters

Present main parameters of Accelerator

Linac	
Accelerated Particles	Negative hydrogen
Energy	400 MeV
Peak Current	50 mA
Pulse Width	0.32 ms for MLF 0.50 ms for MR-FX 0.10 ms for MR-SX
Repetition Rate	25 Hz
Freq. of RFQ, DTL, and SDTL	324 MHz
Freq. of ACS	972 MHz
RCS	
Circumference	348.333 m
Injection Energy	400 MeV
Extraction Energy	3 GeV
Repetition Rate	25 Hz
RF Frequency	0.938 MHz → 1.67 MHz
Harmonic Number	2
Number of RF cavities	12
Number of Bending Magnet	24
Main Ring	
Circumference	1567.5 m
Injection Energy	3 GeV
Extraction Energy	30 GeV
Repetition Rate	~0.4 Hz
RF Frequency	1.67 MHz → 1.72 MHz
Harmonic Number	9
Number of RF cavities	9
Number of Bending Magnet	96

Key parameters of Materials and Life Science Experimental Facility

Injection energy	3 GeV
Repetition rate	25 Hz
Neutron Source	
Target material	Mercury
Number of moderators	3
Moderator material	Liquid hydrogen
Moderator temperature/pressure	20 K/1.5 MPa
Number of neutron beam extraction ports	23
Muon production target	
Target material	Graphite
Number of muon beam extraction ports	4
Neutron instruments *	
Open for user program (general use)	21
Under commissioning/construction	0
Muon Instruments *	
Open for user program (general use)	3
Under commissioning/construction	1/0

(* As of May, 2020)

Events

Events

Formation of the First Industry-Academia Collaborative Consortium at J-PARC

An industry-academia collaborative "Functional Polymer Consortium" has been formed by five corporate groups led by Kuraray Co. Ltd., Sumitomo Bakelite Co., Ltd., DIC Corporation, Nissan Chemical Corporation, and Mitsui Chemicals, Inc., and an academic research team made up of Kyushu University, Nagoya Institute of Technology, Mie University, and KEK. A ceremony to commemorate their cooperation was held on April 5.

J-PARC Hello Science: "From High Intensity Proton Acceleration to Train Acceleration-Wide-Ranging applications of Broadband Cavity System"

On April 26, at a Science Café in Tokai Village, Ibaraki Prefecture, Dr. Chihiro Omori of the Accelerator Division spoke on the "broadband cavity systems" used at J-PARC. This technology is in use not only at J-PARC, but also at many circular accelerators at the European Organization for Nuclear Research (CERN).

Attempts are being made to expand to a broader range of applications for consumer use, such as development of energy-saving transformers for railways.

At Tokai Industry and Information Plaza "Ivil"

The J-PARC Center held a Safety Day meeting to remember the accident of radioactive material leak at the Hadron Experimental Facility that occurred on May 23, 2013

At the information exchange meeting on May 24, J-PARC Center presented the Best Practice Award, Creativity Award, and Sanitation Consideration Award to groups that exhibited performance in safety initiatives at workplaces in the previous fiscal year.

2nd MLF General Meeting held

The second general meeting of the MLF (Materials and Life Science Experimental Facility) was held on July 10 at the Ibaraki Quantum Beam Research Center (IQBRC). Outside researchers, involved in the MLF, from J-PARC, the Comprehensive Research Organization for Science and Society (CROSS), and the Ibaraki Prefecture Beamline (Ibaraki University) took part in it, aiming to exchange information on their current situations and deepen mutual understanding.

Group Photo

J-PARC PAC

Meetings of the J-PARC Program Advisory Committee (PAC) for the Nuclear and Particle Physics Experiments were held from July 16 to 19, and also from January 16 to 18 2020. The committee provided advice on how to proceed with planning of nuclear and particle physics research, using the main ring accelerator (MR) at J-PARC.

Debriefing on the industrial use of J-PARC MLF

The J-PARC Center held its fourth debriefing session on the industrial use of MLF this year on July 18 and 19, with many participants from companies, universities, and research institutes.

J-PARC booth exhibited in GSA

Geo Space Adventure (GSA) is operated by some volunteers from Hida City, Gifu Prefecture, which provides tours to Super-Kamiokande (SK). Every July. J-PARC plays a part in the T2K international collaboration that pursues neutrino research by shooting neutrinos towards SK. "T2K" is an abbreviation of "Tokai to Kamiokande". J-PARC carried out PR activities on July 13 and 14.

Iron balls scattering with a Gauss accelerator

"Eco-Festival Hitachi 2019" in Hitachi City

Eco-Festival Hitachi is the largest environmental event in Ibaraki Prefecture. At present, research on neutron applications is pursued in J-PARC's MLF, and companies are working to develop high-performance tires and storage batteries, which are eco-friendly. On July 20, J-PARC exhibited commercialized eco-tires and explained their activities.

J-PARC Center and DOE sign a cooperative agreement

The J-PARC Center has concluded a new cooperative agreement with the US Department of Energy (DOE) for the purpose of boosting collaboration in the high-power spallation neutron source research and related fields. On August 7, J-PARC Center's Director Naohito Saito and DOE's Office of Science Director Chrisotpher Fall signed the agreement.

Signing ceremony for cooperative agreement with DOE

J-PARC Open House 2019

J-PARC Open House was held on August 25. More than 1,500 visitors attended the event. They had the chance to tour the accelerator, hadron, neutrino, and other facilities opened for the event. Families had fun with many workshops such as light kaleidoscopes, spinning tops, color-changing bead straps, super balls, slime and so on.

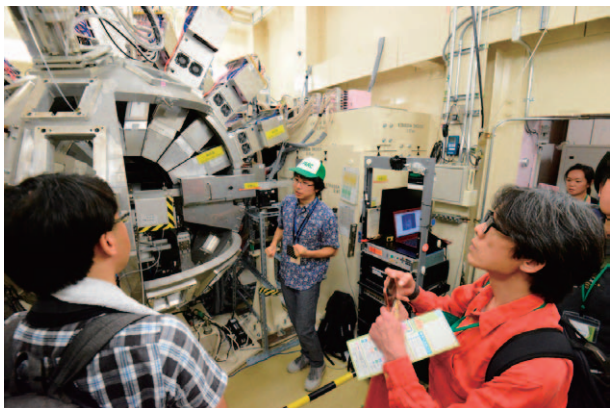

Visitors saw "iBIX (The IBARAKI biological crystal diffractometer) up close.

J-PARC Hello Science: "Identifying Energy Related Materials with Muon Particles"

Hello Science on September 20 featured a talk on research into energy-related materials using muons, by inviting Dr. Jun Sugiyama, Neutron Science and Technology Center of the Comprehensive Research Organization for Science and Society (CROSS).

J-PARC 10th Anniversary Ceremony, J-PARC Symposium 2019

The "10th Anniversary Ceremony, J-PARC Symposium 2019" was held at the Tsukuba International Congress Center to commemorate 10 years of operations at the entire J-PARC facility.

On the first day, the public lecture on the topic of "Searching for the origins of the Universe, Matter and Life" drew around 330 participants. A panel discussion titled "Role of Science in Societies, Role of Japan in the World" took place on the second day. This was followed by the anniversary ceremony to which approximately 600 attendees from Japan and overseas were invited. A commemorative lecture was given by Professor Takaaki Kajita, laureate of the 2015 Nobel Prize in Physics.

The following day, some researchers toured J-PARC.

Tsukuba International Congress Center

Symposium participants

Koichiro Nishikawa Memorial Symposium

Former J-PARC Center deputy director and KEK professor emeritus Koichiro Nishikawa passed away in November 2018. The "Koichiro Nishikawa Memorial Symposium" was held at the KEK Tsukuba Campus Kobayashi Hall on September 27 to commemorate his accomplishments. He made outstanding contributions to the research at J-PARC with his strong leadership skills, including pioneering research into neutrino physics as the spokesperson for the "T2K" experiment.

J-PARC Hello Science: "Creating High-Intensity Beams" – A story of Electricity and Magnets

Dr. Tomohiro Takayanagi of the Accelerator Division is engaged in the development of the bump electromagnets installed in the beam injection section of J-PARC's second-stage circular accelerator, a 3 GeV synchrotron. At the Hello Science event on November 29, he explained that J-PARC employs a world-class high-intensity proton beam to produce secondary particles used in various experiments.

Meeting of the T2K Collaboration Held

From November 18 to 22, a meeting of the T2K collaboration was held at the Ibaraki quantum Beam Research Center (IQBRC). The beam for the T2K experiment had been shut down for about a year and a half, and the data acquisition was resumed on November 5.

The meeting began with reports on the operation situation of each detector. Furthermore, there was a report on a plan by incorporating gadolinium (Gd) into the Super-Kamiokande (SK) neutrino detectors in Kamioka-cho, Gifu Prefecture.

19th Youngsters' Science Festival, Hitachi Event- "Are Magnets and Electricity Friends?!-Single-Pole Motor Project and Experiment"

The Youngsters' Science Festival is sponsored by the Japan Science Foundation and is held in regions throughout Japan. The aim is to show children the wonders of science.

On December 1, the J-PARC Center presented an experiment with a single-pole motor, in which a copper wire spins around a dry-cell battery placed on top of a magnet. Children were trying out various copper wire shapes until their motors spun well.

19th Collaboration Meeting for the Muon g-2/EDM Experiment Held

A collaboration meeting was held from December 2 to 5 for the experiment (E34) on the muon's anomalous magnetic moment (g-2) and electric dipole moment (EDM). The Muon g-2/EDM Experiment is an international collaborative research project. The meeting hosted about 100 participants from seven countries.

Group Phoro

7th Koshien Science Championship for Juniors-Gauss Accelerator demonstration

On December 8, in the Koshien Science Championship for junior high students, teams of six students from 47 prefectures of Japan competed in problem solving ability.

At the exhibition session, J-PARC performed a Gauss accelerator experiments and many students enjoyed observing the speed of a steel ball collision with neodymium magnets.

Collaboration Meeting between SNS and J-PARC on Nuclear Spallation Neutron Sources Held

From December 10 to 13, a collaboration meeting was held between researchers from the Spallation Neutron Source (SNS) of Oak Ridge National Laboratory (OENL) in the U.S. and the Materials and Life Science Experimental Facility (MLF) of J-PARC.

Both use mercury as a target material and are facing similar problems with system equipment. Therefore, related information was exchanged between the two organizations.

Fiscal 2019 J-PARC Center Safety Audit Conducted

On December 16, the J-PARC Center Safety Audit for fiscal year 2019 was conducted by external audit committee members. After that, the J-PARC Deputy Director Tetsuro Ishii led a site inspection of the work implementation situation at the Hadron Experimental Facility.

Site inspection at the Hadron Experimental Facility

J-PARC Hello Science: "Investigating the Origin of Matter in the Universe: with Mysterious Neutrino Particles"

We invited Professor Satoshi Koizumi (Graduate School of Science and Engineering, Ibaraki University) as an instructor on December 20. Dr. Koizumi spoke on the results of research using the neutrons of the MLF to observe the function of shampoo bubbles.

He concluded the lecture by pointing out that a recent experiment was carried out jointly with Nara Women's University and other institutions, using the IBARAKI Materials Design Diffractometer (iMATERIA).

7th Accelerator Facility Safety Symposium Held

From January 23 to 24 2020, the 7th Accelerator Facility Safety Symposium was held at the Ibaraki quantum Beam Research Center (IQBRC). The main themes this time were "Interlocks at Accelerator Facilities" and "Ensuring Safety in Machine Work".

Participants photo

J-PARC Advisory Committee Held

From February 6 to 26, the J-PARC Center held advisory committee meetings in four areas: Transmutation Experimental Facility Technology (T-TAC), Neutron Experimental Facility (NAC), Accelerator Technology (A-TAC), and Muon Experimental Facility (MAC). Experts from all over the world gathered and gave advice and recommendations regarding the status of J-PARC's accelerators and experimental facilities, research progress, and the future plans.

J-PARC Science Experiment Classes

On February 13, students constructed pendulum bell projects in the science club at Shirakata Elementary School in Tokai Village. This time the theme was static electricity. The children worked hard by rubbing vinyl tape with tissue paper and cheered when their bells made a sound.

Pendulum bell generating static electricity using a PVC

Special video class "Introduction to the J-PARC Accelerator – "Let's Learn about Accelerators using a Gauss Accelerator!"

In response to the spread of the novel coronavirus infections, school closures happened all over Japan. The Japan Association of Communication for Science and Technology (JACST), formed by public relations officials of universities and research institutions nationwide, has established a website for elementary, junior high, and high school students who were spending a lot of time at home.

Dr. Tatsunobu Shibata (KEK Associate Professor) produced an exclusive lesson video to explain accelerators in an easy-to-understand manner. It was uploaded on the J-PARC website on March 19.

Dr. Tatsunobu Shibata explaining J-PARC accelerators in the video

Visitors

Chen Yanwei, Director of China Spallation Neutron Source (CSNS), Institute of High Energy Physics (April 24)

Brent K. Park, Deputy Administrator for Defense Nuclear Nonproliferation, Department of Energy (DOE) (August 28)

Ayano Kunimitsu, member of the Diet (November 11)

Laura Thorborg, Minister of Foreign Affairs of Denmark (December 10)

Jiang Xingdong, Vice President of China Institute of Atomic Energy (CIAE) (December 11)

Iulia Georgescu, chief editor of Nature Reviews Physics (January 23 2020)

Sanjay Kumar Verma, Indian Ambassador (February 5 2020)

There were 2,767 visitors to J-PARC for the period from April 2019 to the end of March 2020.

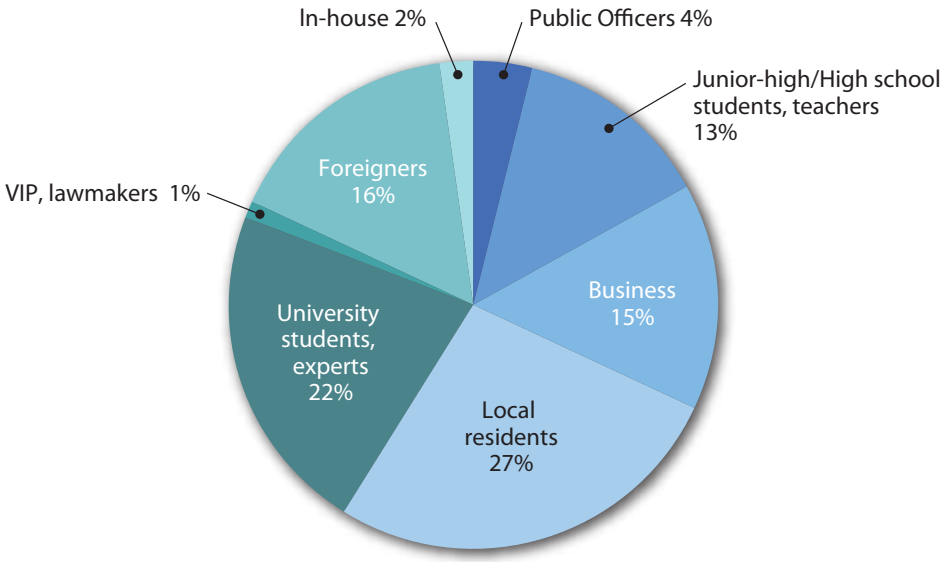

Publications

Publications in Periodical Journals

A-001
K. Mukai, *et al*.
Experimental Visualization of Interstitialcy Diffusion of Li Ion in β-Li2TiO3
ACS Appl. Energy Mater., 2, 5481-5489

A-002
S. Goto, *et al*.
Positive Weiss Temperature in Layered Antiferromagnetic FeNiN for High-Performance Permanent Magnets
ACS Appl. Nano Mater., 2, 6909-6917

A-003
M. Inutsuka, *et al*.
Adhesion Control of Elastomer Sheet on the Basis of Interfacial Segregation of Hyperbranched Polymer
ACS Macro Letters, 8, 267-271

A-004
Y. Sawama, *et al*.
Birch-Type Reduction of Arenes in 2-Propanol Catalyzed by Zero-Valent Iron and Platinum on Carbon
ACS Omega, 4, 11522-11531

A-005
Y. Shibuya, *et al*.
Continuous mesoporous aluminum oxide film with perpendicularly oriented mesopore channels
ACS Omega, 4, 17890-17893

A-006
K. Yamashita, *et al*.
Crystal structure of a high-pressure phase of magnesium chloride hexa-hydrate determined by in-situ X-ray and neutron diffraction methods
Acta Crystallogr. C Struct. Chem., C75, 1605-1612

A-007
A. Ahadi, *et al*.
Reversible elastocaloric effect at ultra-low temperatures in nanocrystalline shape memory alloys
Acta Mater., 165, 109-117

A-008
A. Ahadi, *et al*.
Neutron diffraction study of temperature-dependent elasticity of B19´ NiTi---Elinvar effect and elastic softening
Acta Mater., 173, 281-291

A-009
H. Fukui, *et al*.
Structure change of monoclinic ZrO_2 baddeleyite involving softenings of bulk modulus and atom vibrations
Acta. Crystallogr. B Struct. Sci., 75, 742-749

A-010
Y. Zhong, *et al*.
Determination of fine magnetic structure of magnetic multilayer with quasi antiferromagnetic layer by using polarized neutron reflectivity analysis
AIP Advances, 10, 015323

A-011
H. Kawasoko, *et al*.
Investigation of magnetism and magnetic structure of anti-ThCr2Si2-type Tb2O2Bi by magnetization and neutron diffraction measurements
AIP Advances, 9, 115301

A-012
K. Osamura, *et al*.
Inverted-parabolic and weak strain dependencies on the critical current in practical< 110> and< 100> oriented REBCO tapes
AIP Advances, 9, 75216

A-013
Y. Wang, *et al*.
Pressure-Induced Diels-Alder Reactions in C6H6-C6F6 Cocrystal towards Graphane Structure
Angew. Chem. Int. Ed., 58, 1468-1473

A-014
P. Miao, *et al*.
Revealing magnetic ground state of a layered cathode material by muon spin relaxation and neutron scattering experiments
Appl. Phys. Lett., 114, 203901

A-015
K.M. Kojima, *et al*.
Electronic structure of interstitial hydrogen in In-Ga-Zn-O semiconductor simulated by muon
Appl. Phys. Lett., 115, 122104

A-016
N. Kimura, et.al.
Combined effect of bending and flattening on heat transfer performance of cryogenic sintered-wick heat pipe
Appl. Therm. Eng. 148 (2019), 878

A-017
C. Simpson, *et al*.
Sensitivity of Super-Kamiokande with Gadolinium to Low Energy Antineutrinos from Pre-supernova Emission
Astrophys. J. 885 (2019), 133

A-018
T. Sugiura, *et al*.
Biophysical parameters of the Sec14 phospholipid exchange cycle
Biophys. J., 116, 92-103

A-019
Y. Kameda, *et al*.
Origin of the Difference in Ion-Water Distances Determined by X-ray and Neutron Diffraction Measurements for Aqueous NaCl and KCl Solutions
Bull. Chem. Soc. Jpn., 92, 754-767

A-020
T. Matsunaga, *et al*.
Comprehensive elucidation of crystal structures of lithium-intercalated graphite
Carbon, 142, 513-517

A-021
N. Kitamura, *et al*.
The atomic structure of a MgCo2O4 nanoparticle for a positive electrode of a Mg rechargeable battery
Chem. Commun., 55, 2517-2520

A-022
T. Sugahara, *et al*.
Small-angle neutron scattering study of micelle structure and hydration behavior of oleic acid-based gemini surfactant
Chem. Lett., 48, 1050-1053

A-023
M. Harada, *et al*.
Compositional Segregation in Cross Section of Wet Nafion Thin Film on Platinum Surface
Chem. Lett., 48, 51-54

A-024
M. Nakano
Evaluation of interbilayer and transbilayer transfer dynamics of phospholipids using time-resolved small-angle neutron scattering
Chem. Pharm. Bull, 67, 316-320

A-025
T. Sato, *et al*.
Hydrogen-Release Reaction of a Complex Transition Metal Hydride with Covalently Bound Hydrogen and Hydride Ions
Chem. Phys. Chem., 20, 1392-1397

A-026
S. Benz, *et al*.
Ammonothermal Synthesis, X-Ray and Time-of-Flight Neutron Crystal-Structure Determination, and Vibrational Properties of Barium Guanidinate, Ba(CN3H4)2
Chemistryopen, 8,, 327-332

A-027
N.V. Mdlovu, *et al*.
Iron oxide-pluronic F127 polymer nanocomposites as carriers for doxorubicin drug delivery system

Colloids Surf. A Physicochem. Eng. Asp., 562, 361-369

A-028
K. Suzuki, ,*et al*.
Quench protection for high Tc superconducting rotating gantry model magnet with I-V characteristics measured in the temperature range of 40-83 K
Cryogenics, 100, p.28

A-029
R. Maruyama, *et al*.
Coherent magnetization rotation of a layered system observed by polarized neutron scattering under grazing incidence geometry
Crystals, 9, 383

A-030
TN Lam, *et al*.
Comparing Cyclic Tension-Compression Effects on CoCrFeMnNi High-Entropy Alloy and Ni-Based Superalloy
Crystals, 9, 420

A-031
T. Matsukawa, *et al*.
Average and local structures of κ-phase CeZrO4 crystals by neutron powder diffraction
CrystEngComm, 21, 6335-6339

A-032
M. Sugishima, *et al*.
Bilin-metabolizing enzymes: site-specific reductions catalyzed by two different type of enzymes
Curr. Opin. Struct. Biol., 59, 73-80

A-033
T. Nakane, *et al*.
Magnetic, thermal, and neutron diffraction studies of a coordination polymer: bis(glycolato)cobalt(II)
Dalton Transactions, 48, 333

A-034
Y. Idemoto, *et al*.
Synthesis, crystal structure and electrode properties of spinel-type MgCo2−xMnxO4
Electrochemistry, 87, 220-228

A-035
T. Kawamoto, *et al*.
Sublayered Structures of Hydrated Nafion® Thin Film Formed by Casting on Pt Substrate Analyzed by X-ray Absorption Spectroscopy under Ambient Conditions and Neutron Reflectometry at Temperature of 80°C and Relative Humidity of 30–80%
Electrochemistry, 87, 270-275

A-036
T. Yamaguchi, *et al*.
Ion hydration and association in an aqueous calcium chloride solution in the GPa range
Eur. J. Inorg. Chem., 2019, 1170-1177

A-037
N. Abgrall, *et al*.
Measurements of π±, K± and proton double differential yields from the surface of the T2K replica target for incoming 31 GeV/c protons with the NA61/SHINE spectrometer at the CERN SPS
Eur. Phys. J. C ,79 (2019), 100

A-038
D. Adams, *et al*.
First particle-by-particle measurement of emittance in the Muon Ionization Cooling Experiment
Eur. Phys. J. C, 79 (2019), 257

A-039
K. Furukawa, *et al*.
HE-LHC: The High-Energy Large Hadron Collider
Eur. Phys. J. Spec. Top., 228, 1109

A-040
K. Máthis, *et al*.
In-situ investigation of the microstructure evolution in long-period-stacking-ordered (LPSO) magnesium alloys as a function of the temperature
Front. Mater., 6, 270

A-041
T. Hattori, *et al*.
Development of a technique for high pressure neutron diffraction at 40 GPa with a Paris-Edinburgh press
High Press. Res., 39, 417-425

A-042
K. Suzuki, *et al*.
Test Result of the HL-LHC Beam Separation Dipole Model Magnet With the New Iron Cross Section
IEEE Trans. Appl. Supercond., 29 (2019), 4000905

A-043
M. Sugano, *et al*.
Development of 2-m Model Magnet of the Beam Separation Dipole With New Iron Cross Section for the High-Luminosity LHC Upgrade
IEEE Trans. Appl. Supercond., 29 (2019), 4003607

A-044
S. Takayama, *et al*.
Development of an HTS Accelerator Magnet With REBCO Coils for Tests at HIMAC Beam Line
IEEE Trans. Appl. Supercond., 29 (2019), 4004205

A-045
N. Amemiya, *et al*.
Test of Cryocooler-Cooled RE-123 Magnet on HIMAC Beam Line in S-Innovation Program
IEEE Trans. Appl. Supercond., 29 (2019), 4600305

A-046
T. Yagai, *et al*.
Stability Analysis of MgB2 Coils for SMES Application Consisting of Large-Scale Rutherford Cables
IEEE Trans. Appl. Supercond., 29 (2019), 4602705

A-047
M. Dhakarwal ,*et al*.
Electromechanical Characterization of the MgB2 Wire for Transmission Line Magnet System
IEEE Trans. Appl. Supercond., 29 (2019), 4802404

A-048
M. Jimbo, *et al*.
Investigation on IC Degradation of MgB2 Rutherford Cables by Deformation During Cabling Process
IEEE Trans. Appl. Supercond., 29 (2019), 8003305

A-049
H. Yamaguchi, *et al*.
Development of a CW-NMR Probe for Precise Measurement of Absolute Magnetic Field
IEEE Trans. Appl. Supercond., 29 (2019), 9000904

A-050
D. Schoerling, *et al*.
The 16 T Dipole Development Program for FCC and HE-LHC
IEEE Trans. Appl. Supercond., 29, 4003109

A-051
A. Ballarino, *et al*.
The CERN FCC Conductor Development Program: A Worldwide Effort for the Future Generation of High-Field Magnets
IEEE Trans. Appl. Supercond., 29, 6001709

A-052
C. Ohmori, M. Paoluzzi
Development of Radiation-Hard Solid-State Ampli ers for kilo-Gray Environments using COTS components
IEEE Trans. Nucl. Sci, 66, No. 10, October 2019, p. 2188-2195, DOI: 10.1109/tns. 2019.2937603

A-053
M. Ichikawa, *et al*.
Trigger Merging Module for the J-PARC E16 Experiment
IEEE Trans. Nucl. Sci., 66 (2019), 2022

A-054
F. Tamura, *et al*.
Development of next-generation LLRF control system for J-PARC rapid cycling synchrotron
IEEE Trans. Nucl. Sci., 66(7), p.1242 - 1248, 2019/07

A-055
T. Shimogawa, *et al*.
A Control System of New magnet Power Converter for J-PARC Main Ring Upgrade
IEEE Trans. Nucl. Sci., 66, 1236

A-056
R. Kataoka, *et al*.
Facile Synthesis of LiH-Stabilized Face-Centered-Cubic YH3 High-Pressure Phase by Ball Milling Process
Inorg. Chem. 58, 13102-13107

A-057
J. Hu, *et al*.
A case of multifunctional intermetallic compounds: negative thermal expansion coupling with magnetocaloric effect in (Gd,Ho)(Co,Fe)2
Inorg. Chem. Front., 6, 3146-3151

A-058
Y. Yasui, *et al*.
Discovery of a Rare-Earth-Free Oxide-Ion Conductor Ca3Ga4O9 by Screening through Bond Valence-Based Energy Calculations, Synthesis, and Characterization of Structural and Transport Properties
Inorg. Chem., 58, 9460-9468

A-059
H. Mizoguchi, *et al*.
Zeolitic Intermetallics: LnNiSi (Ln = La–Nd)
J. Am. Chem. Soc., 141, 3376-3379

A-060
Y. Yasuda, *et al*.
Molecular Dynamics of Polyrotaxane in Solution Investigated by Quasi-Elastic Neutron Scattering and Molecular Dynamics Simulation: Sliding Motion of Rings on Polymer
J. Am. Chem. Soc., 141, 9655-9663

A-061
S. Koizumi, *et al*.
Microstructure and water distribution in catalysts for polymer electrolyte fuel cells, elucidated by contrast variation small-angle neutron scattering
J. Appl. Cryst., 52, 791-799

A-062
T. Yamada, *et al*.
Single-crystal time-of-flight neutron Laue methods: application to manganese catalase from Thermus thermophilus HB27
J. Appl. Cryst., 52, 972-983

A-063
T. Kumada, *et al*.
Development of spin-contrast-variation neutron reflectometry for the structural analysis of multilayer films
J. Appl. Crystallogr., 52, 1054-1060

A-064
T. Fukuda, *et al*.
Neutron diffraction study on martensitic transformation under compressive stress in an ordered Fe3Pt
J. Appl. Phys., 126 (2019), 25107

A-065
T. Komori, *et al*.
Magnetic reversal in rare-earth free Mn4–xNixN epitaxial films below and above Ni composition needed for magnetic compensation around room temperature
J. Appl. Phys., 127, 043903

A-066
M. Ooe, *et al*.
Direct observation of mobility of thin polymer layers via asymmetric interdiffusion using neutron reflectivity measurements
J. Chem. Phys., 151, 244905

A-067
H. Iwase, *et al*.
Rheo-SANS study on relationship between micellar structures and rheological behavior of cationic gemini surfactants in solution
J. Colloid Interface Sci., 538, 357-366

A-068
H. Frielinghaus, *et al*.
The locally columnar model for clay/polymer systems: Connections to scattering experiments
J. Colloid Interface Sci., 544, 172-177

A-069
T. Hasegawa, *et al*.
MeV-scale reheating temperature and thermalization of oscillating neutrinos by radiative and hadronic decays of massive particles
J. Cosmol. Astropart. Phys., 12 (2019), 12

A-070
Y. Hino, *et al*.
Aging study of Gd concentration in LAB-based Gd loaded liquid scintillator exposed to passivated stainless steel
J. Instrum., 14 (2019), P09007

A-071
M. Nakazawa, *et al*.
Prototype analog front-end for negative-ion gas and dual-phase liquid-Ar TPCs
J. Instrum., 14 (2019), T01008

A-072
Y. Hino, *et al*.
Stainless steel tank production and tests for the JSNS2 neutrino detector
J. Instrum., 14 (2019), T09001

A-073
J. Park, *et al*.
Production and optical properties of liquid scintillator for the JSNS2 experiment
J. Instrum., 14 (2019), T09010

A-074
Y. Kitanaka, *et al*.
Composition-driven structural variation in ferrielectric phase of (Bi1/2Na1/2)TiO3-Ba(Mg1/3Nb2/3)O3
J. J. Appl. Phys., 58, SLLA04

A-075
K. Shimizu, *et al*.
Neutron Imaging Analysis of Hydrogen Content in Pure Palladium and Aluminum Alloys
J. Japan Inst. Metals, 83, 434-440

A-076
T. Matsushita, *et al*.
Generation of ^{4}He$_2^*$ Clusters via Neutron-^{3}He Absorption Reaction towards Visualization of Full Velocity Field in Quantum Turbulence
J. Low Temp. Phys., 196, 275-282

A-077
K. Asami, *et al*.
Crystal structure analysis and evidence of mixed anion coordination at the Ce3+ site in Y3Al2(Al,Si)3(O,N)12 oxynitride garnet phosphor
J. Mater. Chem. C, 7, 1330-1336

A-078
S. Fujiwara, *et al*.
Dynamic properties of human-synuclein related to propensity to amyloid fibril formation
J. Mol. Biol., 431, 3229-3245

A-079
A. Hyde, *et al*.
Surface Properties of the Ethanol/Water Mixture: Thickness and Composition
J. Mol. Liq., 290, 111005

A-080
H. Abe, *et al*.
Static and dynamic properties of nano-confined water in room-temperature ionic liquids
J. Mol. Liq., 290, 111216

A-081
K. Yoshida, *et al*.
The effect of alkyl ammonium ionic liquids on thermal denaturation aggregation of β-lactoglobulin
J. Mol. Liq., 293, 111477

A-082
H. Iwamoto, S. Meigo
Unified description of the fission probability for highly excited nuclei
J. Nucl. Sci. and Technol, 56 160-171 (2019)

A-083
H. Ishikawa, *et al*.
Neutron spectrum change with thermal moderator temperature in a compact electron accelerator-driven neutron source and its effects on spectroscopic neutron transmission imaging
J. Nucl. Sci. Tech., 56, 221

A-084
A. Kimura, *et al*.
Measurements of the 243Am neutron capture and total cross sections with ANNRI at J-PARC
J. Nucl. Sci. Technol., 56, 479-492

A-085
M. Hirai, *et al*.
Observation of protein and lipid membrane structures in a model mimicking the molecular-crowding environment of cells using neutron scattering and cell debris
J. Phys. Chem. B, 123, 3189-3198

A-086
Y. Kameda, *et al*.
Solvation Structure of Li+ in Methanol and 2-Propanol Solutions Studied by ATR-IR and Neutron Diffraction with 6Li/7Li Isotopic Substitution Methods
J. Phys. Chem. B, 123, 4967-4975

A-087
N. Nishi, *et al*.
Potential-Dependent Structure of the Ionic Layer at the Electrode Interface of an Ionic Liquid Probed Using Neutron Reflectometry
J. Phys. Chem. C, 123, 9223-9230

A-088
H. Akiba, *et al*.
Structural and Thermodynamic Studies of Hydrogen Absorption/Desorption Processes on PdPt Nanoparticles
J. Phys. Chem. C, 123, 9471-9478

A-089
M. Russina, *et al*.
Nanoscale Dynamics and Transport in Highly Ordered Low-Dimensional Water
J. Phys. Chem. Lett., 10, 6339-6344

A-090
S. Fujiwara, *et al*.
Segment Motions of Proteins under Non-native States Evaluated Using Quasielastic Neutron Scatering
J. Phys. Chem. Lett., 10, 7505-7509

A-091
R. Y. Umetsu, *et al*.
Atomic ordering, magnetic properties, and electronic structure of Mn2CoGa Heusler alloy
J. Phys. Condens. Matter, 31, 65801

A-092
K. Abe, *et al*.
Search for neutral-current induced single photon production at the ND280 near detector in T2K
J. Phys. G, 46 (2019), 08LT01

A-093
T. Kim, *et al*.
Hybridization and Decay of Magnetic Excitations in Two-Dimensional Triangular Lattice Antiferromagnets
J. Phys. Soc. Japan, 88, 081003

A-094
R. Kajimoto, *et al*.
Crystal Structures of Highly Hole-Doped Layered Perovskite Nickelate Pr2−xSrxNiO4 Studied by Neutron Diffraction
J. Phys. Soc. Japan, 88, 114602

A-095
S. Asano, *et al*.
Oxidation Annealing Effects on the Spin-Glass-Like Magnetism and Appearance of Superconductivity in T*-type La1−x/2Eu1−x/2SrxCuO4 (0.14 ≤ x ≤ 0.28)
J. Phys. Soc. Japan, 88, 84709

A-096
K. Iwasa
Neutron Scattering Studies on 4f2-Electron Multipoles in Pr-based Systems
J. Phys. Soc. Jpn. , 88, 081005

A-097
K. Shiomi, *et al*.
Approach to New Physics through Kaon Rare Decay Study
J. Phys. Soc. Jpn., 74 (2019), 830

A-098
S. Itoh, *et al*.
Neutron Brillouin Scattering and Low-Q Dynamics in Condensed Matter
J. Phys. Soc. Jpn., 88, 081004

A-099
T. Nakajima, *et al*.
Observation of magnetic skyrmions by neutron scattering
J. Phys. Soc. Jpn., 88, 081006

A-100
K. Kaneko, *et al*.
Unique Helical Magnetic Order and Field-Induced Phase in Trillium Lattice Antiferromagnet EuPtSi
J. Phys. Soc.f Jap., 88, 013702

A-101
Y. Idemoto, *et al*.
Average, electronic, and local structures of LiMn2-xAlxO4 in charge-discharge process by neutron and synchrotron X-ray
J. Power Sources, 410-411, 38-44

A-102
N. Kitamura, *et al*.
Study of atomic ordering across the layer in lithium-rich layered positive electrode material towards preparation process optimization
J. Power Sources, 437, 226905

A-103
K. Ninomiya, *et al*.
Negative muon capture ratios for nitrogen oxide molecules
J. Radioanal. Nucl. Chem., 319, 767

A-104
G. Yoshida, *et al*.
Initial quantum levels of captured muons in CO, CO2, and COS
J. Radioanal. Nucl. Chem., 320, 283

A-105
K. Ninomiya, *et al*.
Development of non-destructive isotopic analysis methods using muon beams and their application to the analysis of lead
J. Radioanal. Nucl. Chem., 320, 801

A-106
W. Huang, *et al*.
Superionic lithium conductor with a cubic argyrodite-type structure in the Li–Al–Si–S system
J. Solid State Chem., 270, 487-492

A-107
T. Kawamoto, *et al*.
In-Plane Distribution of Water inside Nafion Thin Film Analyzed by Neutron Reflectivity at Temperature of 80C and Relative Humidity of 30-80% Based on 4-Layered Structural Model
Jpn. J. Appl. Phys., 58, SIID01

A-108
H. Hotchi, *et al*.
Beam dynamics study for beam loss mitigation in the J-PARC RCS
Kasokuki, 16, no. 2, p. 109 (2019)

A-109
H. Hotchi, *et al*.
Beam dynamics study for beam loss mitigation in the J-PARC RCS
Kasokuki, 16 no. 2, p.109 - 118, 2019/07

A-110
Y. Onuki, *et al*.
Anomalous Twinning as the Macroscopic Deformation Mechanism for AZ31 Magnesium Alloy
Key Eng. Mater., 810, 95-100

A-111
T. Miyazaki, *et al*.
Elucidation of a Heterogeneous Layered Structure in the Thickness Direction of Poly(vinyl alcohol) Films with Solvent Vapor-Induced Swelling
Langmuir, 35, 11099-11107

A-112
K. Imwiset, *et al*.
Novel flexible supramolecular assembly of dioleyldimethylammonium ion in a two-dimensional nanospace studied by neutron scattering
Langmuir, 35, 13977-13982

A-113
T. Sakamaki, *et al*.
Ion-Specific Hydration States of Zwitterionic Poly (sulfobetaine methacrylate) Brushes in Aqueous Solutions
Langmuir, 35, 1583-1589

A-114
S. Lee, *et al*.
Instability of Polystyrene Film and Thermal Behaviors Mediated by Unfavorable Silicon Oxide Inter-layer
Macromolecules, 52, 7524-7530

A-115
N. Itagaki, *et al*.
A Surface Effect on Frictional Properties for Thin Hydrogel Films of Poly(vinyl ether)
Macromolecules, 52, 9632

A-116
Y. Tomota, *et al*.
Dislocation densities and intergranular stresses of plastically deformed austenitic steels
Mater. Sci. Eng. A, 743, 32-39

A-117
H. Chae, *et al*.
Plastic anisotropy and deformation-induced phase transformation of additive manufactured stainless steel
Mater. Sci. Eng. A, 762, 138065

A-118
Y. Koyanagi, *et al*.
Investigation of strengthening mechanism in Ni–38Cr-3.8 Al alloy with fine lamellar structure by in situ neutron diffraction analysis
Mater. Sci. Eng. A, 773, 13822

A-119
T. Wan, *et al*.
Numerical study on the potential of cavitation damage in a lead-bismuth eutectic spallation target
Materials, 12(4), p.681_1 - 681_15, 2019/02

A-120
M. M. Schiavone, *et al*.
The multilevel structure of sulfonated syndiotactic-polystyrene model polyelectrolyte membranes resolved by extended Q-range contrast variation SANS
Membranes, 9, 136

A-121
T. Mibe
Physics of muonium and related topics
Meson, 49 (2019), 37

A-122
Y. Onuki, *et al*.
In Situ Observation of Bainite Transformation and Simultaneous Carbon Enrichment in Austenite in Low-Alloyed TRIP Steel Using Time-of-Flight Neutron Diffraction Techniques
Metall. Mat. Trans. A, 50, 4977-4986

A-123
K. Kiriyama, *et al*.
Development of a biaxial tensile testing machine for pulsed neutron experiments
MethodsX, 6, 2166-2175

A-124
K. Nagura, *et al*.
Size-tunable MRI-visible nitroxide-based magnetic mixed micelles: preparation, stability, and theranostic application
Nanotechnology, 30, 224002

A-125
K. Nawa, *et al*.
Triplon band splitting and topologically protected edge states in the dimerized antiferromagnet
Nat. Commun., 10, 2096

A-126
K. Fukui, *et al*.
Characteristic fast H– ion conduction in oxygen-substituted lanthanum hydride
Nat. Commun., 10, 2578(1-7)

A-127
J. Wang, *et al*.
Evidence for singular-phonon-induced nematic superconductivity in a topological superconductor candidate Sr0.1Bi2Se3
Nat. Commun., 10, 2802

A-128
M. Hirschberger, *et al*.
Skyrmion phase and competing magnetic orders on a breathing Kagome lattice
Nat. Commun., 10, 5831

A-129
Y. Fujishiro, *et al*.
Topological transitions among skyrmion- and hedgehog-lattice states in cubic chiral magnets
Nat. Commun., 1059

A-130
C. Aidala, *et al*.
Creation of quark-gluon plasma droplets with three distinct geometries
Nat. Phys., 15 (2019), 214

A-131
B. Li, *et al*.
Colossal barocaloric effects in plastic crystals
Nature, 567, 506-510

A-132
Y. Onodera, *et al*.
Origin of the mixed alkali effect in silicate glass
NPG Asia Mater., 11, 75

A-133
M. Hagihala, *et al*.
Magnetic states of coupled spin tubes with frustrated geometry in CsCrF4
npj Quantum Mater., 4, 14

A-134
S. Miyahara, *et al*.
The Analytical study of inventories and physicochemical configuration of spallation products produced in Lead-Bismuth Eutectic of Accelerator Driven System
Nucl. Eng. Des., 352, p.110192_1 - 110192_8, 2019/10

A-135
M. Otani, *et al*.
Response of microchannel plates to positrons from muon-decays
Nucl. Inst. Meth A 943, 162475-1 –162475-4 (2019)

A-136
Y. Nakazawa, *et al*.
Beam commissioning of muon beamline using negative hydrogen ions generated by ultraviolet light
Nucl. Inst. Meth. A 937, 164-167 (2019)

A-137
M. Otani, *et al*.
Compact buncher cavity for muons accelerated by a radio-frequency quadrupole
Nucl. Inst. Meth. A 946, 162693-1 – 162693-5 (2019)

A-138
M. Teshigawara, *et al*.
Measurement of neutron scattering cross section of nano-diamond with particle diameter of approximately 5 nm in energy range of 0.2 meV to 100 meV

Nucl. Instr. and Methods Phys. Res. A, 929, 113-120

A-139
C. A. Aidala, *et al*.
The SeaQuest spectrometer at Fermilab
Nucl. Instrum. Methods Phys. Res. A, 930 (2019), 49

A-140
Y. Obara, *et al*.
Profile measurement of circulating electrons in a synchrotron by inserting a carbon wire
Nucl. Instrum. Methods Phys. Res. A, 922 (2019), 108

A-141
Y. Noda, *et al*.
Dynamic nuclear polarization apparatus for contrast variation neutron scattering experiments on iMATERIA spectrometer at J-PARC
Nucl. Instrum. Methods Phys. Res. A, 923, 127-133

A-142
K. Ueno, *et al*.
Design and performance evaluation of front-end electronics for COMET straw tracker
Nucl. Instrum. Methods Phys. Res. A, 936 (2019), 297

A-143
Y. Nakazawa, *et al*.
Radiation study of FPGAs with neutron beam for COMET Phase-I
Nucl. Instrum. Methods Phys. Res. A, 936 (2019), 351

A-144
Y. Fujii, *et al*.
Development of the proton beam monitor based on the thin diamond crystal for the COMET Experiment
Nucl. Instrum. Methods Phys. Res. A, 936 (2019), 669

A-145
S. Shimizu, *et al*.
A new experimental method to search for T-violation using a sequential CeF3 scintillating calorimeter
Nucl. Instrum. Methods Phys. Res. A, 945 (2019), 162587

A-146
A. D. Pant, *et al*.
Characterization and optimization of ultra slow muon beam at J-PARC/MUSE: A simulation study
Nucl. Instrum. Methods Phys. Res. A: Accelerators, Spectrometers, Detectors and Associated Equipment, 929, 129-133

A-147
Z. Fang, *et al*.
Novel auto-startup technology for two cavities of a medical accelerator with one RF source
Nucl. Instrum. Methods Phys. Res. Sect. A, 922, 193

A-148
T. Oyama, *et al*.
Thermal neutron profile inside J-PARC main ring tunnel
Nucl. Instrum. Methods Phys. Res. Sect. A, 937, 98

A-149
S. Li, *et al*.
Iterative learning control-based adaptive beamloading compensation implementations in the J-PARC LINAC
Nucl. Instrum. Methods Phys. Res. Sect. A, 945, 162612

A-150
A. S. Tremsin, *et al*.
Non-destructive mapping of water distribution through white-beam and energy-resolved neutron imaging
Nucl. Instrum. Methods Phys. Res., A, 927, 174-183

A-151
J. K. Ahn, *et al*.
XXVIIth International Conference on Ultrarelativistic Nucleus-Nucleus Collisions (Quark Matter 2018)
Nucl. Phys. A, 982 (2019), 1038

A-152
A. Adare, *et al*.
XXVIIth International Conference on Ultrarelativistic Nucleus-Nucleus Collisions (Quark Matter 2018)
Nucl. Phys. A, 982 (2019), 1053

A-153
H. Sako
Studies of extremely dense matter in heavy-ion collisions at J-PARC
Nucl. Phys. A, 982 (2019), 959

A-154
M. Aoki, *et al*.
XXVIIth International Conference on Ultrarelativistic Nucleus-Nucleus Collisions (Quark Matter 2018)
Nucl. Phys. A, 982 (2019), 985

A-155
S. Yasui, *et al*.
Kondo phase diagram of quark matter
Nucl. Phys. A, 983 (2019), 90

A-156
M. G. Alexeev, *et al*.
Measurement of PT-weighted Sivers asymmetries inleptoproduction of hadrons
Nucl. Phys. B, 940 (2019), 34

A-157
T. Wan, *et al*.
Thermal-hydraulic analysis of the LBE spallation target head in JAEA
Nuclear Technology, 205(1-2), p.188 - 199, 2019/01

A-158
T. Hosobata, *et al*.
Elliptic neutron-focusing supermirror for illuminating small samples in neutron reflectometry
Opt. Express, 27, 26807

A-159
S. Kobayashi, *et al*.
Thermal aging effects on magnetisation reversals in a predeformed Fe-1wt%Cu alloy studied via first-order reversal curves
Philos. Mag. Lett., 99, 217-225

A-160
K. Akutsu-Suyama, *et al*.
Design and Characterization of a 2-(2′-Hydroxyphenyl)benzimidazole-Based Sr2+-Selective Fluorescent Probe in Organic and Micellar Solution Systems
Photochem. Photobiol. Sci., 18, 2531-2538

A-161
K. L. Browning, *et al*.
Role of conductive binder to direct solid-electrolyte interphase formation over silicon anodes
Phys. Chem. Chem. Phys., 21, 17356

A-162
T. Takamuku, *et al*.
Effects of the long octyl chain on complex formation of nickel(II) with dimethyl sulfoxide, methanol, and acetonitrile in Ionic liquid of [C8mim][TFSA]
Phys. Chem. Chem. Phys., 21, 3154-3163

A-163
K. Akutsu-Suyama, *et al*.
Controlled deuterium labelling of imidazolium ionic liquids to probe the fine structure of the electrical double layer using neutron reflectometry
Phys. Chem. Chem. Phys.,21, 17512-17516

A-164
A. Kyono, *et al*.
Crystal structure change of katoite, Ca3Al2(O4D4)3, with temperature at high pressure
Phys. Chem. Minerals, 46, 459-469

A-165
T. Ishikawa, *et al*.
Non-strange dibaryons studied in the γd → π0π0d reaction
Phys. Lett. B, 789 (2019), 413

A-166
S. Ajimura, *et al*.
"K-pp", a K-meson nuclear bound state, observed in 3He(K-, Λp)n reactions

Phys. Lett. B, 789 (2019), 620

A-167
S. Ajimura, *et al.*
"K-pp", a K-meson nuclear bound state, observed in 3He(K-, Λp)n reactions
Phys. Lett. B, 789, p.620

A-168
R. Akhunzyanov, *et al.*
Transverse extension of partons in the proton probed in the sea-quark range by measuring the DVCS cross section
Phys. Lett. B, 793 (2019), 188

A-169
A. AguilarArevalo, *et al.*
Search for heavy neutrinos in π ⟶ μν decay
Phys. Lett. B, 798 (2019), 134980

A-170
F. Tamura, *et al.*
Multiharmonic vector rf voltage control for wideband cavities driven by vacuum tube amplifiers in a rapid cycling synchrotron
Phys. Rev. Accel. Beams (Internet), 22(9), p.092001_1 - 092001_22, 2019/09

A-171
Y. Kondo, *et al.*
Development of a radio frequency quadrupole linac implemented with the equipartitioning beam dynamics scheme
Phys. Rev. Accel. Beams 22, 120101-1 – 120101-8 (2019)

A-172
K. Iida, *et al.*
Coexisting spin resonance and long-range magnetic order of Eu in EuRbFe4As4
Phys. Rev. B, 100, 014506

A-173
S. Klotz, *et al.*
High-pressure structure and electronic properties of YbD_2 to 34 GPa
Phys. Rev. B, 100, 0210101®

A-174
H. Suzuki, *et al.*
X-ray magnetic circular dichroism and neutron diffraction measurements of the magnetic moment of titanium in Sm(Fe0.8Co0.2)11Ti
Phys. Rev. B, 100, 144443

A-175
H. Tamatsukuri, *et al.*
Nonlinear piezomagnetoelectric effect in CuFeO2
Phys. Rev. B, 100, 201105

A-176
S. Ideta, *et al.*
Experimental investigation of the suppressed superconducting gap and double-resonance mode in Ba1−xKxFe2As2
Phys. Rev. B, 100, 235135

A-177
A. Koda, *et al.*
Coupled spin-charge-phonon fluctuation in the all-in/all-out antiferromagnet Cd2Os2O7
Phys. Rev. B, 100, 245113(1-6)

A-178
H. Kadowaki, *et al.*
Spin correlations of quantum-spin-liquid and quadrupole-ordered states of Tb2+xTi2-xO7+y
Phys. Rev. B, 99, 014406

A-179
J. Yamaura, *et al.*
Quantum dynamics of hydrogen in the iron-based superconductor LaFeAsO0.9D0.1 measured with inelastic neutron spectroscopy
Phys. Rev. B, 99, 220505®

A-180
K. P. Kramer, *et al.*
Band structure of overdoped cuprate superconductors: Density functional theory matching experiments
Phys. Rev. B, 99, 224509

A-181
K. Matan, *et al.*
Magnetic structure and high-field magnetization of the distorted kagome lattice antiferromagnet Cs2Cu3SnF12
Phys. Rev. B., 99, 224404

A-182
O. Morimatsu, *et al.*
Renormalization of the unitarized Weinberg-Tomozawa interaction without on-shell factorization and I = 0 KN-πΣ coupled channels
Phys. Rev. C, 100 (2019), 25201

A-183
N. Muramatsu, *et al.*
Measurement of neutral pion photoproduction off the proton with the large acceptance electromagnetic calorimeter BGOegg
Phys. Rev. C, 100 (2019), 55202

A-184
C. C. Haddock, *et al.*
Measurement of the total neutron-scattering cross-section ratios of noble gases of natural isotopic composition using a pulsed neutron beam
Phys. Rev. C, 100, 64002

A-185
S. Ahmed, *et al.*
First ultracold neutrons produced at TRIUMF
Phys. Rev. C, 99 (2019),25503

A-186
J .S. Randhawa, *et al.*
Observation of excited states in 20Mg sheds light on nuclear forces and shell evolution
Phys. Rev. C, 99 (2019), 21301

A-187
A. Adare, *et al.*
Multiparticle azimuthal correlations for extracting event-by-event elliptic and triangular flow in Au + Au collisions at √sNN = 200 GeV
Phys. Rev. C, 99 (2019), 24903

A-188
C. Aidala, *et al.*
Nonperturbative-transverse-momentum broadening in dihadron angular correlations in √sNN = 200 GeV proton-nucleus collisions
Phys. Rev. C, 99 (2019), 44912

A-189
K. Abe, *et al.*
Search for heavy neutrinos with the T2K near detector ND280
Phys. Rev. D, 100 (2019), 52006

A-190
K. Hasegawa, *et al.*
Molecular adsorbed layer formation on cooled mirrors and its impacts on cryogenic gravitational wave telescopes
Phys. Rev. D, 99 (2019), 22003

A-191
L. Wan, *et al.*
Measurement of the neutrino-oxygen neutral-current quasielastic cross section using atmospheric neutrinos at Super-Kamiokande
Phys. Rev. D, 99 (2019), 32005

A-192
K. Abe, *et al.*
Search for light sterile neutrinos with the T2K far detector Super-Kamiokande at a baseline of 295 km
Phys. Rev. D, 99 (2019), 71103

A-193
C. Aidala, *et al.*
Measurements of μμ pairs from open heavy flavor and Drell-Yan in p + p collisions at √s = 200 GeV
Phys. Rev. D, 99 (2019), 72003

A-194
C. Aidala, *et al.*
Measurement of charm and bottom production from semileptonic hadron decays in p + p collisions at √s = 200 GeV
Phys. Rev. D, 99 (2019), 92003

A-195
J. K. Ahn, *et al.*
Search for KL ⟶ π0νν and KL ⟶ π0X0 Decays at the J-PARC KOTO Experiment

Phys. Rev. Lett., 122 (2019), 21802

A-196
J. Guo, *et al*.
Preferred magnetic excitations in the iron-based Sr1-xNaxFe2As2 superconductor
Phys. Rev. Lett., 122, 017001

A-197
H. Wo, *et al*.
Coexistence of ferromagnetic and stripe-type antiferromagnetic spin fluctuations in YFe2Ge2
Phys. Rev. Lett., 122, 217003

A-198
C. Aidala, *et al*.
Nuclear Dependence of the Transverse Single-Spin Asymmetry in the Production of Charged Hadrons at Forward Rapidity in Polarized p + p, p + Al, and p + Au Collisions at √sNN = 200 GeV
Phys. Rev. Lett., 123 (2019), 122001

A-199
N. Kurita, *et al*.
Localized magnetic excitations in the fully frustrated dimerized magnet Ba2CoSi2O6Cl2
Phys. Rev. Lett., 123, 027206

A-200
M. Matsuura, *et al*.
Lattice Dynamics Coupled to Charge and Spin Degrees of Freedom in the Molecular Dimer-Mott Insulator κ–(BEDT–TTF)2Cu[N(CN)2]Cl
Phys. Rev. Lett., 123, 027601

A-201
M. Mogi, *et al*.
Large Anomalous Hall Effect in Topological Insulators with Proximitized Ferromagnetic Insulators
Phys. Rev. Lett.,123, 016804

A-202
Y. Sakaguchi, *et al*.
Structural transformation in GexS100-x (10≤x≤40) network glasses: Structural varieties in short-range, medium-range, and nanoscopic scale
Phys. Rev. Mater., 3, 35601

A-203
J. N. Hendriks, *et al*.
Tomographic reconstruction of triaxial strain fields from Bragg-edge neutron imaging
Phys. Rev. Materials, 3, 113803

A-204
M. Sakurai, *et al*.
Molecular weight component dependence of shish-kebab structure of polyethylene blends with X-ray and neutron scattering measurements covering a wide spatial scale
Polym. Crystallization, 2, e10034

A-205
H. Aoki
Chain dynamics in spin-coated films of poly(methyl methacrylate) in a solvent annealing process
Polym. J., 51, 611-616

A-206
T. Maeda, *et al*.
Thermo-Responsive Nanocomposite Hydrogels Based on PEG-b-PLGA Diblock Copolymer and Laponite
Polymers, 11, 250

A-207
M. Abe, *et al*.
A new approach for measuring the muon anomalous magnetic moment and electric dipole moment
Prog. Theor. Exp. Phys., 053C02-1 – 053C02-22. (2019)

A-208
R. Kitahara, *et al*.
Improved determination of thermal cross section of 14N(n,p)14C for the neutron lifetime measurement
Prog. Theor. Exp. Phys., 2019, 093C01

A-209
H. Ekawa, *et al*.
Observation of a Be double-Lambda hypernucleus in the J-PARC E07 experiment
PTEP2019, (2019), 021D02

A-210
M. Jiang, *et al*.
Atmospheric neutrino oscillation analysis with improved event reconstruction in Super-Kamiokande IV
PTEP2019, (2019), 053F01

A-211
K. Abe, *et al*.
Measurement of the muon neutrino charged-current cross sections on water, hydrocarbon and iron, and their ratios, with the T2K on-axis detectors
PTEP2019, (2019), 093C02

A-212
F. Kaneko, *et al*.
A new simultaneous measurement system of wide Q-range small angle neutron scattering combined with polarized Fouier transform infrared spectroscopy
Rev. Sci. Instrum., 90, 093906

A-213
T. Wu, *et al*.
Nephelauxetic effect of the hydride ligand in Sr2LiSiO4H as a host material for rare-earth-activated phosphors
RSC Adv., 9, 5282-5287

A-214
S. Hayashida, *et al*.
Novel Excitations near Quantum Criticality in Geometrically Frustrated Antiferromagnet CsFeCl3
Sci. Adv., 5, eaaw5639

A-215
A. Machida, *et al*.
Hexagonal closed packed iron hydride behind the conventional phase diagram
Sci. Rep., 9, 12290

A-216
K. Iida, *et al*.
Quantum magnetisms in uniform triangular lattices Li2AMo3O8 (A = In, Sc)
Sci. Rep., 9, 1826

A-217
Y. Kitanaka, *et al*.
Uncovering ferroelectric polarization in tetragonal (Bi1/2K1/2)TiO3–(Bi1/2Na1/2) TiO3 single crystals
Sci. Rep., 9, 19275

A-218
Y. Kitanaka, *et al*.
Ferrielectric-mediated morphotropic phase boundaries in Bi-based polar perovskites
Sci. Rep., 9, 4087

A-219
JG Kim, *et al*.
Synergetic strengthening of layered steel sheet investigated using an in situ neutron diffraction tensile test
Sci. Rep., 9, 43837

A-220
K. Sakurai, *et al*.
Neutron visualization of inhomogeneous buried interfaces in thin films
Sci. Rep., 9, 571

A-221
D. Ikuta, *et al*.
Interstitial hydrogen atoms in face-centered cubic iron in the Earth's core
Sci. Rep., 9, 7108

A-222
A. Shibata, *et al*.
Nature of dynamic ferrite transformation revealed by in-situ neutron diffraction analysis during thermomechanical processing
Scr. Mater., 165, 44-49

A-223
JW Bae, *et al*.
In situ neutron diffraction study of phase stress evolution in a ferrous medium-entropy alloy under low-temperature tensile loading
Scr. Mater., 165, 60-63

A-224
F. Endo, *et al*.
SANS study on the nano-crystalline

network structure of quenched syndiotactic polypropylene gels
Soft Matter, 15, 5521-5528

A-225
K. Mori, *et al*.
Structural and electrochemical features of (Li2S)x(SiS2)100–x superionic glasses
Solid State Ion., 344, 115141

A-226
N. Ishida, *et al*.
Crystal structure and cathode properties of delithiated Li1-xMn1/3Ni1/3Co1/3O2 for Mg rechargeable batteries
Solid State Ionics, 343, 115080

A-227
Y. Iizawa, *et al*.
Energy-resolved neutron imaging with high spatial resolution using a superconducting delay-line kinetic inductance detector
Supercond. Sci. Technol, 32 (2019), 125009

A-228
A. Nishimura, *et al*.
Effect of neutron irradiation on Nb3Sn wire
Supercond. Sci. Technol., 32 (2019), 24004

A-229
J. Sugiyama, *et al*.
Desorption reaction in MgH2 studied with in situ μ+SR
Sustain. Energy Fuels, 3, 956-964

A-230
K. Hanawa, *et al*.
Analysis of Reverse Transformation Behavior in Iron-based Alloys Based on Quantitative Microstructure Information by Neutron Diffraction
Tetsu-to-Hagane, 105, 998-1007

A-231
I. Yamada, *et al*.
Development of a gas distribution measuring system for 2-D beam profile monitor
Vacuum and Surface Science, 62(7), p.400 - 405, 2019/07

A-232
J. Kamiya, *et al*.
Turbomolecular pump as main pump in a high-power proton accelerator vacuum system
Vacuum and Surface Science, 62(8), p.476 - 485, 2019/08

Conference Reports and Books

B-001
S. Kishimoto, *et al*.
64- and 128-pixel Si-APD linear array X-ray detectors with 0.5 ns time resolution
AIP Conf. Proc., 2054 (2019), 60068

B-002
K.Miwa, *et al*.
Σp scattering experiment at J-PARC -- results of commissioning run --
AIP Conf. Proc., 2130 (2019), 20006

B-003
T. Koike, *et al*.
Gamma-ray spectroscopy of single Λ-hypernuclei at J-PARC: results and perspective
AIP Conf. Proc., 2130 (2019), 20011

B-004
T. Nagae, *et al*.
Observation of a Ξ bound state in the 12C(K-, K+) reaction at 1.8 GeV/c
AIP Conf. Proc., 2130 (2019), 20015

B-005
J. Yoshida, *et al*.
Status of J-PARC E07: Systematic Study of Double Strangeness Nuclei with Hybrid Emulsion Method
AIP Conf. Proc., 2130 (2019), 20016

B-006
A. Dote, *et al*.
Fully coupled-channel study of K-pp resonance in a chiral SU(3)-based KbarN potential
AIP Conf. Proc., 2130 (2019), 20018

B-007
T. Yamamoto
Future gamma-ray spectroscopic experiment (J-PARC E63) on 4ΛH
AIP Conf. Proc., 2130 (2019), 30005

B-008
H. Fujioka, *et al*.
5ΛΛH Production Experiment by Use of 7Ξ-H Production and Decay at J-PARC
AIP Conf. Proc., 2130 (2019), 40002

B-009
Y. Ichikawa, *et al*.
K and nucleus system studied by 12C(K-, p) spectrum
AIP Conf. Proc., 2130 (2019), 40017

B-010
H. Asano, *et al*.
Spectroscopic study of the Λ(1405) resonance via the d(K-, n) reaction at J-PARC
AIP Conf. Proc., 2130 (2019), 40018

B-011
H. Asano, *et al*.
Spectroscopic study of the Λ(1405) resonance via the d(K-, n) reaction at J-PARC
AIP Conf. Proc., 2130, 040018

B-012
P. Strasser, *et al*.
New precise measurements of muonium hyperfine structure at J-PARC MUSE
EPJ Web of Conf., 198, 00003

B-013
P. Strasser, *et al*.
New precise measurements of muonium hyperfine structure at J-PARC MUSE
EPJ Web of Conferences, 198 (2019), 3

B-014
HNT Kim, *et al*.
Unitarity of neutrino mixing matrix
EPJ Web of Conferences, 206 (2019), 9009

B-015
S. Kumano
High-energy neutrino-nucleus interactions
EPJ Web of Conferences, 208 (2019), 7003

B-016
S. Hashimoto, *et al*.
Analysis on Enhancement of Thermal Conductivity in Nanofluids
IMPRES2019, D309 (2019)

B-017
R. Wanison, *et al*.
A study of the thermal behavior of a nitrogen heat pipe for a wide range of heat loads at several filling ratios
IOP Conf. Ser. Mater. Sci. Eng., 502 (2019), 012093

B-018
V. Bayliss, *et al*.
The liquid-hydrogen absorber for MICE
IOP Conf. Ser. Mater. Sci. Eng., 502 (2019), 12150

B-019
F. Kaneko, *et al*.
Complexation of syndiotactic polystyrene with branched molecules

IOP Conf. Ser. Mater. Sci. Eng., 580, 012036

B-020
Z. Zong, *et al*.
Commissioning of the SuperKEKB final focusing superconducting magnet cryogenic systems
IOP Conf. Ser.: Mater. Sci. Eng., 502, 012119

B-021
M. Watanabea, H. Nojiri
Pulsed magnet system at MLF in J-PARC
J. Neutron Res., 21, 17-22

B-022
Y. Sakaguchi, *et al*.
High temperature furnace for small-angle neutron scattering instrument at J-PARC
J. Neutron Res., 21, 23-28

B-023
M. Watanabe, *et al*.
Development of Compact High Field Pulsed Magnet System for New Sample Environment Equipment at MLF in J-PARC
J. Neutron Res., 21, 29-38

B-024
M. Shibayama, *et al*.
Phenolic Resins - Recent Progress of Structure and Properties Investigations
J. Neutron Res., 21, 39-45

B-025
H. Hotchi, *et al*.
J-PARC RCS: high-order field components inherent in the injection bump magnets and their effects on the circulating beam during multi-turn injection
J. Phys. Conf. Ser. 1350, 012102 (2019)

B-026
Y. Shobuda, *et al*.
Coupling Impedance of the Collimator Without RF-Shields at the RCS in J-PARC
J. Phys. Conf. Ser. 1350, 012113 (2019)

B-027
H. Takahashi, *et al*.
Development of a beam window protection system for the J-PARC linac
J. Phys. Conf. Ser. 1350, 012142 (2019)

B-028
Y. Nakazawa, *et al*.
Development ofInter-Digital H-Mode Drift-Tube Linac Prototype With Alternative Phase Focusing for a Muon Linac in the J-PARC Muon G-2/EDM Experiment
J. Phys. Conf. Ser., 1350 (2019), 12054

B-029
M. A. Rehman, *et al*.
Beam Control and Monitors for the Spiral Injection Test Experiment
J. Phys. Conf. Ser., 1350 (2019), 12151

B-030
B. Yee-Rendon, *et al*.
Beam optics design of the superconducting region of the JAEA ADS
J. Phys. Conf. Ser., 1350(1), p.012120_1 - 012120_5, (2019)

B-031
F. Tamura, *et al*.
Simulations of beam loading compensation in a wideband accelerating cavity using a circuit simulator including a LLRF feedback control
J. Phys. Conf. Ser., 1350(1), p.012189_1 - 012189_7, 2019/12

B-032
B. Yee-Rendon, *et al*.
Design of the elliptical superconducting cavities for the JAEA ADS
J. Phys. Conf. Ser., 1350(1), p.012198_1 - 012198_6, (2019)

B-033
J. Sugiyama
Spin polarized beam for battery materials research: μ±SR and β-NMR
J. Phys. Conf. Ser., 1350, 012054

B-034
Y. Nakazawa, *et al*.
Development of Inter-Digital H-Mode Drift-Tube Linac Prototype With Alternative Phase Focusing for a Muon Linac in the J-PARC Muon G-2/EDM Experiment
J. Phys. Conf. Ser., 1350, 012054-1 – 012054-7, (2019)

B-035
P. Strasser, *et al*.
New precise measurements of muonium hyperfine structure at J-PARC MUSE
J. Phys. Conf. Ser., 1350, 012067

B-036
M. Otani, *et al*.
Negative Muonium Ion Production With a C12A7 Electride Film
J. Phys. Conf. Ser., 1350, 012067-1 – 012067-6, (2019)

B-037
Y. Kondo, *et al*.
Upgrade of the 3-MeV Linac for testing of Accelerator Components at J-PARC
J. Phys. Conf. Ser., 1350, 012077-1 – 012077-7 (2019)

B-038
M. Otani, *et al*.
Disk and Washer Coupled Cavity Linac Design and Cold-Model for Muon Linac
J. Phys. Conf. Ser., 1350, 012097-1 – 012097-7, (2019)

B-039
Y. Kondo, *et al*.
Upgrade of the 3-MeV Linac for testing of Accelerator Components at J-PARC
J. Phys. Conf. Ser., 1350, 12077

B-040
M. Otani, *et al*.
Longitudinal Measurements and Beam Tuning in the J-PARC Linac MEBT1
J. Phys. Conf. Ser., 1350, 12078

B-041
J. Tamura, *et al*.
The First Replacement of the RF Window of the ACS Cavity
J. Phys. Conf. Ser., 1350, 12079

B-042
J. Tamura, *et al*.
VSWR Adjustment for ACS Cavity in J-PARC Linac
J. Phys. Conf. Ser., 1350, 12080

B-043
T. Shibata, *et al*.
The New Eddy Current Type Septum Magnets for Upgrading of Fast Extraction in Main Ring of J-PARC
J. Phys. Conf. Ser., 1350, 12101

B-044
R. Muto, *et al*.
Current status of slow extraction from J-PARC Main Ring
J. Phys. Conf. Ser., 1350, 12105

B-045
A. Kobayashi, *et al*.
Studies on coherent multi-bunch tune shifts with different bunch spacing at the J-PARC Main Ring
J. Phys. Conf. Ser., 1350, 12114

B-046
K. Sato, *et al*.
Multi-Ribbon Profile Monitor for high power proton beam at J-PARC MR Abort Line
J. Phys. Conf. Ser., 1350, 12152

B-047
K. Moriya, *et al*.
Energy measurement and correction for stable operation in J-PARC
J. Phys. Conf. Ser., 1350, p.012140_1 - 012140_5, 2019/11

B-048
J. Kamiya, *et al*.
Evaluation of 2-D transverse beam profile monitor using gas sheet at J-PARC LINAC
J. Phys. Conf. Ser., 1350, p.012149_1 - 012149_6, 2019/12

B-049
J. Kamiya, *et al*.
New design of vacuum chambers for radiation shield installation at beam injection area of J-PARC RCS

J. Phys. Conf. Ser., 1350, p.012172_1 - 012172_7, 2019/12

B-050
M. Otani, *et al*.
Negative Muonium Ion Production With a C12A7 Electride Film
J. Phys. Conf. Ser., 4, 69

B-051
T. Takayanagi, *et al*.
Development of low inductance circuit for radially symmetric circuit
J. Phys. Conf. Ser., 1350(1), p.012183_1 - 012183_7, 2019/12

B-052
B. Yee-Rendon, *et al*.
Electromagnetic design of the low beta cavities for the JAEA ADS
J. Phys. Conf. Ser., 1350(1), p.012197_1 - 012197_7, (2019)

B-053
F. Tamura, *et al*.
Simulations of beam loading compensation in a wideband accelerating cavity using a circuit simulator including a LLRF feedback control
J. Phys. Conf. Series, 1350, 12189

B-054
S. Koizumi, Y. Noda
A Variety of Small-angle Neutron Scattering Instruments Available in Tokyo Area, Japan —Complimentary Use of Accelerator and Reactor—
JPS Conf. Proc. 25, 011004 (2019)

B-055
I. Tanaka
Necessity and Effectiveness of a Biological Diffractometer for Installation in Second Target Station as a New Neutron Pulsed Source in Japan
JPS Conf. Proc. 25, 011015 (2019)

B-056
Y. Nakazawa, *et al*.
Commissioning of the Diagnostic Beam Line for the Muon RF Acceleration with H- Ion Beam Derived from the Ultraviolet Light
JPS Conf. Proc. 25, 011028-1 - 011028-7 (2019)

B-057
Y. Kondo, *et al*.
Development of RFQs at J-PARC
JPS Conf. Proc. 25, 011030-1 - 011030-5 (2019)

B-058
T. Inada, *et al*.
Micellar Structure of Perfluorooctanesulfonic Acid in Water Investigated by Combination of SAXS and SANS
JPS Conf. Proc. Vol. 25, 11015

B-059
Y. Sakaguchi, *et al*.
Sample environment equipment for light irradiation experiments at J-PARC
JPS Conf. Proc., 25, 11004

B-060
M. Nakamura, *et al*.
Applicability and limitations of G(r, E) analysis transformed from the inelastic neutron scattering data
JPS Conf. Proc., 25, 11005

B-061
S. Ohira-Kawamura, *et al*.
Cryogenic sample environments shared at the MLF, J-PARC
JPS Conf. Proc., 25, 11018

B-062
K. Akutsu-Suyama, *et al*.
Neutron Reflectometry Study of Penetration of Protective Coating Material by Deuterated Sodium Pyruvate
JPS Conf. Proc., 25, 11019

B-063
Y. Sakaguchi, *et al*.
Kinetics of silver photodiffusion into amorphous S-rich germanium sulphide – neutron and optical reflectivity
JPS Conf. Proc., 25, 11019

B-064
K. Kusaka, *et al*.
Current Status and Future Prospects of Single Crystal Neutron Diffractometer iBIX
JPS Conf. Proc., 25, 11024

B-065
S. Kuribayashi, *et al*.
Performance test of the optical interface for Super-FGD in the T2K experiment
JPS Conf. Proc., 27 (2019), 12014

B-066
R. Kajimoto, *et al*.
Study on use of superconducting magnet and first inelastic neutron scattering experiment under magnetic field at 4SEASONS spectrometer
Macromol. Symp., 385, 1800156

B-067
S. Itoh, *et al*.
Progress in High Resolution Chopper Spectrometer HRC by improving collimator and Fermi chopper
Macromol. Symp., 385, 1800181

B-068
T. Kikuchi, *et al*.
Background issues encountered by cold-neutron chopper spectrometer AMATERAS
Macromol. Symp., 386, 1900008

B-069
Y. Ueno, *et al*.
New Precision Measurement of Muonium Hyperfine Structure
Physica B, 556, 26-30

B-070
S. Kanda, *et al*.
Precision spectroscopy of exotic atoms involving muons
Physica B, 562, 148-154

B-071
C. Haddock, *et al*.
A search for deviations from the inverse square law of gravity at nm range using a pulsed neutron beam
Physica B, 564, 45-53

B-072
Y. Nakazawa, *et al*.
Development of Inter-Digital H-Mode Drift-Tube Linac Prototype with Alternative Phase Focusing for a Muon Linac in the J-PARC Muon G-2/EDM Experiment
Physica B, 567, 61-64

B-073
N. Nagakura, *et al*.
New project for precise neutron lifetime measurement at J-PARC
Physica B, 568, 76-80

B-074
W. Liao, *et al*.
Negative and Positive Muon-Induced SEU Cross Sections in 28-nm and 65-nm Planar Bulk CMOS SRAMs
PoS (ICHEP2018), 341, 138

B-075
M. Yotsuzuka, *et al*.
Development of the longitudinal beam profile monitor with high time resolution for realization of low-emittance muon beam in the J-PARC E34 muon g−2/EDM experiment
Proc. 16th Ann. Mtg. Part. Accel. Soc. Jpn. (Internet), 814-817 (2019)

B-076
K. Shinto, *et al*.
Fluctuation of H- beam extracted from a radio-frequency-driven H- ion source
Proc. 16th Ann. Mtg. Part. Accel. Soc. Jpn. (Internet), 824-826 (2019)

B-077
M. Tomizawa, *et al*.
BEAM OPTICS FOR THE MAGNET RECOVERY IN 3-50BT BEAM TRANSFER LINE
Proc. 16th Ann. Mtg. Part. Accel. Soc. Jpan., 2019, 579

B-078
H. Yasuda, *et al*.
J-PARC muon g-2/EDM experiment : Development of the spin rotator for the low

emittance muon beam
Proc. 16th Ann. Mtg. Part. Accel. Soc. Jpn. (Internet), 371-375 (2019)

B-079
Y. Nakazawa, *et al*.
Development of RF input coupler for Inter-digital H-mode drift-tube linac prototype with alternative phase focusing in muon linac
Proc. 16th Ann. Mtg. Part. Accel. Soc. Jpn. (Internet), 404-407 (2019)

B-080
R. Kitamura, *et al*.
Bunch shape monitor for the high-intensity H- beam with 3 MeV using the carbon material
Proc. 16th Ann. Mtg. Part. Accel. Soc. Jpn. (Internet), 51-54(2019)

B-081
K. Ohkoshi, *et al*.
Operation Status of the J-PARC H- Ion Source
Proc. 16th Ann. Mtg. Part. Accel. Soc. Jpn. (Internet), 554-557(2019)

B-082
Y. Sue, *et al*.
Bunch size measurement with high time resolution for RF accelerated muon beam
Proc. 16th Ann. Mtg. Part. Accel. Soc. Jpn. (Internet), 55-60 (2019)

B-083
Y. Kondo, *et al*.
Beam dynamics of a new J-PARC RFQ using equipartitioning scheme
Proc. 16th Ann. Mtg. Part. Accel. Soc. Jpn. (Internet), 558-562 (2019)

B-084
M. Otani, *et al*.
Design of a SRF linac for accelerating muon
Proc. 16th Ann. Mtg. Part. Accel. Soc. Jpn. (Internet), 566-568 (2019)

B-085
Y. Fuwa, *et al*.
Performance Test of J-PARC 324 MHz Klystrons
Proc. 16th Ann. Mtg. Part. Accel. Soc. Jpn. (Internet), 611-613 (2019)

B-086
T. Morishita, *et al*.
Status of Beamline Alignment in J-PARC Linac
Proc. 16th Ann. Mtg. Part. Accel. Soc. Jpn. (Internet), 946-949(2019)

B-087
A. Ono
Development of ignitron alternative semiconductor switch and new kicker power supply for J-PARC accelerator
Proc. 16th Ann. Mtg. Part. Accel. Soc. Jpn. (Internet), p.399 - 403, 2019/08

B-088
F. Tamura, *et al*.
Ten-year oeration and experianced troubles of J-PARC MR timing
Proc. 16th Ann. Mtg. Part. Accel. Soc. Jpn. , 2019, THOI07

B-089
F. Tamura, *et al*.
Next generation timing system for J-PARC
Proc. 16th Ann. Mtg. Part. Accel. Soc. Jpn. (Internet), p.149 - 152, 2019/07

B-090
K. Yamamoto
History of the residual dose distribution and worker doses in J-PARC 3GeV Rapid Cycling Synchrotron
Proc. 16th Ann. Mtg. Part. Accel. Soc. Jpn. (Internet), p.333 - 337, 2019/07

B-091
T. Shibata, *et al*.
THE NEW LOW-FIELD SEPTUM MAGNET FOR UPGRADING OF FAST EXTRACTION IN MR J-PARC
Proc. 16th Ann. Mtg. Part. Accel. Soc. Jpn., 2019, 361

B-092
D. Naito, *et al*.
APPLICATION OF THE BETATRON TUNE CORRECTION SYSTEM IN THE J-PARC MR
Proc. 16th Ann. Mtg. Part. Accel. Soc. Jpn., 2019, 569

B-093
T. Yasui, *et al*.
EFFECT OF THE SPACE-CHARGE FOR THE TUNE AND FOR THE TWISS PARAMETERS IN J-PARC MR
Proc. 16th Ann. Mtg. Part. Accel. Soc. Jpn., 2019, 733

B-094
M. Otani, *et al*.
BEAM DIAGNOSTIC AND TUNING AT THE J-PARC RFQ EXIT
Proc. 16th Ann. Mtg. Part. Accel. Soc. Jpn., 2019, 833

B-095
S. Igarashi, *et al*.
SIMULATION STUDY OF THE BEAM PROFILE OF THE HIGH-POWER BEAM AT THE EXTRACTION OF J-PARC MR
Proc. 16th Ann. Mtg. Part. Accel. Soc. Jpn., 2019, 836

B-096
R. Muto, *et al*.
SIMULATION STUDY FOR THE IMPROVEMENTS OF SPILL STRUCTURE OF THE SLOW EXTRACTION AT J-PARC MR
Proc. 16th Ann. Mtg. Part. Accel. Soc. Jpn., 2019, 849

B-097
M. Furusawa, *et al*.
INVESTIGATION INTO THE INVERTER UNIT MALFUNCTION IN J-PARC MR-RF ANODE POWER SUPPLY
Proc. 16th Ann. Mtg. Part. Accel. Soc. Jpn., 2019, 853

B-098
E. Yanaoka, *et al*.
THE DEVELOPMENT OF A HF AREA MONITOR DEVICE
Proc. 16th Ann. Mtg. Part. Accel. Soc. Jpn., 2019, 967

B-099
H. WATANABE, *et al*.
DEVELOPMENT OF A PARTITION WALL TO PREVENT SCATTERING OF BEAM-WINDOW FRAGMENTS AT J-PARC HADRON FACILITY
Proc. 16th Ann. Mtg. Part. Accel. Soc. Jpn., (2019), 535

B-100
M. Yotsuzuka, *et al*.
DEVELOPMENT OF THE LONGITUDINAL BEAM PROFILE MONITOR WITH HIGH TIME RESOLUTION FOR REALIZATION OF LOW-EMITTANCE MUON BEAM IN THE J-PARC E34 MUON G - 2/EDM EXPERIMENT
Proc. 16th Ann. Mtg. Part. Accel. Soc. Jpn., (2019), 814

B-101
R. Kurasaki, *et al*.
DEVELOPMENT OF A LONG-STROKE PILLOW-SEAL FOR THE J-PARC HADRON HIGH-P BEAMLINE
Proc. 16th Ann. Mtg. Part. Accel. Soc. Jpn., (2019), 302

B-102
H. Sako, *et al*.
PRELIMINARY STUDY OF RADIATION FROM HEAVY-ION BEAMS AT J-PARC HADRON EXPERIMENTAL FACILITY
Proc. 16th Ann. Mtg. Part. Accel. Soc. Jpn., (2019), 344

B-103
E. Hirose, *et al*.
A REMOTE HANDLING MAGNET SYSTEM IN A BRANCH REGION OF A NEW PRIMARY BEAM LINE AT THE J-PARC HADRON FACILITY (2)
Proc. 16th Ann. Mtg. Part. Accel. Soc. Jpn., (2019), 389

B-104
A. Toyoda, *et al*.
DEVELOPMENT OF HIGH SENSITIVITY RESIDUAL GAS IONIZATION PROFILE MONITOR FOR J-PARC HADRON HIGH-P BEAMLINE
Proc. 16th Ann. Mtg. Part. Accel. Soc. Jpn., (2019), 498

B-105
Y. Komatsu, *et al*.
EVALUATION OF BEAM LOSS AT A BRANCHING POINT OF THE J-PARC HADRON HIGH-P BEAMLINE
Proc. 16th Ann. Mtg. Part. Accel. Soc. Jpn., (2019), 61

B-106
M. ABE, *et al*.
MAGNETIC FIELD SHIMMING STRATEGY OF MUON STORAGE MAGNET FOR g-2/EDM PRECISION MEASUREMENT
Proc. 16th Ann. Mtg. Part. Accel. Soc. Jpn., (2019), 95

B-107
N. Hayashi, *et al*.
Beam monitor data analysis of interlocked events at J-PARC RCS
Proc. 16th Ann. Mtg. Part. Accel. Soc. Jpn., 1096-1100 (2019).

B-108
T. Shimogawa, *et al*.
Proposal of nondestructive device for slow extraction
Proc. 16th Ann. Mtg. Part. Accel. Soc. Jpn., 1156-1158 (2019).

B-109
H. Harada, *et al*.
Study of heavy ion beam acceleration in J-PARC
Proc. 16th Ann. Mtg. Part. Accel. Soc. Jpn., 179-182 (2019).

B-110
Y. Kurimoto, *et al*.
EFFECTS OF RIPPLING MAGNETIC FIELD ON THE HIGH POWER OPERATION OF THE J-PARC MAIN RING
Proc. 16th Ann. Mtg. Part. Accel. Soc. Jpn., 2019, 101

B-111
C. Ohmori, *et al*.
NEGATIVE MUON DECELERATOR FOR MATERIAL SCIENCE
Proc. 16th Ann. Mtg. Part. Accel. Soc. Jpn., 2019, 1038

B-112
K. Sato, *et al*.
DEVELOPMENT AND EVALUATION OF MULTI-RIBBON PROFILE MONITOR AT J-PARC MR ABORT LINE
Proc. 16th Ann. Mtg. Part. Accel. Soc. Jpn., 2019, 1118

B-113
Y. Sato, *et al*.
INSTALLATION PLAN OF NEW 2D-BEAM-PROFILE-MONITOR BY OTR AND FLUORESCENCE AT THE J-PARC MAIN RING
Proc. 16th Ann. Mtg. Part. Accel. Soc. Jpn., 2019, 1125

B-114
T. Toyama, *et al*.
ANALYSIS AND UPGRADE PLAN OF THE TRANSVERSE INTRA-BUNCH FEEDBACK SYSTEM IN THE J-PARC MR
Proc. 16th Ann. Mtg. Part. Accel. Soc. Jpn., 2019, 1130

B-115
M. Tajima, *et al*.
DEVELOPMENT OF 16 ELECTRODES BEAM-SIZE MONITORS FOR J-PARC MR
Proc. 16th Ann. Mtg. Part. Accel. Soc. Jpn., 2019, 1134

B-116
T. Shimogawa, *et al*.
PROPOSAL OF NON-DESTRUCTIVE DEVICE FOR SLOW EXTRACTION
Proc. 16th Ann. Mtg. Part. Accel. Soc. Jpn., 2019, 1156

B-117
Y. Liu, *et al*.
BEAM LOSS MITIGATION AND COMISSIONING PROGRESS AT J-PARC LINAC
Proc. 16th Ann. Mtg. Part. Accel. Soc. Jpn., 2019, 1159

B-118
K. Hasegawa, *et al*.
PREPARATION STATUS OF RF SYSTEM FOR J-PARC MR UPGRADE
Proc. 16th Ann. Mtg. Part. Accel. Soc. Jpn., 2019, 1169

B-119
Y. Arakaki, *et al*.
TITANIUM ELECTROSTATIC SEPTA IN J-PARC MR
Proc. 16th Ann. Mtg. Part. Accel. Soc. Jpn., 2019, 1173

B-120
K. Hasegawa, *et al*.
STATUS OF J-PARC ACCELERATORS
Proc. 16th Ann. Mtg. Part. Accel. Soc. Jpn., 2019, 1235

B-121
F. Tamura, *et al*.
NEXT GENERATION TIMING SYSTEM FOR J-PARC
Proc. 16th Ann. Mtg. Part. Accel. Soc. Jpn., 2019, 149

B-122
A. Kobayashi, *et al*.
THE INVESTIGATION ON THE TIME STRUCTURE OF THE WAKE FIELD AT THE J-PARC MR
Proc. 16th Ann. Mtg. Part. Accel. Soc. Jpn., 2019, 223

B-123
Y. Kawabata, *et al*.
FULL-SCALE IMPLEMENTATION OF POSITIONING SENSOR NETWORK DEVICES AND DISASTER PREVENTION APPLICATION IN J-PARC MR
Proc. 16th Ann. Mtg. Part. Accel. Soc. Jpn., 2019, 253

B-124
M. Nomurai, *et al*.
APPLYING NEURAL NETWORKS TO INVESTIGATIONS OF THE INFLUENCE OF WEATHER CONDITIONS ON THE POWER CONSUMPTION OF J-PARC
Proc. 16th Ann. Mtg. Part. Accel. Soc. Jpn., 2019, 258

B-125
M. Yang, *et al*.
RADIATION DOSE MONITOR SYSTEM BASED ON RASPBERRY-PI AND XBEE FOR J-PARC MAIN RING
Proc. 16th Ann. Mtg. Part. Accel. Soc. Jpn., 2019, 275

B-126
K. Sato, *et al*.
DEVELOPMENT AND OPERATION OF THE EPICS-BASED SOFT-MPS IN J-PARC MR
Proc. 16th Ann. Mtg. Part. Accel. Soc. Jpn., 2019, 279

B-127
T. Shibata, *et al*.
THE STUDY OF INVESTIGATION OF THE SHORTED COIL OF MAGNET
Proc. 16th Ann. Mtg. Part. Accel. Soc. Jpn., 2019, 366

B-128
J. Takano, *et al*.
PROCESS AND GUESS OF THE LAYER SHORT IN B15D MAGNET OF J-PARC 3-50BT LINE
Proc. 16th Ann. Mtg. Part. Accel. Soc. Jpn., 2019, 394

B-129
Y. Morita, *et al*.
PERFORMANCE TEST FOR PROTOTYPE OF VHF INPUT COUPLER IN J-PARC MR
Proc. 16th Ann. Mtg. Part. Accel. Soc. Jpn., 2019, 418

B-130
M. Yoshii, *et al*.
SCHOTTKY SIGNAL DURING LONGITUDINAL DEBUNCHING PROCESS AT J-PARC MR SX
Proc. 16th Ann. Mtg. Part. Accel. Soc. Jpn., 2019, 506

B-131
K. Satou, *et al*.
DEVELOPMENT OF GATED IPM SYSTEM FOR J-PARC MR
Proc. 16th Ann. Mtg. Part. Accel. Soc. Jpn., 2019, 510

B-132
K. Ohkoshi, *et al*.

OPERATION STATUS OF THE J-PARC H- ION SOURCE
Proc. 16th Ann. Mtg. Part. Accel. Soc. Jpn., 2019, 554

B-133
M. Otani, *et al*.
DESIGN OF AN SRF LINAC FOR ACCELERATING MUON
Proc. 16th Ann. Mtg. Part. Accel. Soc. Jpn., 2019, 566

B-134
K. Futatsukawa, *et al*.
INVESTIGATION INTO HUMIDITY CHARACTERISTICS OF RF DEVICES AT J-PARC LINAC
Proc. 16th Ann. Mtg. Part. Accel. Soc. Jpn., 2019, 614

B-135
K. Okamura, *et al*.
DEVELOPMENT OF A PULSED POWER SUPPLY UTILIZING 13 kV CLASS SiC-MOSFET
Proc. 16th Ann. Mtg. Part. Accel. Soc. Jpn., 2019, 697

B-136
T. Shibata, *et al*.
THE NEW HIGH-FIELD SEPTUM MAGNET FOR UPGRADING OF FAST EXTRACTION IN MR J-PARC
Proc. 16th Ann. Mtg. Part. Accel. Soc. Jpn., 2019, 85

B-137
M. Shirakata, *et al*.
LAYER SHORT ON B15D MAGNET IN J-PARC 3-50BT LINE
Proc. 16th Ann. Mtg. Part. Accel. Soc. Jpn., 2019, 90

B-138
T. Sugimoto, *et al*.
NUMERICAL SIMULATION OF J-PARC MAIN RING INJECTION KICKER MAGNET TOWARD 1.3MW BEAM OPERATION
Proc. 16th Ann. Mtg. Part. Accel. Soc. Jpn., 2019, 998

B-139
Y. Hashimoto, *et al*.
Status report on multi-ribbon beam-profile monitor at J-PARC main ring and its beam transport line
Proc. 16th Ann. Mtg. Part. Accel. Soc. Jpn., 2019, FRPI039

B-140
T. Kimura, *et al*.
Introduction and background of Soft-MPS in J-PARC MR-MPS
Proc. 16th Ann. Mtg. Part. Accel. Soc. Jpn., 2019, THPH003

B-141
H. Takahashi, *et al*.
Update of MPS modules for J-PARC Linac and RCS
Proc. 16th Ann. Mtg. Part. Accel. Soc. Jpn., 271-274 (2019).

B-142
H. Hotchi, *et al*.
Recent progress of the J-PARC RCS beam commissioning and operation: efforts to realize a higher beam power beyond 1 MW
Proc. 16th Ann. Mtg. Part. Accel. Soc. Jpn., 574-578 (2019).

B-143
M. Chimura, *et al*.
Evaluation of beam-loss suppression method by nonlinear space charge force in a high intensity linac
Proc. 16th Ann. Mtg. Part. Accel. Soc. Jpn., 728-732 (2019).

B-144
N. Kikuzawa, *et al*.
Present status of personnel protection system at J-PARC
Proc. 16th Ann. Mtg. Part. Accel. Soc. Jpn., 877-880 (2019).

B-145
B. Yee-Rendon, *et al*.
Cavity and optics design of the accelerator for the JAEA-ADS project
Proc. 16th Ann. Mtg. Part. Accel. Soc. Jpn., p.107 - 111, (2019)

B-146
S. Meigo, *et al*.
Development of profile monitors on target for high-intensity proton accelerators
Proc. 16th Ann. Mtg. Part. Accel. Soc. Jpn., p.515 - 519, (2019)

B-147
Z. Zong, *et al*.
CRYOGENIC SYSTEMS OF THE FINAL FOCUSING SC MAGNETS IN THE SuperKEKB ACCELERATOR PHASE 2&3 COMMISSIONINGS
Proc. 16th Ann. Mtg. Part. Accel. Soc. Jpn., p.983

B-148
N. Ohuchi, *et al*.
QUENCHES OF THE FINAL FOCUS SUPERCONDUCTING MAGNETS IN THE SuperKEKB PHASE-2 AND PHASE-3 BEAM OPERATIONS
Proc. 16th Ann. Mtg. Part. Accel. Soc. Jpn., p.987

B-149
C. Ohmori, *et al*.
STATUS OF LIU (LHC INJECTOR UPGRADE) RF COLLABORATION --DEVELOPMENTS OF RAD-HARD SOLID-STATE AMPLIFIER-
Proc. 16th Ann. Mtg. Part. Accle. Soc. Jpn., 2019, 232

B-150
P. K. Saha, *et al*.
Development of two-mirror multi-pass laser system to reduce laser power for laser stripping injection at J-PARC 3-GeV RCS
Proc. 16th Ann. Mtg. Part. Soc. Jpn., 841-845 (2019).

B-151
H. Takei, *et al*.
Long beam pulse extraction by the laser charge exchange method using the 3-MeV linac in J-PARC
Proc. IBIC 2019, p.595 - 599, (2019)

B-152
N. Tsverava, *et al*.
Development of Ultrathin 12 μm Thick Straw Tubes for the Tracking Detector of COMET Experiment
Proc. IEEE NSS/MIC 2019 (2019), 9060032

B-153
M. Otani, *et al*.
NEGATIVE MUONIUM ION PRODUCTION WITH A C12A7 ELECTRIDE FILM
Proc. IPAC 2019 (2019), 1175

B-154
M. Otani, *et al*.
DISK AND WASHER COUPLED CAVITY LINAC DESIGN AND COLD-MODEL FOR MUON LINAC
Proc. IPAC 2019 (2019), 1924

B-155
M. A. Rehman, *et al*.
BEAM CONTROL AND MONITORS FOR THE SPIRAL INJECTION TEST EXPERIMENT
Proc. IPAC 2019 (2019), 2557

B-156
H. Nishiguchi, *et al*.
EXTINCTION MEASUREMENT OF J-PARC MR WITH 8 GEV PROTON BEAM FOR THE NEW MUON-TO-ELECTRON CONVERSION SEARCH EXPERIMENT - COMET
Proc. IPAC 2019 (2019), 4372

B-157
K. Yamamoto, *et al*.
Operation status of J-PARC rapid cycling synchrotron
Proc. IPAC 2019 (Internet), p.2020- 2023, 2019/06

B-158
Y. Sue, *et al*.
A Bunch Structure Measurement of Muons Accelerated by RFQ Using a Longitudinal Beam-Profile Monitor With High Time Resolution
Proc. IPAC 2019 , 37-40 (2019)

B-159
H. Yasuda, *et al*.
Design of the Wien-Filter Type Spin Rotator

for the Low-Emittance Muon Beam
Proc. IPAC 2019 , 622-625 (2019)

B-160
J. Tamura, *et al*.
The First Replacement of the RF Window of the ACS Cavity
Proc. IPAC 2019 , p.971-973(2019)

B-161
J. Tamura, *et al*.
VSWR Adjustment for ACS Cavity in J-PARC Linac
Proc. IPAC 2019 , p.974-976(2019)

B-162
K. Miura, *et al*.
MAGNET POWER SUPPLY CALIBRATION WITH A PORTABLE CURRENT MEASURING UNIT AT THE J-PARC MAIN RING
Proc. IPAC 2019, 1263

B-163
T. Shimogawa, *et al*.
NEW POWER SUPPLY OF MAIN MAGNETS FOR J-PARC MAIN RING UPGRADE
Proc. IPAC 2019, 1266

B-164
A. Kobayashi, *et al*.
STUDIES ON COHERENT MULTI-BUNCH TUNE SHIFTS WITH DIFFERENT BUNCH SPACING AT THE J-PARC MAIN RING
Proc. IPAC 2019, 167

B-165
P. K. Saha, *et al*.
DYNAMIC VARIATION OF CHROMATICITY FOR BEAM INSTABILITY MITIGATION IN THE 3-GeV RCS OF J-PARC
Proc. IPAC 2019, 171 (2019)

B-166
Y. Liu, *et al*.
PROGRESS OF J-PARC LINAC COMMISSIONING
Proc. IPAC 2019, 1990

B-167
T. Shibata, *et al*.
THE NEW EDDY CURRENT TYPE SEPTUM MAGNETS FOR UPGRADING OF FAST EXTRACTION IN MAIN RING OF J-PARC
Proc. IPAC 2019 , 1997

B-168
T. Shibata, *et al*.
THE NEW HIGH FIELD SEPTUM MAGNETS FOR UPGRADING OF FAST EXTRACTION IN MAIN RING OF J-PARC
Proc. IPAC 2019, 2001

B-169
M. Shirakata, *et al*.
RADIATION DESIGN OF NEW 30 kW BEAM DUMP OF J-PARC MAIN RING
Proc. IPAC 2019, 2005

B-170
M. Yamamoto, *et al*.
VACUUM TUBE OPERATION ANALYSIS FOR 1.2 MW BEAM ACCELERATION IN J-PARC RCS
Proc. IPAC 2019, 2017

B-171
R. Muto, *et al*.
CURRENT STATUS OF SLOW EXTRACTION FROM J-PARC MAIN RING
Proc. IPAC 2019, 2311

B-172
K. Okumura, *et al*.
A CONSIDERATION ON THE TRANSFER FUNCTION BETWEEN RQ FIELD AND SLOW EXTRACTION SPILL IN THE MAIN RING OF J-PARC
Proc. IPAC 2019, 2315

B-173
M. Tomizawa, *et al*.
8 GeV SLOW EXTRACTION BEAM TEST FOR MUON TO ELECTRON CONVERSION SEARCH EXPERIMENT AT J-PARC
Proc. IPAC 2019, 2322

B-174
Y. Hashimoto, *et al*.
BEAM PROFILE MONITOR FOR SLOW EXTRACTED BEAM USING MULTI-LAYERED GRAPHENE AT J-PARC
Proc. IPAC 2019, 2532

B-175
K. Sato, *et al*.
MULTI-RIBBON PROFILE MONITOR FOR HIGH POWER PROTON BEAM AT J-PARC MR ABORT LINE
Proc. IPAC 2019, 2561

B-176
M. Yotsuzuka, *et al*.
Development of the Longitudinal Beam Monitor with High Time Resolution for a Muon LINAC in the J-PARC E34 Experiment
Proc. IPAC 2019, 2571-2574 (2019)

B-177
F. Tamura, *et al*.
SIMULATIONS OF BEAM LOADING COMPENSATION IN A WIDEBAND ACCELERATING CAVITY USING A CIRCUIT SIMULATOR INCLUDING A LLRF FEEDBACK CONTROL
Proc. IPAC 2019, 2863

B-178
T. Yasui, *et al*.
TUNE SHIFTS AND OPTICS MODULATIONS IN THE HIGH INTENSITY OPERATION AT J-PARC MR
Proc. IPAC 2019, 3148

B-179
H. Takahashi, *et al*.
DEVELOPMENT OF A BEAM WINDOW PROTECTION SYSTEM FOR THE J-PARC LINAC
Proc. IPAC 2019, 3886

B-180
T. Toyama, *et al*.
IMPROVED FREQUENCY CHARACTERISTICS USING MULTIPLE STRIPLINE KICKERS
Proc. IPAC 2019, 3893

B-181
S. Li, *et al*.
THE REALIZATION OF ITERATIVE LEARNING CONTROL FOR J-PARC LINAC LLRF CONTROL SYSTEM
Proc. IPAC 2019, 4155

B-182
T. Sugimoto, *et al*.
RECENT IMPROVEMENTS AND FUTURE UPGRADES OF THE J-PARC MAIN RING KICKER MAGNET SYSTEMS
Proc. IPAC 2019, 4167

B-183
S. Igarashi, *et al*.
CHALLENGES TO HIGHER BEAM POWER IN J-PARC: ACHIEVED PERFORMANCE AND FUTURE PROSPECTS
Proc. IPAC 2019, 6

B-184
C. Ohmori, *et al*.
CONCEPTUAL DESIGN OF NEGATIVE-MUON DECELERATOR FOR MATERIAL SCIENCE
Proc. IPAC 2019, 610

B-185
Y. Kondo, *et al*.
UPGRADE OF THE 3MeV LINAC FOR TESTING OF ACCELERATOR COMPONENTS AT J-PARC
Proc. IPAC 2019, 960

B-186
M. Otani, *et al*.
LONGITUDINAL MEASUREMENTS AND BEAM TUNING IN THE J-PARC LINAC MEBT1
Proc. IPAC 2019, 968

B-187
J. Tamura, *et al*.
THE FIRST REPLACEMENT OF THE RF WINDOWOF THE ACS CAVITY
Proc. IPAC 2019, 971

B-188
R. Kitamura, *et al*.
Development of the bunch shape monitor using the carbon-nano tube wire
Proc. IPAC 2019, p.2543-2546(2019)

B-189
M. Kinsho, *et al*.
Effect of nitric hydrofluoric acid treatment on brazing of alumina ceramics and pure titanium
Proc. IPAC 2019, p.4161 - 4163, 2019/06

B-190
H. Matsuda, *et al*.
Measurement of activation cross sections of aluminum for protons with energies between 0.4 GeV and 3.0 GeV at J-PARC
Proc. ISORD-9, 171 - 174 (2019)

B-191
N. Watanabe, *et al*.
Immortal experimental loop at JAEA; Post-process and validation
Proc. NURETH-18, (USB Flash Drive), p.248 - 261, 2019/08

B-192
H. Obayashi, *et al*.
Steady-state and transient experiments in mock-up of J-PARC LBE spallation target system using mock-up loop IMMORTAL
Proc. NURETH-18, 13p. (USB Flash Drive)

B-193
K. Mishima, *et al*.
Neutron scattering cross section of diamond nanoparticle
Proc. PPNS 2018

B-194
M. Ishikado, *et al*.
Q Dependence of Magnetic Resonance Mode on FeTe0.5Se0.5 Studied by Inelastic Neutron Scattering
Proc. PPNS2018, EPJ Web Conf., 219, 03003

B-195
R. Kajimoto, *et al*.
Status of neutron spectrometers at J-PARC
Proc. PPNS2018, EPJ Web Conf., 219, 05002

B-196
A. Lavakumar, *et al*.
In-situ neutron diffraction study on the deformation of a TRIP-assisted multi-phase steel composed of ferrite, austenite and martensite
Proc. PPNS2018, EPJ Web Conf., 219, 10005

B-197
K. Sakai, *et al*.
Search for Cosmic-Ray Antideuterons with BESS-Polar II
Proc. Sci. ICRC 2019 (2019), 134

B-198
S. Mihara
Status of MEG experiment at PSI
Proc. Sci. NuFact 2019 (2019), 81

B-199
K. Sakai, *et al*.
Search for Cosmic-Ray Antideuterons with BESS-Polar II
Proc. Sci., 358

B-200
J. Tamura, *et al*.
Electromagnetic Design of the Prototype Spoke Cavity for the JAEA-ADS Linac
Proc. SRF 2019, p.399-402(2019)

B-201
M. Sugano, *et al*.
DEVELOPMENT OF SUPERCONDUCTING MAGNETS FOR LHC LUMINOSITY UPGRADE (6) - FROM DEVELOPMENT OF 2 M-LONG MODEL MAGNET TO CONSTRUCTION OF SERIES MAGNET -
Proc. the 16th Ann. Mtg. Part. Accel. Soc. Jpn., p.80

B-202
K. Yamamoto, *et al*.
SAXS and SANS studies on the phase-separated network structure of amphiphilic copolymer composed of poly(dimethyl siloxane) and poly(N,N-dimethyl acrylamide) gels swollen in water and a water/methanol mixture
Pure Appl. Chem., 91, 1821-1835

KEK Reports

C-001
Safety Division, J-PARC Center
Annual Report on the Activities of Safety in J-PARC, FY2018
KEK Internal 2019-6

C-002
I. Yamane
Charge-exchange of 400 MeV H- beam with laser beam for J-PARC RCS injection
KEK Report 2019-2

JAEA Reports

D-001
Safety Division, J-PARC Center
Annual Report on the Activities of Safety in J-PARC, FY2018
JAEA-Review 2019-043(2019)

D-002
K. Nakajima, *et al*.
Presentation Materials Related to Neutron Instruments in the Technical Study Meetings for Future MLF
JAEA-Review / J-PARC

Others

E-001
H. Hotchi
Study on beam dynamics of high intensity proton beam and mitigation of beam loss in J-PARC RCS
Foundation for High Energy Accelerator Science, 18, 18, (2019)

E-002
C. Ohmori, *et al*.
From Proton beam acceleration to train acceleration
High Energy News, 38, 1

E-003
J. Kamiya, *et al*.
Technolofy of vacuum, Large vacuum system, J-PARC
New Practical Vacuum Technology, p.908 - 917, 2019/02

Photograph : Person in Tank
Image credit : Yasuhiro MAKIDA

J-PARC Annual Report 2019
Vol.1: Highlight

January 2021

J-PARC

JAPAN PROTON ACCELERATOR RESEARCH COMPLEX

High Energy Accelerator Research Organization (KEK)
Japan Atomic Energy Agency (JAEA)

2-4 Shirakata, Tokai-mura, Naka-gun, Ibaraki 319-1195, Japan

http://j-parc.jp/